TECHNISCHE UNIVERSITÄT WIEN
Vienna University of Technology

Dissertation

Vehicular Service Delivery via Hybrid Access and Antennas

Submitted in partial fulfillment of the requirements for the degree of "Doktor der technischen Wissenschaften" (Dr.techn.)

to the

Vienna University of Technology
Faculty of Electrical Engineering and Information Technology

by

Dipl.-Ing. Levent Y. Ekiz
Matrikelnr.: 1125490

Vienna, 16th October 2014

Advisor:

Prof. Dr. Christoph F. Mecklenbräuker

Institute of Telecommunications

Vienna University of Technology

Examiner:

Prof. Dr. Erik G. Ström

Department of Signals and Systems

Chalmers University of Technology, Sweden

Abstract

In this work two key topics are investigated; assessment of hybrid antenna systems and the service delivery for driver information and assistance systems using cellular and ad-hoc networks. The evaluation of prototypical antenna systems focuses on the networks Long Term Evolution (LTE) and the vehicle-to-vehicle (V2V) standard IEEE 802.11p. Key performance indicators KPIs are identified on component and on system level to determine the ability of antenna systems to support dependable communication. On component level KPIs relating to the antenna impedance and radiation efficiency are analyzed. Statistical metrics for link performance evaluation are introduced to quantify the deviation of the prototypical antenna systems from the expected values. On system level applied KPIs differ as safety applications are mainly considered for 802.11p communication systems, whereas LTE systems are intended for safety as well as infotainment applications. Consequently, the evaluation of LTE antennas focuses on their capability to support spatial multiplexing SMX transmission techniques, whereas for 802.11p antenna systems their ability to enable diversity transmission schemes is investigated. Both transmission schemes are evaluated on system level by a real-world drive test using active probing, which causes additional traffic for the purpose of measurements, and also by passive listening. In case of passive listening KPIs are derived from the channel matrix being estimated from pilot symbols broadcasted periodically by the base station. For LTE antenna systems the impact on the KPIs, such as channel condition number and mutual information, are shown subject to the antenna isolation and antenna gain deviations. The assessment of the 802.11p systems in drive test illustrates the influence of different solutions for positioning the antennas in a multiple antenna arrangement to achieve a high diversity gain.

In the second part of this work the additional value of using hybrid radio access including cellular and wireless local area based networks is analyzed for the service delivery in infotainment and safety applications. For infotainment applications a network selection algorithm is presented, which is able to incorporate KPIs from different data sources to exploit the advantages of the diverse access networks. A simulation based evaluation is presented illustrating improved service delivery by avoiding throughout drops and reducing the occurring transmission costs. By performing simulations and measurements it is illustrated that KPIs from the backend, such as the load of the access networks and network coverage maps, are key to achieve such improvements. Analysis carried out for driver assistance applications show that the combined use of LTE and 802.11p radios allows to compensate for the deficiencies of each network. The investigated KPIs for safety applications include the yielded range, the latency of the messages, the network load in the LTE network and the supported networks by the vehicles. Using 802.11p radios to forward safety messages received over LTE, it is shown that communication gaps resulting from the low communication range of 802.11p radios are overcome. The simulations also illustrate that the base load in the LTE network causes an increase in the latency of the message delivery. It is thus the primary performance deteriorating factor for the deployment of safety applications using LTE.

Kurzfassung

Diese Arbeit setzt sich aus zwei thematischen Schwerpunkten zusammen; Zum einen wird die Leistungsfähigkeit hybrider Antennensysteme bewertet und zum anderen wird der Mehrwert von hybriden Funknetzen für Fahrerinformations- und assistenzsysteme analysiert. Die Bewertung von prototypischen hybriden Mehrantennensystemen befasst sich im Vordergrund mit dem zellularen Funkzugangssystem Long Term Evolution (LTE), sowie dem Fahrzeug-zu-Fahrzeug Kommunikationsstandard IEEE 802.11p. Für die Bestimmung der Leistungsfähigkeit der Antennensysteme werden Performance Kenngrößen verwendet, die eine Bewertung auf Komponenten- als auch auf Systemebene erlauben. Auf Komponentenebene werden Performance Indikatoren (KPI)s verwendet, welche die Impedanz und Strahlungscharakteristika der Mehrantennensysteme fassen. Abweichungen von Mindestperformancekennwerten werden mit Hilfe von statistischen Kenngrößen festgehalten. Resultierend von den unterschiedlichen Anwendungsbereichen der Funkzugangssysteme LTE und 802.11p im Automobilumfeld, kommen für die Beurteilung ihrer Leistungsfähigkeit auf Systemebene voneinander abweichend KPIs zum Einsatz. Da 802.11p Systeme in erster Linie für Sicherheitsapplikation ausgelegt sind, liegt hierbei der Schwerpunkt auf der Erhöhung der Robustheit der Kommunikation durch Diversität. Wohingegen bei LTE Antennen, die sowohl für Sicherheits- als auch für Infotainmentanwendungen ausgelegt sind, vordergründig der erzielte Raummultiplex-Gewinn im Fokus steht. Beide Mehrantennensysteme werden durch Testfahrten evaluiert, wobei einerseits passives Absuchen von Signalen als auch aktive Messungen, wo zu Messzwecken eine Datenlast erzeugt wird, zum Einsatz kommen. LTE Antennensysteme, die sich zum größten Teil durch ihre Isolation und Einbrüchen im Antennengewinn unterscheiden, werden anhand der Transinformation und der Konditionszahl der Kanalmatrix beurteilt. Aus den Ergebnissen der 802.11p Systeme wird abgeleitet mit welcher Konstellation der zellularen und ad-hoc Antennen ein hoher Diversitätsgewinn erreicht wird.

Im zweiten Teil dieser Arbeit wird der Mehrwert der hybriden Kommunikation, d.h. die kombinierte Nutzung von LTE und 802.11p Funksystemen, für Sicherheits- und Infotainmentapplikationen analysiert. Im Bereich von Infotainmentapplikationen wird ein mehrkriterielle Netzwahlalgorithmus betrachtet, der es erlaubt KPIs aus Fahrzeuginternen wie -externen Quellen zu berücksichtigen. Mit Hilfe von Simulationen und Messungen wird gezeigt, dass insbesondere Daten aus externen Quellen, wie z.B. Güteinformationen aus vergangenen Verbindungen oder Karten zur Netzverfügbarkeit, die Dienstgüte für Fahrerinformationsdiensten erheblich verbessern und zu Entgeltersparnissen führen. Untersuchungen zu Sicherheitsapplikationen zeigen, dass durch hybride Kommunikation Unzulänglichkeiten der Funkzugangssysteme kompensiert werden. Durch die Nutzung der hybriden Kommunikation wird die Reichweite von Fahrerassistenzsystemen und die Wahrscheinlichkeit für die rechtzeitige Zustellung von Sicherheitsnachrichten erhöht. Die Untersuchungen zeigen, dass solche Verbesserung sogar bei einer prozentual geringen Penetration von hybriden Radios erzielt werden. Ferner wird durch die Nutzung der hybriden Kommunikation unter Berücksichtigung von volkswirtschaftlichen Gesichtspunkten eine bessere Ausnutzung der Kommunikations-Ressourcen erreicht.

Acknowledgements

First, I like to thank my PhD Advisor Christoph Mecklenbräuker to agree to supervise my thesis and for his continuous support throughout my work. It was a privilege to work with him towards my PhD. I enjoyed the social events, dinners and bar nights during the COST meetings and my visits in Vienna to discuss my progress. One of the highlights of my thesis was when Christoph put his trust in me and nominated me to chair the vehicular working group in the COST IC 1004 action. Another key person in my professional life during the last years was Oliver Klemp, who is the reason why I started at BMW Research and Technology in the first place. From being my lecturer at the university, he went on to supervise my Master Thesis and afterwards my PhD. He is a constant source of motivation, knows very well how to keep you on your toes and to strive you to your best. The diverse projects we worked together on, thought me a lot and formed the foundation of my professional life. Through Christoph and Oliver I got to know Erik Ström with whom I currently co-chair the aforementioned vehicular working group. I am grateful of our fruitful discussions and will always keep in mind the various social events and nights out during meetings and conferences. I am really glad that Erik accepted to be my second examiner. During my PhD I had the privilege to work with some great people; I really appreciate that my department head Karl-Ernst Steinberg always had an open ear for the requirements of my research projects and always supported me to achieve my goals. Over the years I become one of the most frequent travelers to workshops, meetings and conferences. I am thankful to Mr. Steinberg for supporting me to go on all these travels. I am also very grateful to my former team leader Michael Schraut, who offered me a position in his research team and continuously supported my work.

One of the most memorable and greatest experiences during a PhD is working towards your goals with great colleagues. I am very glad to have been in a team, where the team spirit and the sense of community had a significant value. Therefore I like to thank my current team leader Sebastian Zimmermann and the Automotive Connectivity and Security Solutions group. I will always hold our various 'Stammtisch' events in great memory. I especially like to thank Mladen Botsov for taking the time to thoroughly proof read my thesis and giving me valuable feedback. Moreover, I appreciate the continuous support of Adrian Posselt, Dennis Lenz, Michael Rosenfelder and Pascal Hervé for the measurements and the post-processing of all the gigabytes of data we collected. I also had the pleasure of supervising some great students, namely Roland Wilhelm, David Öhmann, Timo Patelczyk, Christian Arendt, Anne-Claire Morvan, Martin Waltl, Martin Bayer and Florence Vogl with whom I enjoyed working together very much. In particular I like to thank Christian Arendt for his great work and support in over 2 years. From the TU Vienna I like to thank Mona Shemshaki and Veronika Shivaldova for the fruitful discussions and support when I was visiting.

Lastly I am really thankful to my parents for their endless love and support. Without my parents I would have never gotten this far.

Contents

Chapter 1

Introduction

Within three years, vehicles are likely connected with each other and to the road infrastructure to provide traffic information services for ITS. Research projects, such as *CoCarX* [1], showed that in the cellular domain the 4G communication standard 3GPP Long Term Evolution (LTE) is very suitable for time-critical driver assistance services. In the ad-hoc domain the recently completed project *simTD* [2] evaluated the performance of IEEE 802.11p for different vehicle-to-vehicle (V2V) and vehicle-to-infrastructure (V2I) applications. An analysis of key characteristics of V2V and V2I channels was provided in [3]. IEEE 802.11p is in the U.S. standardized by the IEEE regulated by the Federal Communications Commission (FCC) and is allocated a spectrum of 75 MHz in the 5.9 GHz band. In Europe the ETSI allocated 802.11p, also known as ETSI ITS-G5, a spectrum of 30 MHz. Although research projects determined the general suitability of the access networks for driver assistance systems, it was shown that both access networks also suffer from shortcomings. Cellular networks, such as LTE, are used commercially by non-automotive users, thus the LTE performance is depending on the instantaneous load conditions in the network [1]. IEEE 802.11p is intended only for vehicular applications, however due to the high operating frequency at 5.9 GHz, it does not allow to cover long communication ranges. To handle the disadvantages and to exploit the merits of IEEE 802.11p and the LTE network, the research project *CONVERGE* [4] explores, among other research interests, ways to efficiently combine both domains. Such a hybrid approach, by merging the aforementioned access networks, allows to use the available spectrum efficiently as well as to enable reliable connectivity and improved quality of service (QoS) for vehicular infotainment and safety applications. However, this hybrid approach also necessitates that electronic components, such as antenna systems and the corresponding electronic control units, are capable to work with cellular as well as ad-hoc standards. The presently deployed systems in different vehicle models work only at cellular frequencies.

In this work requirements for next generation of hybrid antenna systems and corresponding electronic components are considered enabling future vehicular infotainment and safety applications, see Figure 1.1. In case of antenna systems the focus is on the design of a methodology to determine the performance of different systems and thus

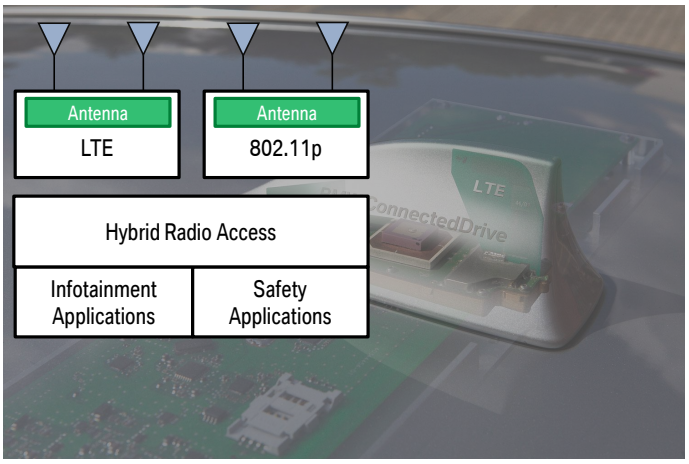

Figure 1.1: Assessment of LTE and 802.11p antennas and hybrid access for infotainment and safety applications are the two key aspects of this work.

to establish key performance indicators (KPIs) for antenna specification documents. The second corner stone of this thesis, after an investigation of hybrid antenna systems, covers the analysis of the combined use of LTE and 802.11p access networks for vehicular applications.

Hybrid antenna systems are integrated in a single antenna housing on the vehicle rooftop. An in-depth analysis of various antenna integration volumes was researched in [5]. In this work, however, the focus is on the conventional mounting volume on the vehicle rooftop as new antenna systems are feasible to be integrated without changing the vehicle design or manufacturing process. Due to design considerations the volume within the housing is confided posing challenges on the one hand to integrate additional antennas and on the other to ensure that the antennas do not interfere with each other. Interactions of cellular antennas in confided volumes were analyzed in diverse research papers, such as [6, 7]. In [6] it was shown by measurements in a live LTE network that differences in the gain of the employed antennas decrease the spatial multiplexing (SMX) gain of the multiple input multiple output (MIMO) antenna system. A fallback from SMX to diversity transmission was found to be occurring predominantly in line of sight (LOS) scenarios with the base station. The investigated MIMO antenna system was analyzed in detail in [8]. Comparing the antenna gain measurements to a reference monopole system, yielded that such deterioration result from the low separation of the cellular antennas. However, a methodology to assess the performance of MIMO antennas on system level has not been carried out so far. Thus current antenna systems are rated based on component level KPIs, such as the antenna gain or scattering parameters, without a deeper insight into the impact of single KPIs on the achieved end-to-end performance. In this work various prototypical antenna system are evaluated to illustrate the impact of component level KPIs on system level. Thus a methodology is established to rate the SMX capability of the LTE MIMO antennas. Component level analysis focuses on KPIs relating to the antenna isolation, radiation efficiency and antenna gain. To take into consideration regional degradation of the antenna radiation pattern statistical metrics are also applied. For system level evaluation test

drives are conducted to assess SMX performance of the antennas. Depending on the measurement methodology KPIs, such as the channel condition number (κ), mutual information (C) or data rate are evaluated.

In contrast to cellular antenna systems, the current analysis for 802.11p antennas in the literature focuses predominately on the occurring performance deterioration when mounting such systems on the vehicle. In [9] it was shown that roof railings and sunroofs have a significant impact on the antenna performance. Analysis in [10] illustrated that due to the high operating frequency the antenna housing substantially influences the antenna radiation pattern resulting in blind spots for certain angles in the azimuth. Research into positioning of 802.11p antennas to optimally exploit diversity efficiency was conducted in [11]. It was shown that from an antenna performance perspective the side mirror and the rear end of the vehicle rooftop are suitable positions in specific channel conditions. Due to economic considerations distributing antenna systems on the vehicle is challenging, all antenna systems are thus spaced in a confided volume. Thus necessitating to determine the impact of 802.11p antennas positioned close to other antennas in such a volume. In this work the yielded diversity efficiency is evaluated as a KPI for various 802.11p systems performing measurements on a test track. The diversity efficiency is assessed subject to the received signal strength (RSS) values of both antennas of the prototypical systems. On component level the same KPIs are applied to the prototypical systems as analyzed for LTE antennas. However, an emphasize is put on regional degradation in the antenna radiation pattern in order to allow for reception and transmission of safety messages regardless of the direction they yield from.

To exploit the merits of both access networks LTE and 802.11p for vehicular safety and infotainment applications, see [12], this thesis also focuses on a radio resource management (RRM) as also analyzed in [13, 14]. Using a RRM for vehicular safety applications ensures that performance degradation, for instance, of the communication range by integration impairments of 802.11p antenna system, due to the high operating frequency, is feasible to be compensated by the LTE network. Besides compensation efforts, the combined use of both access networks also allows for redundant transmissions via the different networks in order to increase the robustness of the communication [15]. The key difference between safety and infotainment application domains is that safety applications are of a cooperative nature whereas infotainment application are user-centric [13, 16]. Thus a RRM for infotainment applications works independently of other users to optimize the communication link according to the requirements and demands of the user. Due to the dynamic nature of the vehicular radio channel it is not sufficient for a RRM to derive a decision for network selection only from passively monitored KPIs, such as the signal strength of the access networks [17]. Additional on-board values from vehicular electronic control units and context-aware external information from, for instance, original equipment manufacturer (OEM) backends is capable to improve the network decision. Such context-aware information includes the current traffic conditions, the load of the access networks or user experience maps of the network reliability for a specified location and time. In [18] an overview of different RRM strategies is given to satisfy the different needs of users and application demands for infotainment use cases.

The authors in [19] illustrate by simulations that a multi-criteria approach is best suited for a RRM strategy for complex scenarios found in the vehicular environment. The analysis conducted in [20] reveals that most multi-criteria RRM yield similar results. Consequently, to satisfy the demands it is key to set proper weights for the considered inputs. The combined use of cellular and ad-hoc access networks for infotainment applications has been analyzed in [21, 22, 23]. The results show that the use of WLAN offloading substantially decreases the load in cellular networks and consequently reduces the transmission costs for customers. However, due to the scheduling of the download to use transmission cost-efficient networks the necessary time span is also increased. Thus in this case a trade-off is made between cost-efficiency and required time to perform the download. The potentially lower traffic in the cellular network due to WLAN offloading is also capable to increase the probability of on-time delivery of latency sensitive messages or packets, such as for video calls [16]. Such an on-time delivery is especially key for reliable functioning of safety applications using cellular as well as ad-hoc radios. However, the use of hybrid radio access especially in the domain of vehicular safety applications has not been explored so far. In [24] an overview is given regarding the suitability of cellular and ad-hoc networks for vehicular safety applications. It is proposed that cellular communication systems are suitable for long range V2I communication. For delay sensitive and short range communication IEEE 802.11p is found to be best suited. In [25] it is stated that LTE radios are able to compensate the drawbacks of 802.11p system, such as system scalability and coverage. However, it is also pointed out that LTE is predominately used commercially by end consumers, thus making it more challenging to reliably support delay intolerant applications in contrast to 802.11p communication. In [25, 26] it is concluded that LTE unicast connections are not suited for beaconing applications, as those substantially increase the network load and incur in high transmission costs. It is suggested that using network resource efficient broadcasting schemes are in the future a possibility to also support beaconing applications via LTE. As LTE broadcasting schemes are currently not widely deployed, hybrid access is considered for event-driven applications only, whereas ad-hoc systems are regarded for beaconing applications. Consequently, this work also focuses on event-driven applications, to illustrate that combining both LTE and 802.11p access networks is a suitable approach to exploit the merits of both domains and to meet ITS application requirements.

1.1 Outline

This thesis is structured as follows: The assessment methodology for hybrid antenna systems is discussed in Chapter 2. Different approaches to perform such an assessment are analyzed with emphasize on the vehicular environment. Furthermore, various KPIs are investigated to determine the suitability of MIMO antenna prototypes for the access networks LTE and 802.11p. The RRM using hybrid access for safety and infotainment applications is investigated in Chapter 3. The Section on infotainment applications includes a discussion on available on- and off-board KPIs to achieve a high

QoS in terms of an overall high throughput and transmission cost efficient connectivity. The next Section discusses the major difference in the use of hybrid access for infotainment and safety applications. Based on this analysis use case dependent safety message dissemination methodologies are examined, for instance, to increase reliability by redundant transmission. Following this, prototypical hybrid antenna systems are evaluated in Chapter 4. The cellular antennas of four prototypical hybrid systems are compared to a reference antenna system by performing measurements drives in different channel conditions. KPIs rating the SMX efficiency are identified for future vehicular antenna specification data sheets. The second part of the Chapter includes an analysis of KPIs for the diversity gain efficiency of 802.11p antennas. Moreover, is a methodology introduced to eliminate nulls in the antenna radiation pattern, which is key for receiving safety messages independent of the direction. Test drive measurements are presented to determine the yielded communication range of different antenna positions. Next, simulations and measurements are presented in Chapter 5 determining that the use of on- and off-board KPIs significantly enhance the yielded QoS for infotainment applications. As such an overall high throughput is achieved and momentarily connection outages are avoided. It is shown that a hierarchical assessment approach to rank different access networks and their KPIs is a suitable way to achieve a context aware high QoS for infotainment applications. The analysis of safety applications in the second part of the Chapter discusses the cooperative nature of safety applications with special regards on the impact of access network penetration on the dissemination of safety messages. It is shown that the combined use of LTE and 802.11p radios significantly reduces communication gaps as well as increases the communication range and service availability of safety applications. The conclusions of this thesis are drawn in Chapter 6.

1.2 Publications

The following papers were published in the context of this thesis:

- [6] 'MIMO Performance Evaluation of Automotive Qualified LTE Antennas' by L. Ekiz, A. Thiel, O. Klemp, and C.F. Mecklenbräuker presents active measurements, carried out with a prototypical MIMO antenna system in a LTE live network. The results show that differences in the antenna gain significantly reduce the SMX performance of the analyzed prototypical MIMO antenna system.
- [27] 'System Level Assessment of Vehicular MIMO Antennas in 4G LTE Live Networks' by L. Ekiz, A. Posselt, O. Klemp, and C.F. Mecklenbräuker investigates a methodology for carrying out reproducible antenna benchmarks. The introduced methodology evaluates KPIs yielded from pilot symbols, which are transmitted continuously by the base station. It is shown that suitable KPIs for the benchmark of MIMO antennas are the channel condition number and the mutual information.
- [28] 'Compensation of Vehicle-Specific Antenna Radome Effects at 5.9 GHz'

by L. Ekiz, T. Patelczyk, O. Klemp, and C.F. Mecklenbräuker presents a methodology to eliminate nulls in the radiation pattern of 802.11p antenna systems. By modifying the thickness of the antenna housing it is illustrated that nulls in the pattern are compensated. Performing simulations it is shown that such a compensation results in considerable improvements on system level.

- [29] 'Assessment of Design Methodologies for Vehicular 802.11p Antenna Systems' by L. Ekiz, A. Posselt, O. Klemp, and C.F. Mecklenbräuker analyzes different positions of 802.11p antennas among similar locations for cellular antennas to limit the interaction between both systems. The results show that positioning the 802.11p antennas one on each side of the antenna housing yields the highest diversity efficiency.
- [17] 'Potential of Cooperative Information for Vertical Handover Decision Algorithms' by L. Ekiz, C. Lottermann, D. Öhmann, T. Tran, O. Klemp, C. Wietfeld and C.F. Mecklenbräuker investigates the service delivery for infotainment applications in hybrid access networks. It is illustrated that KPIs from the backend are key in increasing the throughput and avoiding outages in the communication link.
- [16] 'System Level Impact of Hybrid Radio Access for Vehicular Safety Applications' by L. Ekiz, C. Arendt, O. Klemp and C.F. Mecklenbräuker illustrates that the service delivery of safety messages is improved using hybrid radio access. The shortcomings of each access network, such as the limited communication range of 802.11p range and an increased delay in the LTE network for high base loads, are feasible to be compensated. This journal article is currently under review.
- [7] 'System Level Evaluation for Vehicular MIMO Antennas in Simulated and Measured Channels' by A. Posselt, L. Ekiz, O. Klemp, B. Geck and C.F: Mecklenbräuker illustrates the impact of antenna correlation and antenna isolation for a reliable LTE link. A metric for evaluating LTE MIMO antennas is derived with the help of a Kronecker MIMO channel model including fading.
- [8] 'Automotive Grade MIMO Antenna Setup and Performance Evaluation for LTE-Communications' by A. Thiel, L. Ekiz, O. Klemp, M. Schultz gives insights into the design process of a LTE MIMO antenna system fitting in a conventional antenna housing on the vehicle rooftop. Moreover, measurements are presented, which are obtained in a LTE live network measuring at the center frequency (796 MHz) of the operator's band.
- [30] 'System-Level Assessment of Volumetric 3D Vehicular MIMO Antenna Based on Measurement' by A. Posselt, A. Friedrich, L. Ekiz, O. Klemp and B. Geck evaluates the performance of a 3D MID cellular MIMO antenna and compares it to a reference antenna system with identical feed point positions. It is illustrated that the 3D antenna yields a higher mutual information and lower condition number, as it exploits the available antenna integration volume more efficiently.

Chapter 2

Antennas for Hybrid Radio Access

Hybrid antenna systems are currently not yet commercial state-of-the-art in the automotive industry. Vehicular applications requiring an Internet connection employ either the 2nd generation GSM standard or its successor the 3rd generation UMTS standard [6]. Ad-hoc based networks to connect the vehicle to the Internet via, for instance, WLAN outdoor access points APs or 802.11p RSUs are also in their infancy. Resulting from the increased bandwidth, scalability and largely reduced latency LTE the 4th generation of cellular communication systems attracts increased attention by the automotive industry [25]. Especially newly developed applications for electrical vehicles, such as intermodal route guidance [31] determining the fastest mode of transportation, benefit from the characteristics of LTE. To achieve higher bandwidths LTE is able to use up to four antennas simultaneously [32, pp.131]. Its evolution LTE-Advanced (LTE-A), which is currently in standardization allows even higher data rates of up to 1 Gb/s using a bandwidth of 100 MHz [25]. Whether diversity or SMX is used for the transmission depends on the network state, such as the load, on the agreed QoS class [33] and on the capability of an antenna system to support the transmission scheme in the respective channel [32, pp.131].

In the ad-hoc domain IEEE 802.11p has gained attention in recent years especially for vehicular connectivity applications [26]. In comparison to LTE the ad-hoc standard 802.11p, is primarily intended for safety or traffic efficiency applications. For 802.11p communication a two antenna system is envisioned to increase the reliability of the transmission and to compensate for integrational impairments mounting such an antenna systems on the vehicle [3]. Thus not for increased data rates due to the use of SMX as transmission scheme. As the transmission schemes vary between the access networks 802.11p and LTE, a different benchmark methodology is applied to the corresponding antennas.

In the first part of this chapter methodologies for evaluating LTE antenna systems are reviewed and rated according to their accuracy and practicality. It is analyzed by which KPIs the current specification sheets for vehicular antenna systems have to be expanded to ensure that the supplied MIMO antenna systems are properly performing. Measurement as well as simulation-based approaches are reviewed, with a focus on measurement-based approaches. The proposed measurement-based methodology is

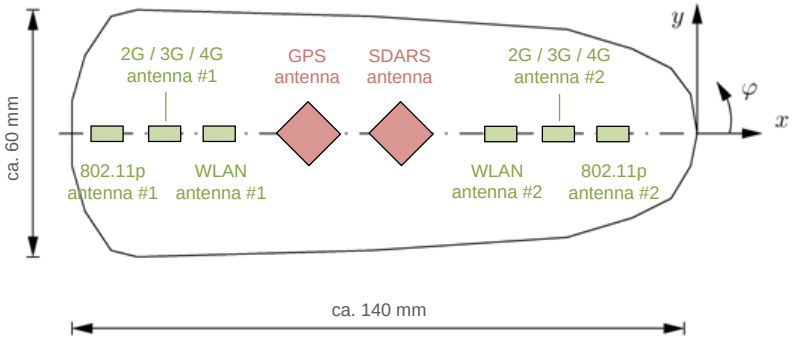

Figure 2.1: Antenna system offering MIMO for relevant communication standards.

feasible to be applied regardless of the carrier frequency, which in case of LTE varies between countries. The evaluation of the methodology performed in Chapter 4 is carried out in the frequency Band 20 (791 MHz - 862 MHz) in Germany [32], as this is in regards to antenna isolation of a compact MIMO antenna system the worst case scenario. Differences in performance of the analyzed prototypes are thus feasible to be visualized best in this frequency band.

In the second part of this Chapter a benchmark and ranking methodology is introduced for 802.11p antenna systems, to assess them in regards to the achieved diversity efficiency. A set of KPIs is proposed to be defined in future antenna specification sheets. It is also discussed in which way the antenna performance is likely to be evaluated with the help of measurements in the 5.9 GHz band. The suggested approach is applied in Chapter 4, where 802.11p antenna prototypes are benchmarked. Furthermore, an approach is introduced to reduce the impact of the antenna housing on the performance of antennas systems working at the frequency band of 5.9 GHz. A simulative approach is proposed to determine the impact of improvements on component level to the overall system level performance. In the last part of this Chapter the component level KPIs applied for cellular as well as 802.11p systems are discussed.

2.1 Benchmark of Cellular Antennas

Currently MIMO-qualified antennas are fairly new to the automotive industry. Thus current specification sheets for antenna systems include, in most cases, KPIs for single input single output (SISO) systems only. The predominantly requested KPIs and characteristics for such antenna systems, excluding thermal, mechanical and electrical characteristics are:

- a broadband antenna matching of at least 10 dB, covering all the required cellular frequency bands in the country, where the vehicle is sold
- a radiation efficiency of at least 70 %
- an omni-directional antenna pattern having a gain of at least 0 dBi for the required cellular frequency bands

A potential antenna system has to fit in the integration volume of approx. 60 mm × 140 mm × 70 mm (width, length, height) on the vehicle rooftop, see Figure 2.1. Other constraints for the design of cellular antennas result from sharing the integration volume with further antenna systems for location services, such as GPS or antennas for broadcast services like Satellite Digital Audio Radio Services (SDARS) [34, pp.175]. The antenna systems also vary depending on the country, where the vehicle is sold. Designing entirely different antennas for each market is, considering the arising cost, out of the question. It is more likely that the antenna systems are designed in such a way, which allows to add or remove antenna systems according to the market requirements. In order to support SMX in LTE at least one further antenna has to be added. LTE is able to support up to four antennas [32, pp.131]. However, such complex systems are currently not in the primary focus of the CE device or the automotive industry. The KPIs and characteristics included in current specification sheets are applicable to the second antenna as well. However, none of these KPIs describe the degree to which MIMO antenna systems support SMX [7]. It is possible to define thresholds for antenna coupling and correlation, but it is unclear how these KPIs translate into an increase in system performance in the highly dynamic vehicular environment. The interaction of all antenna KPIs on component level is complex, which makes ranking different MIMO antenna systems from various suppliers difficult. Considering that requesting high thresholds for KPIs in antenna specification sheets potentially results in higher research and production cost, defining a reasonable and sufficient threshold for KPIs is of great importance. Consequently, it is key for the evaluation and benchmarking of MIMO antenna systems that KPIs on system level are defined, which describe the end-to-end link quality, see Figure 2.2. Such KPIs are potentially the data rate or the latency of the communication link, which are also perceivable by customers. A further requirement is to ensure that the selected KPIs for antenna specification sheets are reproducible. In order to fulfill the dynamic requirements of the vehicular environment, it is thus advantageous to perform such system level evaluations always under the same conditions. Figure 2.2 illustrates the concept of component level as well as system level evaluation and shows KPIs for benchmark of antenna systems. Besides the given selection of system level KPIs a further analysis of KPIs is presented for the access networks LTE and 802.11p in [15]. KPIs on component level are discussed further in Section 2.3 and summed up in Table 2.1. The suitability of power related physical layer KPIs for antenna benchmark is investigated in Section 4.1.2.

Three interfaces are indicated in Figure 2.2, where the evaluation and, consequently, the benchmark of antenna systems is possible. These locations include the antenna feed, the radio frequency (RF) frontend and the output of the signal processing taking place in the modem [7]. The industry-wide employed impedance and radiation level KPIs on component level are thus evaluated at the antenna feed. These KPIs or antenna characteristics include, as mentioned, the reflection loss, radiation efficiency, antenna gain and the radiation pattern. The RF frontend is the first interface within the link, where the impact of impedance and radiation level KPIs is feasible to be assessed on system level. KPIs at the RF frontend include, for instance, the employed modulation scheme or signal strength related KPIs, such as received signal

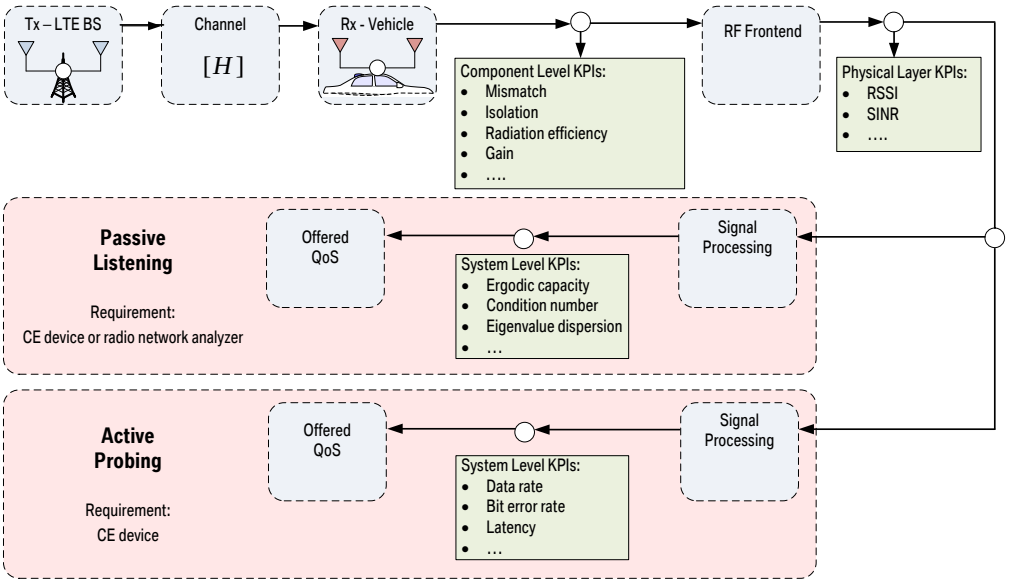

Figure 2.2: Component and system level benchmark methodology of MIMO antennas.

strength, signal-to-noise ratio (SNR) or signal-to-interference-plus-noise ratio (SINR). It was shown in [6] that the SINR values relate well to the achieved throughput thus enabling to gauge the link performance. An extensive discussion of further KPIs for the LTE access network is found in [15]. The subsequent signal processing interface offers access to KPIs, which are suited to be directly used for determining the offered QoS of the connection. Accessible KPIs include, for instance, the data rate, frame error rate, latency and many more, which depend on the specific application or the access network [15]. Considering LTE as access network the available KPIs at the signal processing interface also depend on the employed measurement methodology, see Figure 2.2. Active probing, also called active measurements in this work, requires a subscription to an operator's network and a CE device. The accessible KPIs depend on the application running on the CE device and its capabilities. On the other hand using passive listening, also referred to as passive measurements, uses radio network analyzers to evaluate KPIs extracted from pilot symbols from, for instance, the LTE base stations. The pilot symbols are send periodically by base stations [35] and are thus part of the signaling traffic in LTE. They enable CE devices to estimate the channel and report results for the purpose of scheduling of network resources back to the operator [35]. Devices such as radio network analyzers, are capable to make use of the pilots to gauge the quality of the communication link without being a subscriber of the network. Considering that a better performing MIMO antenna systems has, in case of SMX, better decorrelated sub-channels, the channel estimation is likely to be used as means of antenna benchmark [7]. Naturally comparing the complex elements of the estimated channel is not feasible. Thus KPIs have to be derived from the channel matrix to allow comparing measurements obtained with different antenna systems. As KPIs it is proposed in [7, 27] to use the condition number (κ), which is the quotient of the lowest and highest singular value, see Eq. (2.1). In Eq. (2.1) σ_{max} and σ_{min} are the maximum respectively the minimum singular value of the channel matrix. The condition number κ is interpreted as the noise enhancement of a zero-forcing receiver [36, 37].

$$\kappa = \frac{\sigma_{max}}{\sigma_{min}} \qquad (2.1)$$

$$ED = \frac{\left(\prod_{i=1}^{K} \lambda_i\right)^{1/K}}{\frac{1}{K} \cdot \sum_{i=1}^{K} \lambda_i} \qquad (2.2)$$

Another suggested KPI is the eigenvalue dispersion (ED) of the channel matrix, which takes into consideration all eigenvalues, see Eq. (2.1). The main difference between ED and κ is that κ takes into consideration only the maximum and minimum singular values. Thus for systems employing arrays with more than two antennas κ potentially yields less relevant results, as always only two singular values of the channel matrix are analyzed. As, however, only two antenna MIMO systems are considered, either of the aforementioned KPIs are feasible to be used for the benchmark without encountering imprecise measurements. As the employed measurement equipment[1] only allows to evaluate the condition number during the drive test, solely κ is used in the following to have a better reference between the values during the measurements and the location they are gathered.

As further KPI the mutual information (C), Eq. (2.3), is evaluated. The mutual information is an indicator close to the capacity according to Shannon [39]. In comparison to determining the capacity with an application performing down- or uploads of large data files, the mutual information yielded from the channel matrix is more suitable for antenna benchmarking, since it is independent of a specific application having its own measurement methodology [40]. Moreover, as discussed in the forthcoming Section 2.1.2 the mutual information is also independent of any influences on the ongoing traffic on the operators network or on the employed server for up- and download. All of the aforementioned KPIs are applied and discussed in Chapter 4, where prototype antennas are benchmarked and ranked.

$$C = \sum_{i=1}^{K} \log_2 \left(1 + \lambda_i \cdot SINR\right) \qquad (2.3)$$

An alternative approach to benchmark antenna systems is to use simulations. Simulations are advantageous in comparison to measurement campaigns as they allow exact reproducibility of the results. As measurements campaigns are subject to changes in the traffic flow or the environment, multiple measurements are essential to assess their correlation and thus the reliability of the results. Although simulation do not suffer from this drawback building an accurate simulation model for assessing the performance of antenna systems in different environments, such as rural, urban and suburban is time consuming and complex. The complexity arises mostly from modeling rich scattering environments as found in urban and suburban environments, which are key in the MIMO antenna benchmark [41]. Furthermore, in order to perform an antenna benchmark on system level, a simulative approach requires a full, 3-dimensional characterization of the antenna radiation pattern on the vehicle rooftop. Otherwise effects arising from integrating the antenna system on the vehicle rooftop are not taken into consideration. Nevertheless, once the simulation model with a propagation environment for cellular systems and a mobility model for the

[1] Rohde & Schwarz TSMW universal radio network analyzer [38]

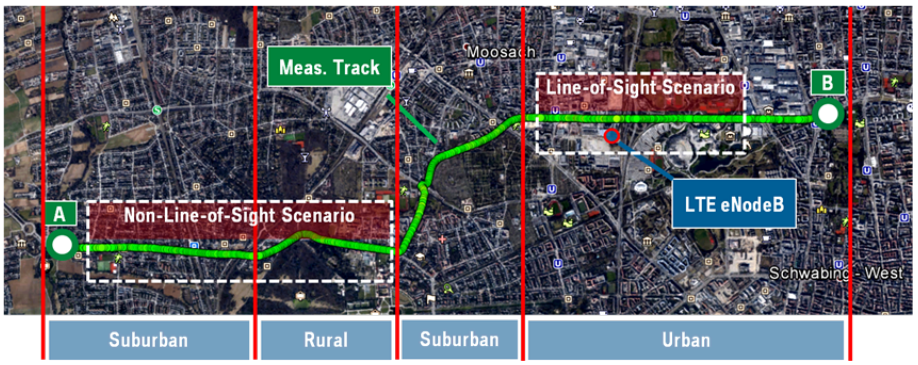

Figure 2.3: LTE 800 MHz drive track bearing different channel conditions, cf. [44].

vehicles is designed, benchmarking of antenna systems is able to be performed with less effort by the end-user. Publications, such as [42, 43], show that the results from simulations are reliable by verifying them with measurement drives. In [42] it is also pointed out that such simulations do require extensive computation resources. However, compared to measurements, where just gathering the results for one antenna system requires two engineers, one driving, the other one measuring, with a time effort of at least two business days, simulations are a non-negligible alternative, see also Chapter 4. For cellular antennas a simulation-based approach is not pursued in favor of measurements. This is resulting mainly from the fact that the simulation environments available for this work, such as FEKO [43], currently do not allow to evaluate the channel matrix of the transmission. Moreover, to validate the results with measurements a model of the environment in the reception area of the base station is necessary.

2.1.1 Measurement Methodology

The measurements to benchmark cellular antennas are carried out in a live LTE network, which is served by one 800 MHz LTE base station, utilizing dual-polarized antennas. The test track, see Figure 2.3, covers sections with urban, suburban and rural environments at the vehicle end, cf. [44]. The measurements presented in Chapter 4 were conducted at 796 MHz, which is the center frequency of the operator's LTE band. The route for the measurements includes both LOS conditions (when the vehicle is nearby the base station) and non line of sight (nLOS) conditions (when the vehicle is further away from the base station). This enables to evaluate the antenna systems under different channel characteristics. The start and the end point of the measurement track are denoted with the letters 'A' and 'B'. Depending on the driving direction, the notation Route AB, respectively, Route BA is used. Measurements, which are carried out in a live LTE network are subject to shadowing periods due to other vehicles and waiting periods at traffic lights to name a few incidents [45, 3]. Such effects need to be compensated to a sufficient degree to ensure reliable and reproducible measurements. Moreover, in order to compare consecutive measurement runs the effect of small scale fading has to be filtered out as well. In [46] it is proposed that a spatial filtering is carried out over nine wavelengths to ensure that the channel

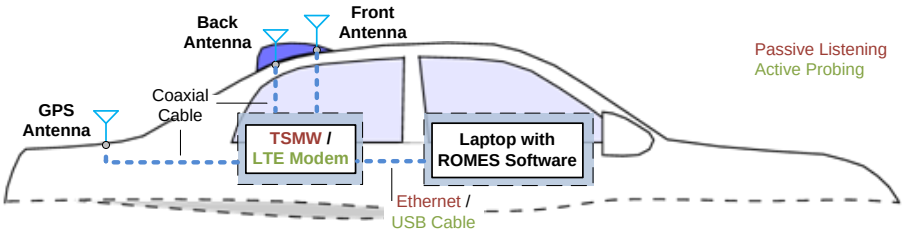

Figure 2.4: Setup for active and passive measurements.

still fulfills the wide-sense stationarity condition. At 796 MHz nine wavelengths results in a distance of approximately 4 m, which poses difficulties considering the employed GPS receiver's accuracy. According to [47] the mean accuracy of commercial of the shelf GPS receivers is around 8 m, which is double the required accuracy. Furthermore, the radio network analyzer TSMW [38], which is used together with its corresponding measurement software ROMES[2], allows only to record two measurements per second. Considering that even at 30 km/h only one measurement is recorded every 4 m, even if the GPS accuracy is potentially higher, the equipment does not allow to obtain enough measurement data to correct for small scale fading. So in order to correct for small scale fading and thus average measurement data over 4 m, it is either necessary to drive below 30 km/h or to use measurement equipment being able to record more data during one second. Consequently, with the current measurement setup it is not possible to correct for small scale fading within a city unless on a closed track, where a lower speed than 30 km/h does not interfere with the traffic. However, considering that the performed antenna benchmarks are relative comparisons between antenna prototypes and a reference system, not being able to correct for small scale fading is not a considerable drawback. All obtained results include similar effects and thus ranking the antenna systems between one another is still feasible to do. In order to correct for waiting periods at traffic lights or other traffic incidents, it is proposed to take measurements every 10 m into consideration when post-processing. A distance of 10 m is approximately twice the length of the measurement vehicle. Consequently, such an interval allows that no cluttering of the measurements occurs when the vehicle is moving slowly or stopping at traffic lights. Performance evaluations of MIMO LTE antenna systems primarily in terms of the maximum achievable data rate have already been carried out in multiple publications, such as [6, 49, 50, 51, 52]. To better illustrate the measurement setup employed in this work the active probing and passive listening approaches are presented in Figure 2.4. The main difference in the setup is that in case of passive listening the radio network analyzer is connected to the illustrated laptop via an Ethernet cable, whereas for a active measurements the CE is attached using an Universal Serial Bus (USB cable). The antenna under test is connected either to the CE device or the radio network analyzer depending on the used assessment methodology. The measurement software requires that the GPS antenna is always connected to the radio network analyzer for evaluating the GPS signal, even when carrying out active measurements with a CE device. In this case pilots of the LTE base stations are not picked up, the network analyzer goes idle.

[2]ROMES4 Drive Test Software v4.69 [48]

2.1.2 Active and Passive Measurements

The benchmark of cellular antenna is likely to be carried out, as mentioned in Section 2.1, using active probing or passive listening measurements, see also [15]. Radio network analyzers are due to the missing subscription to an operators network only able to perform passive measurements. On the other hand CE devices are feasible to be used for passive as well as active measurements. Active probing measurements are, in general, common tools for consumers to determine their data rate of their Internet connection [40]. For such measurements it is common to down- or upload large data files to determine the data rate of the transmission. Small files are mainly used to determine the round trip time of the transmission i.e. the time span between sending a file and receiving an acknowledgment of its reception. Active probing measurements are carried out with LTE qualified CE devices with a USB port. The CE device intended for the measurements needs to be selected according to the compatibility with the employed measurement software [48], so that the required KPIs are able to be extracted. Further restrictions result from the modem of the CE device being accessible and the ability to deactivate the internal antennas. Thus in order to perform benchmark measurements a prospective device has to support SMX with at least two antennas and be equipped with external connectors for the vehicular antennas. For such devices a subscriber identity module (SIM) card is needed in order to connect to the network of the operator. Regular consumer SIM cards have the drawback of offering limited data plans or bandwidths. Thus for the purpose of reliable measurements SIM cards with no such limitations are essential. A further requirement is that such measurements necessitate the use of a server for the purpose of performing up- and downloads as stated in [40] and illustrated in [6]. Such servers need to contain data files, which are large enough so that completing the transfer is not achievable during one measurement drive. Using smaller files causes inaccuracies in the determined data rate, as once a file download is completed it takes time until the next download is initiated even if the process is automated. Such interruptions likely lead to momentarily drops in the data rate and thus cause misleading results. Moreover, it has to be ensured that the used server does not limit the bandwidth of file transfers and all its bandwidth resources are allocated to the measurement. Thus ideally a server has to be used, which is only intended for the measurements. Consequently, in an ideal scenario such evaluations have to be carried out on a closed test track, where the serving base station does not allow other users to connect to the network. The disadvantage of such closed facilities is that their use is in most cases expensive and they are located in isolated areas, where the environment is mostly rural. Thus such settings are inadequate for the end-to-end evaluation of performance limits of antenna systems with varying vehicle velocities in different scattering environments. Nonetheless closed facilities, where the environment is controllable, are advantageous, if fixed angular relations between the base station and vehicle antenna need to be analyzed, for instance, in the design phase. Considering, however, that users potentially use connectivity services in urban, suburban and rural environments, the antenna performance has to be evaluated also in these environments. This necessitates for obtaining reproducible antenna benchmark results that the evaluation is carried out under single user conditions on

a test track as shown in Figure 2.3, where all network resources are allocated to the measurement. Another possibility is to obtain the results with a guaranteed QoS from the network operator. Taking into consideration that the antenna benchmark results presented in Chapter 4 take up to two days to collect for a single antenna system, both possibilities seriously deteriorate the network performance for other users making it infeasible from a network operator's point of view. Even if an agreement is found with the network operator, such as performing the measurements during the night, the antenna benchmark results are gathered with consumer electronic (CE) devices, which is not their primary functional purpose. Although they come closest to the perceived quality of the user, their measurement uncertainties are higher compared to, for instance, a radio network analyzer from an electronic test equipment manufacturer, cf. [38]. In Release 9 of the LTE standard it is defined that CE devices are allowed an inaccuracy of at least 6 dB to comply with the standard [53], whereas the employed network analyzer has an accuracy of around 1 dB [38]. Naturally evaluating an antenna system under the conditions of how consumers perceive such systems is important, but for accurate benchmark of antenna systems from different suppliers active measurements are not feasible. Another drawback resulting from the use of CE devices is that the full set of relevant KPIs from CE devices is only available with special diagnostic software from the chipset manufacturers. For instance, the estimated channel matrix, which is used for reporting back the determined channel quality to the base station [35], is for chipsets of the manufacturer Qualcomm only accessible through its proprietary software [54]. In addition, KPIs, such as the signal power, which are accessible through the chipset drivers [55] are given only as the mean of the antenna system and not for each antenna separately. Thus analyzing the antennas separately is not possible, unless a proprietary software from a chipset manufacturer is used [54]. Having to use proprietary software to access KPIs derived from the channel matrix increases the difficulty to analyze the MIMO performance of the antenna system. A further disadvantage results from the diagnostic software likely not being implemented in a commercial measurement systems for drive tests. Thus using CE devices for passive measurements is not feasible. Considering the discussed drawbacks of active and passive measurements for the benchmark of cellular MIMO antenna systems, it is proposed to use radio network analyzers being only capable of passive measurements. The analyzers need to offer, as in the case of CE devices, two channels for 2x2 MIMO antenna evaluation. As the measurement equipment determines its KPIs based on pilot signals from the base station and by scanning the signal power on selected frequencies [38], the data rate of a transmission is not possible to be determined. Nevertheless, the end-to-end link quality is feasible to be described with the mutual information as an indicator close to the capacity according to Shannon [39, 56, 57]. The greatest advantage of passive listening measurements is that they do not require a connection to the network of an operator, as the pilot signals used for evaluation are exchanged in any event between the base station and the CE devices. Thus no SIM card is necessary and the evaluations are capable to be carried out without feedback from the network operator. Consequently, no attempts have to be made to have all network resources allocated to the measurements.

2.2 Benchmark 802.11p Antennas

Antennas for 802.11p working at 5.9 GHz are currently not deployed in vehicles. Thus also specification sheets for these antenna systems are also not available. However, due to the emphasize on the diversity transmission scheme to increase the robustness of the link, see [58], most of the specifications from singular cellular antenna systems are suitable to be reused, see Section 2.1. Consequently, KPIs, such as the reflection loss, radiation efficiency and antenna gain are applied to these antennas as well. To ensure reliable communication links regardless of the direction an omni-directional radiation pattern is also key. As multiple antenna systems are applied for 802.11p systems to improve the communication link by redundancy, KPIs for evaluating the SMX capability, such as κ and ED, are not suitable for the antenna benchmark in this case. Investigation into the channel characteristics of the 5.9 GHz frequency band of 802.11p [45] and antenna systems revealed that the transmission is subject to performance deterioration due to the high operating frequency. The performance deterioration on the vehicular end is resulting from the finite size of the vehicle roof, roof curvatures, insets and the antenna housing. The deteriorating effect of these characteristics was explored by means of simulations and measurements in multiple publications, such as in [10, 59, 60, 9]. To illustrate the impact of the aforementioned effects on the communication link research into a link budget was performed in [61]. Accounting for the aforementioned effects by performing measurements, it was found that depending on the vehicle type and thus the roof characteristics a mean range reduction of 20 % occurs, see also Figure 2.5. Considering also sun rooftops the range was shown to be further decreasing by 23 %. Adding the losses of the antenna housing (7 %), the antenna position on the roof (5 %) and the cable losses (5%) the total range reduction yielded 60 %. In other words only 40 % of the initial communication range was determined to be remaining for any application running on 802.11p, in case no countermeasures are taken. The aforementioned performance deteriorating effects are the main reason to use a diversity transmission scheme to increase the robustness of 802.11p communication. The antenna systems are deployed in such a way that one antenna primarily covers the front and the other the rear of the vehicles. As the resulting efficiency from using a two antenna diversity system is key in regards to the deployment of reliable safety applications [58, 62], the diversity gain is an essential KPI for the benchmark of 802.11p antenna systems. The evaluation of different 802.11p prototype antenna systems carried out in Section 4.2 is thus exploring the signal strength of both antennas separately and the maximum signal strength of both $max\{SNR_1, SNR_2\}$. In addition to maximal-ratio combining as diversity scheme

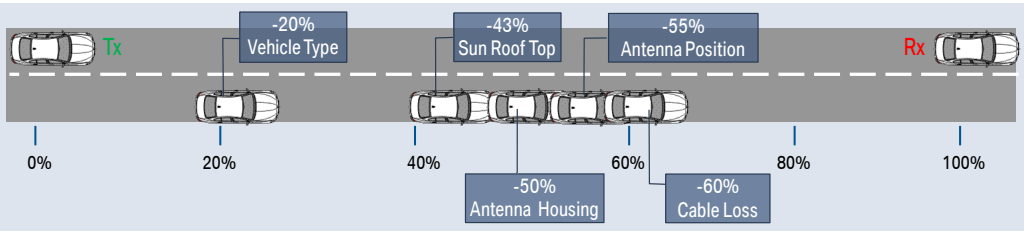

Figure 2.5: Range Reduction in 802.11p communication.

also selection combining is considered [63]. The employed urban testsite is located at the BMW Research and Technology headquarters in Munich, see Figure 2.6(b). The topology of the testsite, see Figure 2.6(a), shows that it is equipped with five outdoor WLAN access points, which are capable of the standard 802.11g. Each outdoor WLAN location also offers one omni-directional 802.11p antenna, which is pointing upwards, whereas the 802.11g antenna are directed downwards, see Figure 2.6(b). The 802.11p antennas are omni-directional antennas with a gain of 6 dBi [64]. The WLAN antennas also have an omni-directional characteristic and a gain of 5.2 dBi [65]. The corresponding radios, not shown in the Figures, are placed indoors. In case of 802.11p three radios are available, which are able to be mounted at either one of the locations. Not equipping all locations with 802.11p radios simultaneously allows to rate the antenna performance in areas with low signal strength without reducing the signal power of other RSUs. As such it is possible to rank different antenna systems based on their diversity efficiency in low as well as high signal conditions.

Evaluating the diversity efficiency in a testsite, such as the one seen in Figure 2.6, is a suitable means to determine the overall system-oriented antenna performance. However, in most cases, the antenna performance is only evaluated in certain regions of the radiation pattern. Thus for more or less fixed angular relations between the vehicle and the RSU. Moreover, is the accuracy of the antenna assessment subject to the used 802.11p modem and the surrounding vehicles, which potentially cause shadowing. As such, for instance, the impact of distinctive nulls in the radiation pattern on the system level performance is likely difficult to be identified. Thus measurements in a chamber are key to determine the antenna pattern on the vehicle rooftop in order to ensure that safety messages are likely to be received regardless of the direction of the impinging wave front. Consequently, evaluating the antenna radiation pattern in addition to the diversity efficiency is key in the benchmark of 802.11p antenna systems, see Section 2.3. Such measurements are suited to be carried out in a variety of test environments. A common and in regards to the measurement costs feasible way to determine the radiation pattern is in a semi-anechoic chamber. Compared to a fully anechoic chamber the floor of the chamber is not covered with absorbers. In order to save costs by not equipping the walls with absorbers as well some facilities are located in a free space environment with no scatterers in the surrounding. An enclosure, which is made from a material not attenuating the transmitted electromagnetic signals, is protecting the site against environmental influences. The measurements in such facilities are usually carried out in the near-field and are then transformed to the far-field [59]. The system level evaluations presented in Chapter 4 are obtained in such a chamber. Another possibility for such evaluations is to characterize the antenna with spherical near-field antenna test systems [66]. The vehicle is placed in an fully anechoic chamber allowing to investigate the antenna characteristics with virtually no effect from its surrounding. The measurements in such chambers are thus not only the most accurate but also the most expensive way of researching vehicular antenna systems. Consequently, specifying such measurements in a call of bids for suppliers is potentially not feasible. Therefore in addition to defining KPIs for accurately assessing the performance, it is essential to select KPIs, which are likely to be obtained with reasonable efforts.

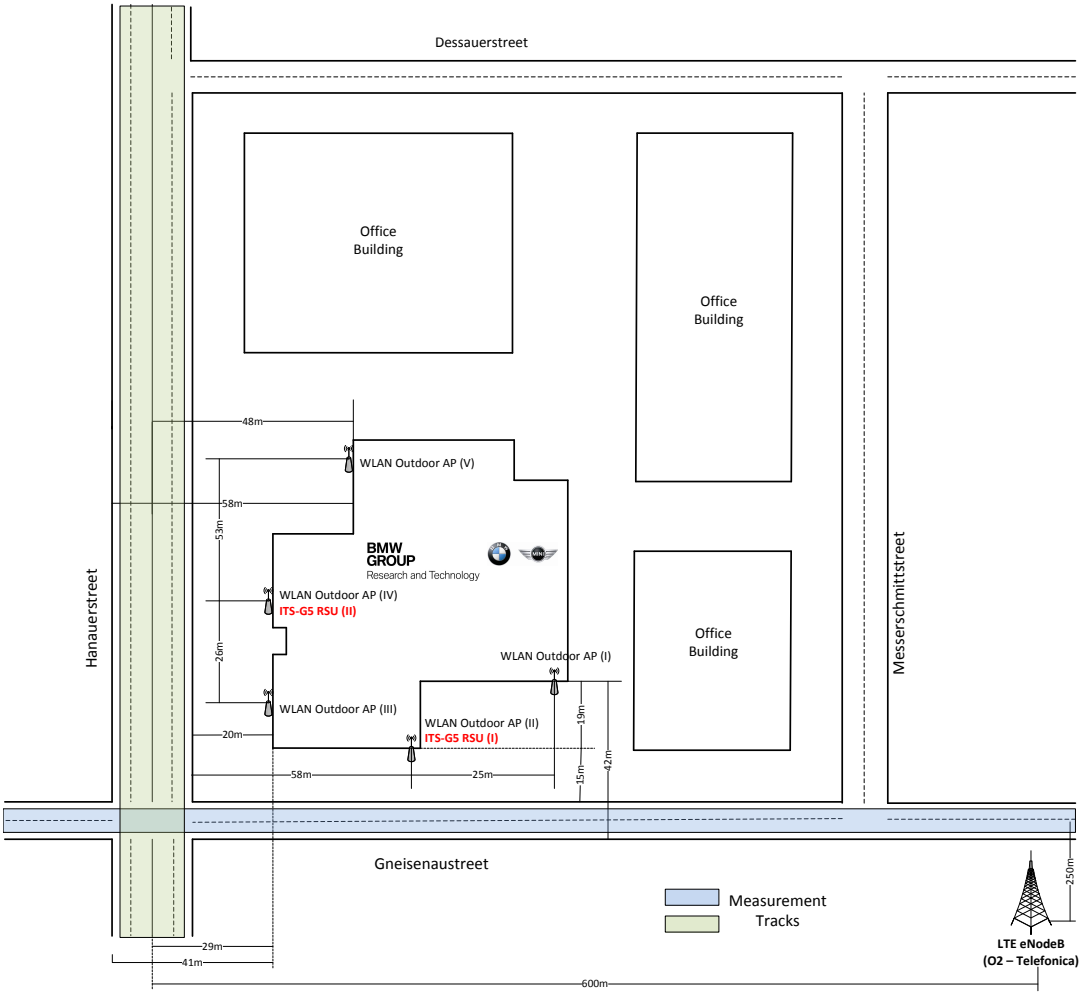

(a) Topology of the hybrid testsite.

(b) Surrounding and the employed RSU antennas of the testsite.

Figure 2.6: Topology and the surrounding of the hybrid testsite including the access networks IEEE 802.11p, WLAN 802.11g and the cellular network LTE.

2.2.1 Radiation Pattern Optimization

An omni-directional antenna pattern in addition to the diversity efficiency is key for the benchmark of 802.11p antenna systems. Performance deterioration caused by, for instance, the vehicle sunroof or the roof curvature are difficult to compensate in an ongoing production cycle by attempting to change exterior of the vehicle. However, compensating deteriorating effects of the antenna housing [10] is straightforward, as only modifications of the housing are required. The currently deployed dielectric antenna housings, which protect the rooftop antenna against environmental influences, consist of PC-ABS (Polycarbonate-Acrylnitril Butadien Styrol) material having a dielectric permittivity in the order of magnitude of 2.9 and dielectric loss tangent in the order of magnitude of 0.005, see [28]. The physical dimensions of antenna compartments used for BMW vehicles typically covers a volume of $(l \times h \times w) \simeq (190 \times 60 \times 50)$ mm. The size of the antenna housing is approximately in the range or a multiple of the free-space wavelength $\lambda_0 \simeq 50\,\text{mm}$ for 802.11p communication at 5.9 GHz. The performance deterioration thus results from wave reflections impinging e.g. at the bounding sidewalls of the dielectric antenna compartment, which lead to interactions with the directly radiated electromagnetic waves. Consequently, the resulting interference patterns exhibit geometry and frequency dependent behavior resulting from reflection and refraction effects inside the antenna housing [28]. Depending on whether the interference of the waves is constructive or destructive, publications, such as [60], have shown that a significantly deteriorated radiation pattern is yielded. Nulls in the pattern are occurring in areas with destructive interference, whereas the radiation power is amplified in areas with constructive interference. To compensate the effects of the antenna housing an approach was presented in [28]. By altering the thickness of the antenna housing it was achieved that the antenna radiation was directed from directions benefiting from constructive interference towards nulls. The advantage of this approach is that changes in the thickness of the antenna housing are feasible to be applied even during a running production cycle without any alterations to the exterior design of the vehicle. The approach is investigated in detail in Section 4.2.3, where the wall thickness of the antenna housing is modified to achieve a dielectric lens effect obtaining a radiation pattern with maximum pattern flatness at $\vartheta = 90^\circ$ in the $xy-$plane. It is also shown to which degree simplified geometrical shapes are likely to be used to model the impact of an antenna housing resembling a shark fin-shaped integration volume.

Another approach to compensate effects of the antenna housing, which is not investigated further in this thesis, is achieved by placing parasitic elements close to the antenna systems [67]. Such elements share the same grounding as the radiating antenna system. However, they are not connected to the antenna feed but rather are excited by the radiating antenna. By matching these elements to the frequency used to radiate they interfere, subject to their location, constructively or destructively with the field of the radiating antenna. Key to such an approach is to determine the quantity of required parasitic elements and place them in such a way to compensate nulls in the radiation pattern. Thus applying this approach requires a substantial

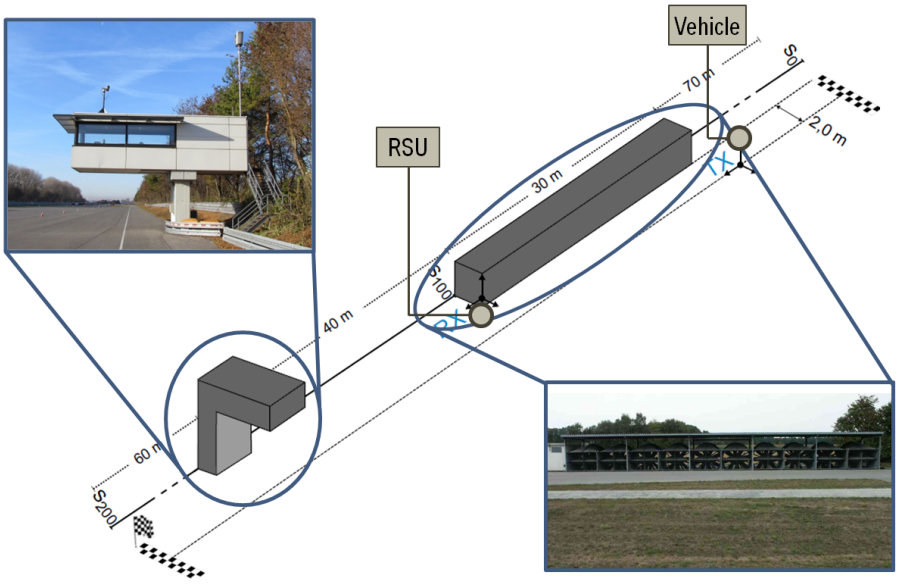

Figure 2.7: Modeled testtrack for simulation based antenna assessment.

redesign of the antenna systems to achieve the desired compensation. Within the design phase it also needs to be ensured that the parasitic elements do not cause any destructive interference to other antenna systems. Considering that the antenna systems, based on the frequency allocated for radio standards, vary between different markets such a parasitic elements approach potentially needs to be evaluated for all derivatives of an antenna system. Due to the adjustment to one antenna design the parasitic elements approach necessitates additional efforts, if, for instance, the supplier and thus the antenna design is changed. Considering the impact of such investigations on research cost and consequently on higher production costs, as more derivatives of one antenna have to be manufactured, this approach is not feasible.

2.2.2 System Level Simulations

An alternative approach to measurements to determine the impact of antenna integration aspects on system level, is performing simulations. Naturally measurements are essential for evaluating prototypical antenna systems, but evaluating each design phase by measurements is time consuming and thus costly. For 802.11p antenna systems, which have a lower communication range compared to most cellular systems [25], using simulations allows to substantially decrease the necessary efforts to assess the system level performance of such systems. In addition performing simulations allows to evaluate a range of different propagation environments, such as urban, rural or suburban within the design phase with less effort. Using measurements for such evaluations require either a fixed infrastructure or the use of mobile RSUs in each of these environments. Nevertheless also for simulations it is beneficial to choose environments, where the result are feasible to be validated later. In Section 4.2.3 the performance of 802.11p antenna systems is evaluated by simulations on a BMW testtrack including two building on the sides, cf. Figure 2.7. Both buildings are

approximated by simplified geometrical shapes being perfectly conducting and thus ideal scatterers. With the help of such a scenario a variety of antenna systems as well as different concepts of antenna housings are feasible to be evaluated. However, ahead of performing evaluations on system level, the antenna radiation pattern on the vehicle rooftop has to be obtained. It is key to gather the pattern on the vehicle rooftop and not on a generic ground to include all antenna performance degrading effects resulting from its integration. Multiple electromagnetic (EM) field simulators, currently available, offer to obtain such patterns. In this thesis the simulator CST Microwave Studio (CST MWS) [68] is used. The patterns are obtained using the transient solver of CST MWS with an automatic hexahedral and tetrahedral mesh generation. In case of system level simulations a hybrid solver approach including optical methods is required, as for a 200 m long test track about 4000 wavelengths at an operating frequency of 5.9 GHz have to be considered [69]. Even with state of the art computing resources a full electromagnetic simulation performed with, for instance, CST MWS is not feasible. A hybrid solver, such as FEKO [70, 71], which is used in this thesis, is essential. The hybridization implies that different solution techniques are applied to different parts of the same simulation model. FEKO hybridizes the current based method of moments (MoM) approach with the uniform theory of diffraction (UTD) [71]. For accuracy bidirectional coupling between the MoM and UTD is being maintained in the solution, i.e. modification of the interaction matrix. UTD being an asymptotic high frequency numerical method, which is also used in physical optics, is commonly applied where electrically large structures are considered [71]. However, currently the UTD numerical formulation only allows to be applied to flat polygonal plates with minimum edge length in the order of a wavelength or to single cylinders. The described approach to determine the impact of component level changes to the system level performance is carried out in Section 4.2.3. With the help of the simulations it is shown that an improved antenna housing substantially increase the efficiency of 802.11p antenna systems.

2.3 Component Level Analysis of V2X Antennas

The previous Sections on the benchmark of cellular and ad-hoc antenna systems revealed fundamental differences in the applied methodology to assess the system level performance. For MIMO cellular standards, such as LTE, it was derived that the antenna performance is best captured by KPIs assessing SMX capability of the antenna system. In contrast to cellular systems it was determined that 802.11p antennas are primarily assessed in terms of the achievable diversity efficiency. Although the system level KPIs upon which the antenna systems are benchmarked differ, the applied component level KPIs are the same. Considering, however, the specific services to be performed with the LTE and 802.11p antenna systems the importance of the component level KPIs varies. In both cases the antenna mismatch has to be as low as possible and antenna isolation as well as radiation efficiency as high as possible. However, an omni-directional antenna characteristic with high antenna gain is more crucial for 802.11p systems primarily intended for V2V safety

applications rather than for infrastructure based cellular systems. As regional performance degradation in the antenna radiation pattern likely leads to blind spots around vehicles statistical metrics for antenna benchmark is essential to quantify this degradation [72]. The crossing or outage rate ρ_{TH} gives an indication of the severity of this degradation. It is calculated according to Eq. (2.4), where the parameter N defines the increment upon which all angular values $0° \leq \varphi \leq 360°$ in the radiation pattern are swept. Naturally for benchmark of different antenna systems N has to be kept at the same value in order to ensure comparability of the results.

$$\rho_{TH} = \frac{1}{N} \cdot \sum_{i=1}^{N} (G_i | G_i < G_{TH}) \tag{2.4}$$

$$\rho_{Diff} = \frac{1}{N} \cdot \sum_{i=1}^{N} (|G_{main,N} - G_{aux,N}| \mid |G_{main,N} - G_{aux,N}| > G_{\delta}) \tag{2.5}$$

Perf. Ind.	*Antenna*	*Region*	*Perf. Ind.*	*Antenna*	*Region*
Mismatch	main	n/a	G_{max}	main	front
	aux	n/a			rear
Isolation	main-aux	n/a		aux	front
Radiation Eff.	main	n/a			rear
	aux	n/a	G_{min}	main	front
ρ_{TH}	main	front			rear
		rear		aux	front
	aux	front			rear
		rear	G_{mean}	main	front
ρ_{TH}	main	front			rear
		rear		aux	front
	aux	front			rear
		rear			

Table 2.1: KPIs for assessment of hybrid MIMO antennas.

As a further statistical metric the occurrence of gain differences below a threshold is defined, see Eq. (2.5). Evaluations in [6] showed that a difference in antenna gain of more than 6 dB led to a performance degradation in the LTE link and allowed only diversity as transmission scheme instead of SMX. Thus applying ρ_{TH} for cellular antenna benchmark allows to determine a potential deterioration in the SMX capabilities of the analyzed antenna system. The performance indicator ρ_{Diff} is also an important metric for 802.11p communication, as in this case it gives an indication on the achievable redundancy of the antenna system. As long as the gain difference of the main and aux antenna are small, the same safety messages are potentially picked up by them both.

In Chapter 4 the prototypical systems are analyzed separately for the LTE and 802.11p antennas. The antenna located in the rear of the prototypical system is referred to as the 'main' antenna and the one in the front is denoted the auxiliary

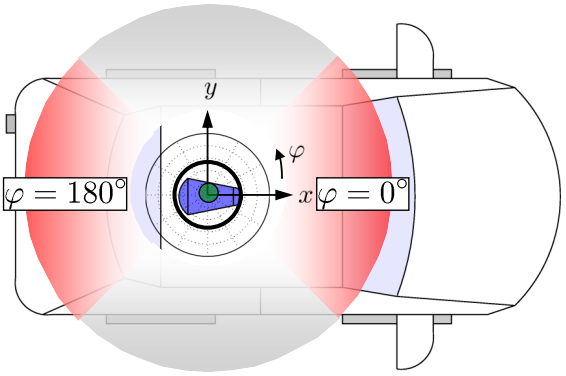

Figure 2.8: Regions to assess the antenna performance on the vehicle roof.

(aux) antenna. In case of LTE the main antenna covers all relevant frequency bands, whereas the aux antenna is in most cases designed only for the bands used for SMX transmission. This is resulting from the smaller integration volume in the front making it more efficient and less challenging to design the antenna. As mentioned before two antenna systems are also used for 802.11p communication to compensate for integrational impairments and to exploit diversity, see Section 2.2. Naturally increasing the number of antennas, as shown in [11], enables to take advantage of diversity even further, however it also increases significantly the investment costs. Thus the discussed prototypical systems in this work include only two 802.11p antennas. The main antenna is primarily intended to cover the rear while the aux antenna is designed predominantly for the front of the vehicle. To assess the direction dependent performance of the analyzed prototypical antenna systems the aforementioned gain related KPIs are investigated for the two regions of the vehicle. As the evaluations in [6] revealed a difference in SMX performance whether the vehicle was facing the base station with its rear or front, these two regions are distinguished as follows: Region I ($\varphi = 0° \pm 90°$) for the front part of the vehicle and Region II ($\varphi = 180° \pm 90°$) for the rear, see Figure 2.8. Both regions are also applied for the assessment of 802.11p antennas to better visualize the performance deterioration resulting from their integration on the vehicle rooftop. The KPIs ρ_{TH} and ρ_{Diff} are consequently evaluated for both regions separately. To have a complete picture of the antenna performance the peak gain values G_{min} and G_{max} are analyzed for both antennas in both regions as well. By evaluating these values on top of the level crossing rates the minimum and maximum occurring deviations in antenna gain are revealed. To obtain a full picture of the antennas without over- or underestimating the performance by taking the peak values into consideration also the mean value G_{mean} is investigated for both antennas in both regions. All previously considered KPIs on component level are summed up in Table 2.1. The KPIs are used in the forthcoming Chapter 4 to benchmark the LTE and 802.11p antennas.

Chapter 3

Service Delivery in Hybrid Networks

This Chapter focuses on improvements of the service delivery by using hybrid radio access, which is the second key topic of this thesis. The service delivery is investigated in the first part of this Chapter for vehicular infotainment applications and in the second part for safety applications. It is discussed that infotainment applications are user-centric, whereas safety applications are of a cooperative nature [15], where multiple users need to work together to ensure that the system works efficiently. Research into using hybrid radio access technologies especially for vehicular safety applications are not well explored so far. Related work for infotainment applications have, for instance, been carried out in [17]. It was shown that using KPIs from the backend of an OEM improves substantially handover decisions. Handovers within hybrid access networks are feasible to be optimized in such a way that throughput drops, thus a reduction in the QoS is prevented. As KPIs for deriving a decision on the network selection, the current network load and coverage maps of the access networks are considered from a backend. A similar approach is presented in [73], where the network load of the cellular access network UMTS is gathered to investigate data dissemination policies. A discussion of KPIs for handovers in hybrid radio networks and their corresponding weights is carried out in [74]. An approach to incorporate contextual information, such as user preferences and application requirements in vertical handover decision algorithms, is presented in [75]. The authors divide the presented algorithms in different groups based on the KPIs they incorporate and benchmark the algorithms in regards to the QoS they offer.

For vehicular safety applications [24] provides a good survey of available radio access networks and their aptitude to fulfill the necessary application requirements. It is discussed that cellular communication systems are suitable for applications requiring a long range V2I communication. For safety of life applications IEEE 802.11p is found to be suited, whereas for safety applications with relaxed delay requirements also cellular systems are considered to be apt. In order to make use of the merits of both access networks the research project *CONVERGE* [4] explores among other research interests to efficiently combine the cellular and ad-hoc domain. The combination of, in this case LTE and 802.11p networks, is pursued to meet the delay and communication range requirements of safety applications. Discussed use cases within the project include

the local hazard warning (LHW) and the wrong-way driver warning (WWDW) [14]. For a LHW a warning of a construction site in a highway scenario is considered. The WWDW is a special case of the LHW, as for this particular application the wrong-way driver is the hazard, which other parties have to be notified about. In both the general LHW and the WWDW the traffic incident has to be identified in a first step and in the next step distributed to the affected parties, see Figure 3.1. The identification of a hazard by the vehicle is in case of a construction site potentially not necessary, as it feasible that such a warning is broadcasted by the site itself. On the other hand in case of a WWDW [76] the wrong-way driver has to be identified in order to warn others of the particular incident. In *CONVERGE*, see Figure 3.1, the wrong-way driver is detected using a 802.11p based RSU. Naturally also cellular system or sensors at the drive-up way are feasible to be employed, however these are not considered in the *CONVERGE* project [14]. The particular research interest is on the second step, which is the distribution of the traffic incident or generally speaking the safety message. As shown in Figure 3.1 various options are available to distribute the safety messages using cellular or ad-hoc networks. In particular for cellular networks, such as LTE, also broadcast protocols like evolved multimedia broadcast multicast service (eMBMS) [77] are feasible to be used for message dissemination purposes. However, limitations in the vehicular environment potentially occur from the supported access networks by the vehicles.

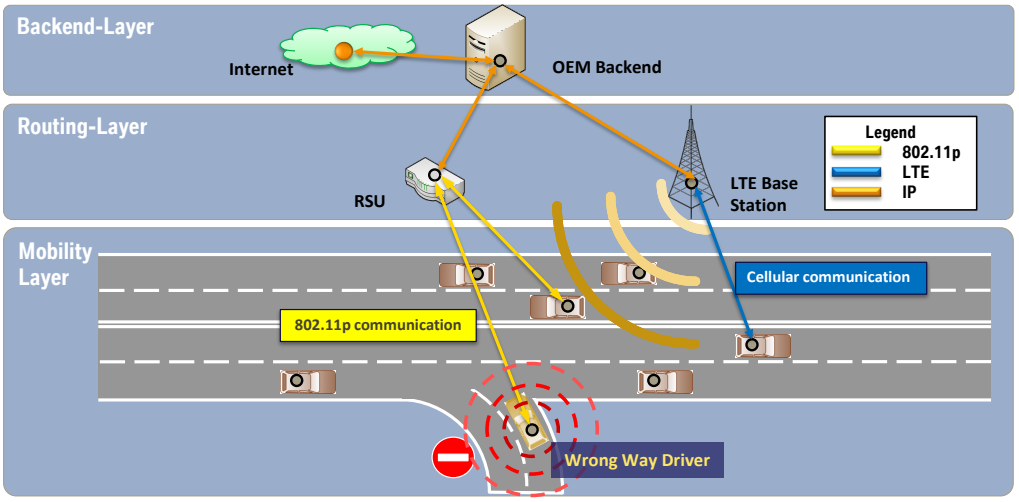

Figure 3.1: Wrong-Way driver warning using hybrid radio access [4].

The first part of this Chapter focuses on infotainment applications and KPIs for an improved network selection to yield an overall high throughput and no outages in the communication link. Moreover, are network selection algorithms introduced, which are used to derive the potential of KPIs from external sources to improve handover decisions. The second part of this Chapter focuses on safety applications. The additional value of using hybrid radio instead of a single access network to disseminate safety is elaborated. Furthermore, are various message disseminate policies discussed focusing on the combined use of LTE and 802.11p networks.

3.1 Infotainment Applications

Key for an improved service delivery for infotainment application using hybrid radio access are the considered KPIs for network selection and their assigned weights [18]. Section 3.1.1 gives an overview of the available KPI and differentiates them in two categories on-board and off-board. To satisfy the demands of the dynamic vehicular environment not only accounting for various KPIs is essential, but also the way in which these KPIs are included in network selection algorithms. Thus this necessitates a multi-criteria approach to incorporate the KPIs and prioritize them according to user and application demands, see Section 3.1.2.

3.1.1 Data Sources

In general data sources are feasible to be divided in on-board and off-board KPIs. On-board KPIs include values, which are collected by the electronic control unit (ECUs) of the vehicle. These ECUs include any kind of vehicular sensor data, such as the velocity, as well as measurements from the telematic ECU, which incorporates the modems of all access networks. These on-board KPIs are further categorized in whether they are obtained by active probing measurements, which cause additional traffic in the network, or by passively monitoring the ECU [15]. Naturally in case of vehicular sensor data all values are obtained by passive monitoring, as this information is read from the vehicle bus. Consequently, active probing measurements only relate to the telematic ECU. One of the most relevant vehicular sensor information for network selection is the previously mentioned vehicle velocity. Evaluating the current velocity enables to conduct a pre-selection of the access networks subject to the application or user requirements. WLAN networks, which have a limited range [78], are feasible to be filtered out at high speeds, since shortly after the vehicle is part of the network, it is most probably not in the range anymore. However, for high speeds even some cellular networks are potentially not the best choice. For instance, in the case of a storage intensive download application, selecting an access network offering an increased range, such as LTE at 800 MHz, is a better choice rather than UMTS working at 2.1 GHz. Due to the increased communication range of LTE the number of handovers is likely lower and thus the connection is potentially more reliable [75]. In case of lower velocities or even when the vehicle stops, for instance at traffic lights, WLAN networks offer the possibility to perform offloading of mobile data. Finding WLAN networks for such purposes is achievable by additional on-board data from the navigation system of the vehicle. As such WLAN APs are able to be considered as point of interests (POI)s, which are included in the navigation route. These POIs are likely to be used in addition to an on-demand selection of access networks for scheduling the transmission of certain applications, such as downloads of large files. Thus due to the scheduling of the transmission, as shown in Section 5.1.2, considerable transmission costs are feasible to be saved.

Besides vehicular sensor data on-board KPIs also include RF values of the access networks. RF values are aggregated on different ways: Recalling from Section 2.1.2

by passively monitoring an active connection, by scanning without transmitting any data packets or else by active probing. Naturally performing active probing measurements is, as discussed in Section 2.1.2, costly due to the generated additional traffic. However, in contrast antenna benchmark active probing [40] is only carried out for a short time frame, as only the momentary connection is of relevance. Nevertheless, the drawback of probing for a short time frame is that the results are likely to be accurate for only a limited time span. Still such measurements are for infotainment applications a feasible way to rate the performance of the momentary connection as long as such evaluations are not done repeatedly and consequently incur in high transmission costs. On the other hand just monitoring the ongoing transmissions or scanning radio channels is carried out anyway by CE devices to find networks to connect to or to report the quality of the connection back to the operator [35]. Consequently, using those results to determine the quality of the connection for infotainment applications does not require further resources. Evaluations, such as in [79], have shown that KPIs gathered in such a manner, like the SINR values, are reliable performance metrics to assess the quality of the communication channel. However, the available RF values depend on the modem of the access networks, thus by monitoring or scanning it is possible that the required KPIs to rate the channel are not accessible.

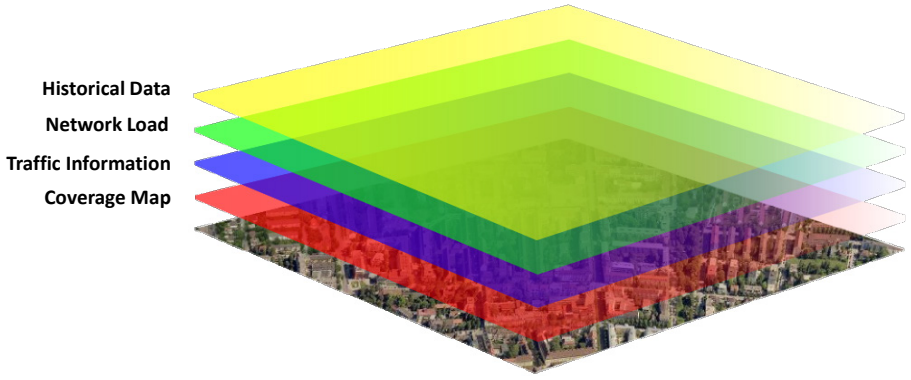

Figure 3.2: Off-board KPIs for network selection.

Thus additional KPIs, see Figure 3.2, have to be considered to enable a reliable network selection [15]. These KPIs are accessible online and are either aggregated over different vehicles or are yielded from additional data sources, such as from network operators. Aggregation over different vehicles also known as floating car data (FCD) is, for instance, currently used to gather information on the traffic flow, thus to provide better navigation routes for vehicles. Alternatively to the traffic situation FCD also potentially comprises information on the network connection of the vehicles, such as the results of active probing measurements or monitored transmissions. Similar to the traffic condition those KPIs on the current network conditions are feasible to enable a better informed network selection. An even higher potential of such aggregated KPIs is achievable, as shown in Section 5.1.2, if historical data and network coverage maps from a backend are considered for the access network selection. Historical data comprises monitored or scanned KPIs, which are in general aggregated over a longer time frame by different vehicles. By mapping such time

related aggregated historical data on the traffic grid the network conditions are likely to be predicted, to ensure that preferably networks offering in general a better performance are selected. Consequently in, for instance, a traffic congestion occurring always at the same downtown area during rush hour, the network condition are feasible to be anticipated and measures taken beforehand. Such a measure is that data intensive applications perform downloads before the area is reached or that networks in that area are in general avoided. In Section 5.1.2 an intelligent, transmission cost reducing download application is considered, where based on historical data, access networks, which are overloaded, are neglected from the network selection. Besides historical data network coverage maps, potentially bought from network operators, are also an additional way to further improve the network selection.

3.1.2 Network Selection Algorithms

Recently, various vertical handover decision algorithms (VHDAs) have been proposed by different research groups for infotainment applications [18, 75, 74]. The differences between the algorithms arise from the KPIs they take into consideration, the way the selection is derived and the targeted optimization. A comparison of different network selection algorithms is provided in [20]. The authors show that the selection of the algorithm is not the most crucial factor for network selection but rather the prioritization of the included KPIs.

$$(RSS_{serving} < T_{HO}) \cap (RSS_{alt.} > RSS_{serving} + H) \tag{3.1}$$

Traditional VHDAs, employed predominantly for horizontal handovers between wireless networks using the same technology, take only RSS values into consideration [80]. The handover decision is initiated, if the RSS value of the current access network $RSS_{serving}$ is lower than the pre-defined threshold T_{HO} and the RSS value of the alternate network $RSS_{alt.}$ is higher than the one of the current access network plus a hysteresis margin H. Such an algorithm is, for instance, expressed in Eq. (3.1).

Data: RSS value
Result: Network with superior RSS value
while *on the way towards destination* **do**
  Determine $RSS_{serving}$;
  Determine alternate network with highest RSS value;
  Normalize RSS values;
  Assign the highest RSS value to $RSS_{alt.}$;
  if *(*$RSS_{serving} < T_{HO}$*) and (*$RSS_{alt.} > RSS_{serving} + H$*)* **then**
    Perform handover to an alternate network;
  else
    stay connected to the current network;
  end
end

Algorithm 1: Pseudocode of the RSS algorithm from Eq. (3.1).

Data: Throughput, RSS, CPU load, power consumption
Result: Ranking matrix of all networks
while *on the way towards destination* **do**
  Determine $RSS_{serving}$;
  Determine RSS values of alternate networks;
  Normalize RSS values;
  while *alternate networks available* **do**
    Assign the highest RSS value to ($RSS_{alt.}$);
    if *(*$RSS_{serving} < T_{HO}$*) and (*$RSS_{alt.} > RSS_{serving} + H$*)* **then**
      include network for Fuzzy algorithm;
    else
      exclude network from further analysis;
    end
    Normalize network KPIs;
    Evaluate membership degree of each KPI (fuzzification);
    Calculate impact indexes of each KPI for all available network;
    Compute membership value of all available networks;
    Calculation of the performance score (PS) of each access network;
    To avoid a ping-pong effect in network selection perform a handover to an alternate network only if $PS_{alternate} > PS_{current} + PS_H$;
  end
end

Algorithm 2: Pseudocode of the Fuzzy algorithm according to [81].

Algorithm 1 shows a pseudocode of an implementation of the RSS algorithm from Eq. (3.1). The only dynamic input KPI is the measured RSS value. The hysteresis margin H is a constant value, which is used to avoid ping-pong effects in the network selection. So called ping-pongs, cf. [81], are numerous handovers carried out in a short time frame causing in most cases disruptions in the connection. The output of the algorithm is thus the network offering the highest RSS value.

As the handover decision is based on a single parameter, in this case the RSS value, the handover decision is potentially not able to meet multiple QoS requirements of an application. For handling multiple decision metrics and to fulfill such QoS requirements, artificial neural and Fuzzy logic based methods are able to achieve good results [82, 83, 84]. The Fuzzy logic method, taking multiple KPIs into account, is a way to realize efficient handover decision algorithms and is able to handle, e.g. RSS fluctuations [18]. Fuzzy algorithms also take inaccurate inputs, such as user preferences into account, that are likely not able to be defined accurately. For the evaluation carried out in Section 5.1.2 the Fuzzy logic based algorithm proposed in [81] is used as a reference algorithm. It incorporates the RSS value, the throughput of the access networks as well as the energy consumption and the central processing unit (CPU) load of the telematics ECU. This enhanced Fuzzy based algorithm consists of a three step process: During metric fuzzification, the chosen decision metrics are normalized to enable direct value comparisons. Following this, the influence of these normalized metrics on the handover decision, by using specific membership functions,

are computed [81]. Based on the previous steps, the last process determines the target network showing the best prospects for a handover.

Algorithm 2 presents a pseudocode of a implementation of the Fuzzy algorithm from [81]. It takes, as aforementioned, four KPIs into consideration and gives in contrast to the RSS algorithm as output a performance score of all access networks. To limit the number of considered access networks a filtering based on the RSS value is carried out. The filtering seen in line 7 of the pseudocode is performed with the previously discussed RSS algorithm. The main part of the Fuzzy algorithm is starting in line 12. The first step is the normalization of the input KPIs in order to enable comparison of KPIs from different sources. The so called fuzzification evaluating the membership degree of each KPI is carried out in the next step. This is followed by the calculation of the impact indexes of each KPI for all networks and the computation of the membership value. The performance scores of each access network are yielded in the last step. To avoid ping-pongs in the network selection a threshold PS_H is set in line 17 by which the network score of an alternate network has to exceed the performance score of the current network for a handover to occur.

Using the analytical hierarchy process (AHP) algorithm for network selection is another approach to satisfy the diverse application requirements while taking into account multiple KPIs [85]. For the evaluations carried out in Section 5.1.2 an AHP algorithm is developed consisting of an implementation based on the work of Kassar et al. [19]. The designed AHP is shown in Figure 3.3. In the top level category a differentiation is done between local and external KPIs. The local values are divided into two subordinate categories: network KPIs measured on-board the vehicle and static KPIs, which are constant over a long time period. The inputs characterizing the radio access networks, static KPIs and the external information are shown in the lowest level of the hierarchy. The indicators of the radio networks include the RSS, SINR and latency, which are subsequently evaluated for each considered radio access network. Further incorporated KPIs are the energy consumption, transmission costs as well as external information like the network load and an user experience map. The user experience map contains previous stable or unstable connections in terms of the achieved throughput. The external KPIs are aggregated centrally and are geo- and time-referenced in an off-board server. Based on the selected navigation route the previously described information is then requested for the purpose of network selection by the vehicle.

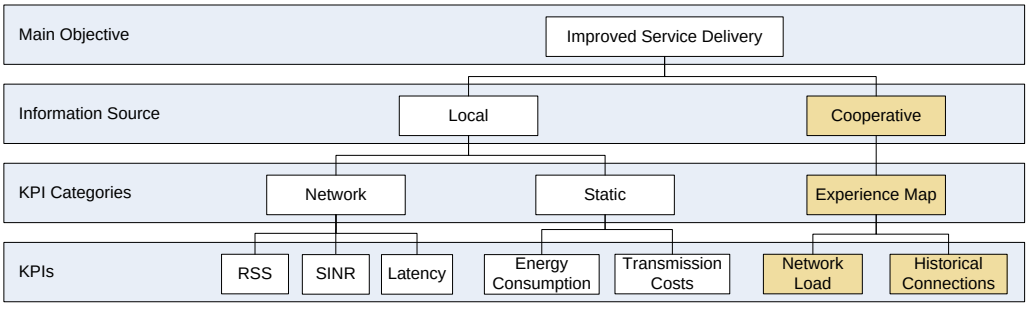

Figure 3.3: Developed AHP algorithm including external KPIs.

Data: RSS, SINR, latency, energy consumption, transmission cost, Optional: network load & historical connections
Result: Ranking matrix of all networks

while *on the way towards destination* **do**
  Set weights for KPI comparison matrix [85];
  Calculate eigenvalues of KPI comparison matrix;
  while *alternate networks available* **do**
    Measure KPIs of all available networks;
    Calculate network performance scores according to upper and lower limits of each KPI [85];
    Create normalized network performance score matrix by calculating relative quality scores of each KPI [85];
    Compute eigenvalues of normalized network performance score matrix;
    Calculate sum of products of KPIs and network performance score matrix elements per available network [85];
    Each sum is the quality score of an available network;
  end
  if *score of alternate networks > score of current network* **then**
    Bucket of each access network is decremented by one;
    Calculate network score difference of current and all alternate networks;
    if *Score difference > network score difference threshold* **then**
      Increment score of bucket of the alternate network by $1 + \frac{\text{difference}}{\text{network score difference threshold}}$;
    end
  else
    Empty all buckets of the access networks;
  end
  if *Level of a bucket of an alternate network > bucket level threshold* **then**
    Perform handover to an alternate network;
  else
    Stay on current network;
  end
end

Algorithm 3: Pseudocode of the AHP algorithm.

The presented AHP hierarchy is mathematically evaluated by means of comparison matrices normalizing in a first step all inputs, cf. Algorithm 3. The elements of each category are weighted against each other according to their assigned priority. As the lowest hierarchy level includes KPIs from three different superordinate elements (network, static, external) three comparison matrices are used in this category level, if external KPIs are also considered, otherwise only two. The eigenvalues are calculated for the comparison matrices of all categories and the ratings of the radio access networks are determined according to [19]. It is feasible to exclude networks, such as WLAN from the network selection due to their lower communication range [23] in case the the vehicle velocity a certain threshold. In the simulation, however, shown

in Section 5.1.2 such a pre-filtering is not carried out as a traffic congestion scenario is evaluated. Also the measurements discussed in Section 5.1.3 do not include such a filtering as the measurements are conducted at velocities lower than 30 km/h. After calculating the weights a newly developed bucket concept is applied to determine the necessity of initiating a handover and thus avoiding ping-pong effects in the network selection. Each radio access network is assigned a bucket including a counter. The counter of the network receiving a better rating than the current network is incremented. A handover to an alternative network is only performed, when a previously determined threshold of the bucket counter is met. After this all counters are reset.

The AHP algorithm is especially suited for vehicular applications, as comparison matrices are used not only to rate the KPIs against one another but also to prioritize the radio access networks depending on the application demands. Moreover, the AHP also enables to use application or user specific profiles prioritizing certain KPIs. Thus, for instance, a profile putting a large weight on the latency is feasible to be used just for delay-sensitive applications, such as for video streaming applications, to impact the handover decision towards delay intolerant access networks. Moreover, modifying the weights of KPIs gathered from off-board sources according to, for instance, the current traffic flow or the network load is likely to be achieved in a simple manner. The simulation based evaluations in Section 5.1.2 show that such a VHDA approach is well suited to increase the overall obtained throughput by reducing the number of handovers. These findings are also validated with measurements, which are shown in Section 5.1.3.

3.2 Safety Applications

Safety applications are in comparison to user-centric infotainment applications of a cooperative nature, hence require full collaboration between different parties. For one user it is not irrelevant anymore what application another user is performing or whether he is offered a low QoS by the network operator. Consequently, the different users act dependent from one another and share a common interest. This is the key difference between safety and infotainment applications. Due to cooperative nature of safety applications the reliability of the system is contingent upon the weakest link in the communication chain. Thus it is essential to set common minimum performance requirements to allow reliable communication between the different parties. As such a required minimum communication range of an access network is feasible to be considered. In case of 802.11p communication this potentially means that performance deterioration due to integrational impairments are compensated in a similar manner. For vehicular safety application an overview of these degradation and on the characteristics of V2I and V2V channels is given in [3]. A special focus of using LTE for safety applications is performed in [25]. It is stated that LTE radios are in general able to compensate the drawbacks of 802.11p systems, such as their scalability and communication range. LTE is regarded as key for the deployment of vehicular networks especially in the beginning when the penetration of 802.11p

radios is low and consequently dissemination of safety messages through multihop [86] mechanisms is not possible. A comparison between LTE and 802.11p for their ability to support safety applications is done by means of simulations in [26]. It is concluded that LTE is not suited for beaconing applications as this increases the network load substantially and causes high expenses for transmission costs. The authors in [26, 87] establish that cooperative awareness message (CAM) based applications, such as intersection assistance, are not suited for cellular networks as the required number of messages considerably increase the load in the network. Thus yielding that cellular systems in the area of vehicular safety applications are predominantly apt for decentralized environmental notification message (DENM) events [88].

In the following Section 3.2.1 an analysis of the advantages of using hybrid radio access for safety applications is provided. Section 3.2.2 includes a discussion on a dissemination methodology to distribute safety messages exploiting the benefits of hybrid radios.

3.2.1 Hybrid Communication for Safety

A multitude of radio access networks in the ad-hoc as well as in the cellular domain have been deployed in the past, which are especially suited for vehicular communication applications, see [15, 25, 89] for an overview. However, approaches to merge both domains to exploit their merits for safety applications have only been pursued lately. In the ad-hoc domain the vehicular-specific IEEE 802.11p was primarily investigated for automotive connectivity applications. IEEE 802.11p radio access is used either for V2V or V2I communication. V2V is mainly intended for safety applications having stringent delay requirements, such as rear collision avoidance systems [12]. V2I communication, for instance using 802.11p RSUs, employs the infrastructure to broadcast safety related messages. As such the system reliability is potentially due to the redundant message transmission increased further. However, the main focus of V2I communication is broadcasting safety as well as traffic efficiency messages from operators, such as traffic control centers. Other current uses also include road tolling systems. Various research projects have already investigated the reliability, usability and limitations of 802.11p communication systems. The recently finalized research project *simTD* [2] analyzed the feasibility of 802.11p communication systems for vehicular safety applications. One of the major goals was the definition and validation of scenarios for rolling out ITS applications for road safety and traffic efficiency applications. The scenarios were validated with over 100 vehicles in highway, rural and urban environments [2]. In the cellular domain the communication standard 3GPP UMTS and 3GPP LTE have recently been investigated for vehicular safety applications. The investigations were mainly conducted in the already finalized research projects within the *AKTIV* initiative [1], i.e. *CoCar* and *CoCarX*. LTE offering increased bandwidth, scalability and largely reduced delay constraints, was found to be enabling the provisioning of driver assistance and information services, whereas UMTS was found to be inapt [90]. Attempts to exploit the merits of cellular and ad-hoc networks is currently pursued in the *CONVERGE* project [4] to improve the dependability of vehicular safety applications.

Such improvements necessitate the use of a message dissemination engine (MDE) to route safety messages depending on the application requirements and the performance of the networks using the most suitable radio. To increase reliability by redundancy a MDE is also able to distribute safety messages using all available access networks. This is likely required for delay stringent safety messages considering that 802.11p communication does not provide a guaranteed QoS due to its decentralized channel access nature [91]. Such a decentralized channel access is likely to lead to packet collisions and thus increase the latency [92]. Naturally the probability of packet collisions rises with the number of vehicles. Furthermore, distributing safety messages over longer distances using 802.11p requires the use of RSUs, which are currently not widely available. LTE on the other hand offers two QoS categories, one where different QoS classes are guaranteed and the other category where no prioritization occurs (best effort) [33]. The best effort QoS class is comparable to the transmission in 802.11p; an attempt is made for transmitting a message, but it is not guaranteed that the safety message goes through in the required time frame. An additional advantage of LTE is, compared to 802.11p, the increased communication range. On the other hand an increased communication range results especially for low frequencies, such as 800 MHz in a higher number of users, who are able to connect to the network. As conventionally most consumers use a best effort QoS class [93], the probability of getting, for instance a safety message transmitted on-time, is potentially not very high, if the network resources are divided among a multitude of users. To limit the impact of additional vehicular users on the network resources broadcasting such messages as done in 802.11p is potentially better suited than unicast connection to each participant. Moreover, is broadcasting also worthwhile when safety messages, such as for a wrong-way driver incidents, are not only relevant for one user but rather for all vehicles in a certain geographical region. This illustrates that a context-based and situation-aware network management is key for the proper dissemination of safety messages. Requiring a guaranteed QoS in LTE for every message to be disseminated is in consideration of economic reasons not expedient. It is also not feasible in regards to the use of the available network resources. Thus to keep the consumption of network resources low, to be transmission cost-efficient and still ensure a high penetration of safety messages a dissemination strategy is required. Besides an increase in reliability of the message by redundant transmission, a strategy is also able to distribute a message over different networks to increase the communication range. Thus in case of a local hazard warning the vehicles closest the incident are likely to be alerted using all available networks, whereas in areas further away only one access network likely suffices. The arising different dissemination strategies by using hybrid access networks are explored in the subsequent Section 3.2.2.

3.2.2 Messages Dissemination using Hybrid Access

As described in the previous Section the use of a MDE enables to route safety messages depending on the application requirements, network conditions and availability. To illustrate that an MDE allows for such improvements and to establish that MDEs

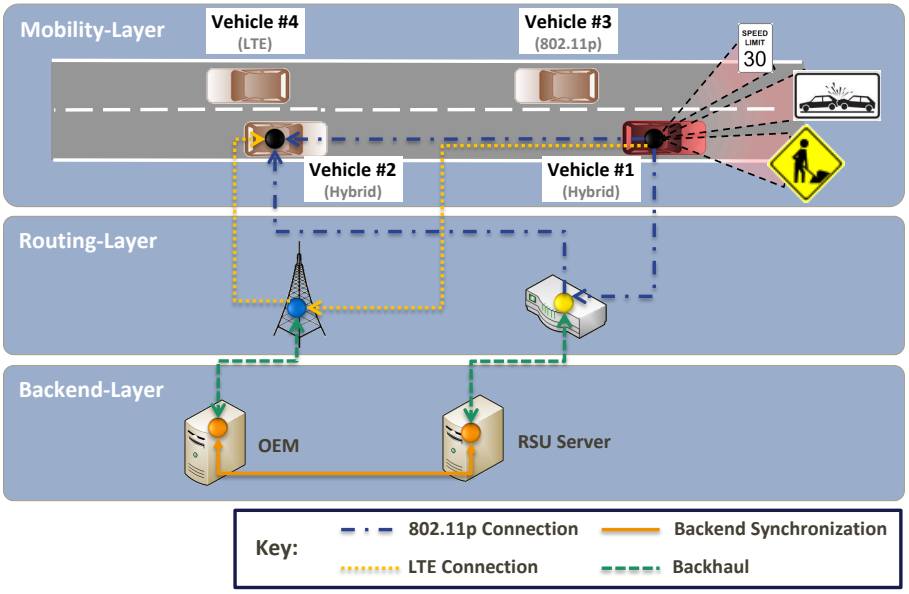

Figure 3.4: Messages dissemination strategies in hybrid radio environments.

of different vehicles need to work cooperatively the scenario shown in Figure 3.4 is analyzed. In Figure 3.4 Vehicle #1 has detected a safety related traffic incident, for instance, a construction site or a change of the speed limit. Vehicle #1 and Vehicle #2 are equipped with hybrid radios, whereas Vehicle #3 supports only 802.11p and Vehicle #4 only LTE communication. Vehicle #1 requires to distribute the DENM in such a way that all affected vehicles are notified of this warning.

To better visualize the message dissemination a sequence diagram is shown in Figure 3.5. As in this case Vehicle #1 supports hybrid access networks, it is able to distribute the message via LTE and 802.11p. Assuming that both Vehicle #2 and Vehicle #3 are in range of the 802.11p communication range both receive the message via 802.11p. In addition to both vehicles the 802.11p RSU, which is in the communication range as well, also receives the safety message. Consequently, Vehicle #2, Vehicle #3 and the RSU are able to relay the message to other participants. To reduce the complexity of the sequence diagram only the re-broadcast of the RSU is shown in Figure 3.5, excluding Vehicle #2 and Vehicle #3. Both have also the option to route the safety message through the backend of an operator or the OEM backend. In case broadcast protocols, such as eMBMS [77], are not considered for LTE, vehicles equipped with LTE radios, Vehicle #2 and Vehicle #4 in this example, are notified with an unicast connection.

Consequently, it is possible to implement MDEs on multiple layers, as shown in Figure 3.6, see also [14]: (1) Vehicles, (2) OEM backends, (2) third party backends as, for instance, from mobile network operators or traffic control centers. Vehicles have in general the best knowledge on the presence and mobility of the ongoing traffic in their immediate surrounding. However, besides their immediate surrounding vehicles have a limited overview of others, which are further away. Thus achieving a high message penetration over a wide range poses to be difficult. The OEM backend on the other hand has a bird's eye view of all vehicles, which for proper

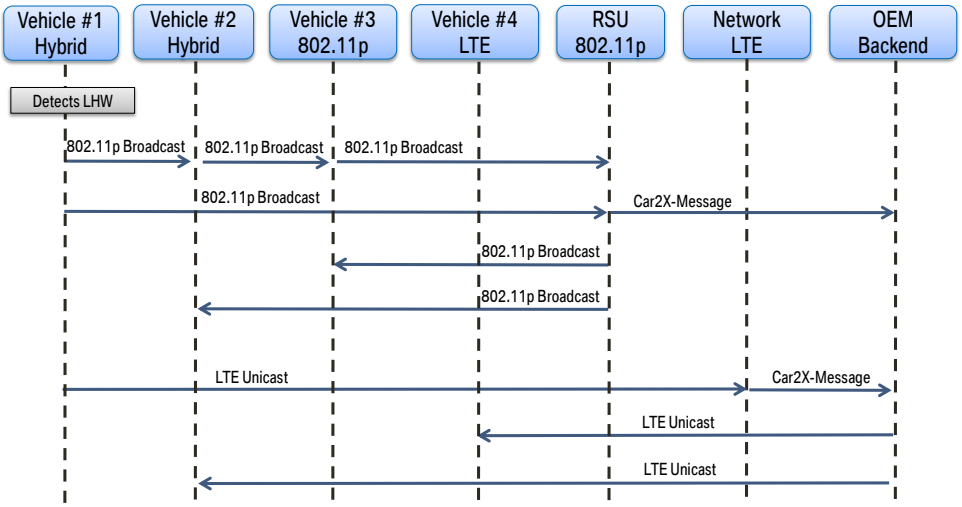

Figure 3.5: Sequence diagram of the safety message dissemination in Figure 3.4.

message dissemination purposes is ideal. Nevertheless, in a given scenario the vehicles are most likely from different manufacturers. Thus a bird's eye of the surrounding vehicles has to be obtained from a decentralized Car2X Systems Network, where a complete bird's eye view regardless of the manufacturer is feasible to be gathered. The dissemination of safety messages in the rapidly changing vehicular environment requires synchronization between the different MDEs on the different layers, which consumes time and network resources. Without synchronization of MDEs on different layers it is difficult to accomplish improvements in the service delivery of safety messages and to use the network resources efficiently. Moreover, a strategy is necessary to account for up-to-date sensor information of single vehicles as well as information aggregated from the entire vehicle fleet. For improved system performance in terms of used radio resources and message penetration a trade-off has to be found between synchronization and the application needs. Considering that in case of safety applications with stringent delay constraints, such as collisions warnings, every millisecond counts. Synchronization between different MDEs are in case of these applications not feasible to be performed in order not to compromise the functionality and thus endanger lives. Consequently, the primary use case of MDEs is more in the area of less delay stringent applications as found for traffic information services. Considering the sequence diagram in Figure 3.4 synchronization between MDEs is able to lower consumption of network resources as redundant transmissions are likely to be avoided. Thus in the shown simplified example the LTE unicast transmission to Vehicle #2 is feasible to be avoided or deliberately triggered for the purpose of redundancy. Naturally this is a very simplified example and the necessary effort to save network resources in this case is not worthwhile the synchronization attempt. However, in a greater scenario as discussed in the following with the example shown in Figure 3.7 the potential benefits for the service delivery are more apparent.

Most possibilities for dissemination of safety messages arises for equipping all vehicles with cellular as well as ad-hoc radios. However, this does not reflect future development in the area of vehicular communication systems. Due to different manufactures

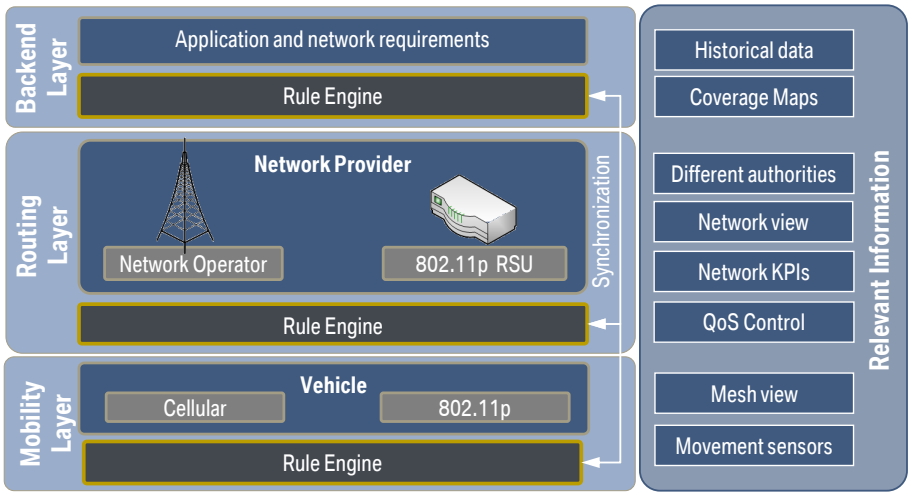

Figure 3.6: Localization and Synchronization of a MDEs.

and a variety of different vehicle models, it is more likely that vehicle with one or both access radios are likely to co-exist. Besides the compatibility of vehicles with a certain access network a methodology and thus a synchronization attempt for dissemination is essential to make use of the available radio resources as efficiently as possible. As it is likely that vehicles from various OEMs have contracts with different network operators a dissemination methodology with a MDE located at network layer is not advisable, in a first instant, for an improved service delivery. Similar to locating the MDE at the network layer is the backend layer also not feasible, as converging the various OEM backends intended for the distribution of safety message, similar to the proposal in *CONVERGE*, will be challenging as a short term goal. Thus an approach working at the mobility layer and having a low dependency on the OEM or the network operator is a more feasible way.

Clustering of vehicle is one possible way to achieve this, cf. Figure 3.7. As currently a direct device-to-device communication is only possible using ad-hoc communication, it is suggested to use 802.11p to build different clusters. The additional benefit of 802.11p communication arises from the already occurring communication between the vehicles in the form of status updates, the CAM messages. Making use of CAM messages is potentially an efficient way to use the network resources as economically as possible for the purpose of clustering. Different approaches to perform clustering are, for instance, given in [94]. In [92] clustering is used to evaluate a newly developed 802.11p media access control (MAC) protocol in a highway scenario. Clustering is not only an approach to disseminate safety messages more efficiently but also to collect FCD [95]. FCD is feasible to be aggregated at one vehicle and forwarded only by certain vehicles in order to reduce the overall number of connections, thus the transmitted data. Due to the use of the cellular network as a backbone to forward the message, vehicles having only 802.11p are also feasible to be included in the dissemination. Naturally this requires that the vehicle disseminating and aggregating messages is equipped with cellular as well as ad-hoc networks.

One of the easiest ways to perform clustering and in the same time being compatible to CAM messages is to use the Lowest-ID method [94]. With this approach each

vehicle is assigned a certain ID, which is periodically broadcasted together with the ones of its neighbors. The vehicle having the lowest ID number among its neighbors announces itself to be a cluster head. The other vehicles on the ID list are consequently assigned the role of a cluster member. To disseminate a safety message it is only necessary to notify the cluster head, using for instance the LTE network, the cluster members are than notified by the cluster head using 802.11p communication. To better illustrate the benefits of clustering, a LHW, see [14], is considered in Figure 3.7. For the purpose of simplification it is assumed that all vehicles are equipped with cellular as well as ad-hoc radios. Notifying the 18 vehicles of the LHW incident, which is detected by the red colored vehicle, results in at least 17 LTE connections, if no ad-hoc communication is used. This number is potentially even higher taking into consideration re-transmissions due to status updates on the LHW. In case of clustering this number of transmission is likely to be substantially reduced. In the shown scenario using clustering only 4 connections are necessary to notify the cluster heads. They in turn are able to disseminate the message further within their cluster using 802.11p communication. The only requirement is that the chosen cluster heads supports both access networks, in order to receive messages via cellular and distribute them using 802.11p. Naturally the selection of cluster heads is key to ensure that such a forwarding scheme works properly. As, for instance, a LHW is likely to be initiated by the backend of a manufacturer and distributed via a cellular network, it is key that a selected cluster head remains to serve as such for a long time period. A frequent change of a cluster head potentially increases the network load, as the new cluster head has to be notified again by the backend of the safety incident and in turn needs to re-distribute the message. This also shows that an approach like clustering is most feasible in scenario like in a highway, as in an urban setting intersections potentially result in frequent changes of the cluster. Another key factor in clustering is the number of cluster heads [96]. To most efficiently make use of clustering the number of cluster heads need to be as low as possible. All vehicles, which are not associated with a cluster are considered to be their own cluster heads. Thus this number needs to be minimized in order to achieve an additional value using such an approach. In a worst case scenario all vehicles are thought to be cluster heads, which in turn means notifying all vehicles by a unicast transmission. Due to the emphasize on the service delivery of delay intolerant safety applications and the impact of differently equipped vehicles the additional value of using clustering is not investigated further in this work.

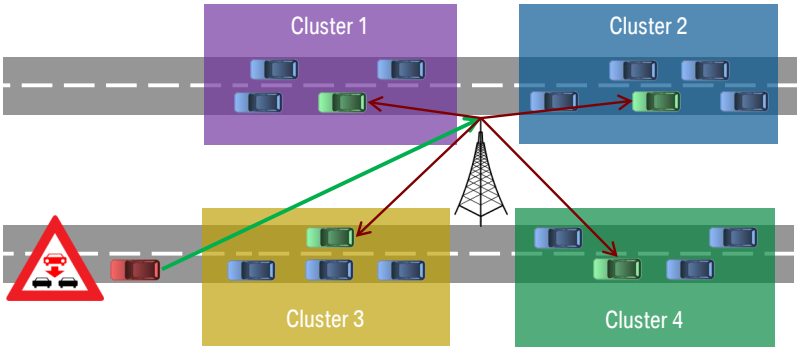

Figure 3.7: Clustering methodology for a local hazard warning.

Chapter 4

Assessment of Antennas for Hybrid Radio Access

The assessment methodologies introduced in Chapter 2 are applied here for the benchmark of prototypical hybrid antenna systems. The evaluation is divided in two parts; assessing their ability to support LTE in the first and their 802.11p capabilities in the subsequent part. In the following Section 4.1 the prototype antenna systems are assessed based on their capability to support SMX in LTE at 800 MHz. Similar investigations were also carried out in [51, 50, 49]. The characteristics of the prototype antennas are evaluated with metrics introduced in Chapter 2. The prototype systems are compared to different reference antenna setups to illustrate the impact of antenna isolation on the SMX capability. The results also illustrate a target antenna isolation value for future antenna systems, which in consideration of design efforts and yielded SMX performance is justifiable. On system level the cellular antennas are benchmarked with the help of passive measurements. The evaluated performance metrics are the mutual information C and the condition number κ, see also [30, 7, 97]. Assessment of each antenna system is carried out on the 9 km long measurement track introduced in Section 2.1.1, which is served by a 800 MHz base station, see also [6]. The KPIs are analyzed for the entire measurement track as well as for a LOS and nLOS scenario, cf. [27]. Although the LOS and nLOS scenario provide, on their own, essential inputs on the antenna performance, the evaluation conducted on the entire measurement track including both scenarios comes closest to the overall user experience. With the help of active measurements it is shown that differences in the gain of the main and aux antenna, especially in a LOS scenario to the base station, are crucial.

Assessment of vehicular antenna systems for 802.11p communication are carried out in Section 4.2. Evaluations on the occurring performance deterioration when mounting such antennas on the vehicle rooftop are illustrated in [59, 60, 61]. The different antenna prototypes are evaluated on their yielded diversity efficiency and communication range in a testbed, see [29]. The considered prototypical antenna systems employ different design methodologies to limit the interaction between their 802.11p and cellular antennas. The different design methodologies are assessed by

comparing the prototypical systems based on mismatch, antenna isolation and KPIs taking into consideration the antenna gain. Moreover, is a methodology introduced to compensate the antenna performance deteriorating effects of the antenna housing causing nulls in the radiation pattern, see also [28]. Simulations are performed on component level and are verified with measurements in an anechoic chamber showing that such a compensation is achieved by altering the thickness of the antenna housing. Furthermore, it is shown that geometrically simplified shapes for an antenna housing are feasible to be used as a proof of concept approach to investigate its impact on the antenna performance. The effect of such component level improvements on the system level performance are evaluated by performing virtual measurement drives with different antenna housing prototypes.

4.1 Cellular Antenna Benchmark

The assessment of cellular antennas on component as wells as on system level is carried out in this section. The analyzed antenna systems are fully hybrid, thus cover cellular and 802.11p frequencies. In the cellular domain the antenna systems cover the frequency bands GSM, UMTS and LTE, which are rolled out in Germany [98]. The frequencies for each cellular network is listed in Table 4.1. The prototypical systems are designed in such a way that the main antenna, Figure 4.1, has to be compatible with all of the denoted frequency bands. The aux antenna on the other hand is only required to cover the frequency bands LTE 800 and LTE 2600. All prototypical systems are specified to cover the frequency bands with a reference mismatch value of -10 dB. Analyzing the systems at 800 MHz, the worst case scenario for antenna isolation due to the low separation of the main and aux antenna, reveals that this requirement is met in most cases, cf. Table 4.3. The prototypes fall below this reference value yielding mismatch values as high as -6 dB. In case of the isolation between the main and aux antenna a value of -12 dB is targeted for the SMX capable LTE frequency bands. This targeted value is crossed in the low LTE 800 MHz frequency band due to the scarce antenna integration volume causing inter-element correlation and coupling of the antennas [50, 51]. Values as low as -5.5 dB are yielded in this frequency band. In the LTE 2600 frequency band all obtained isolation values are above the defined reference value, since in this case the integration volume is sufficient for decoupling the main and aux antenna. Due to the arising challenges especially in the low frequency band the focus of this work is the LTE 800 band. The other frequency bands mentioned in Table 4.1 are not discussed further.

LTE 800	GSM 900	GSM 1800	UMTS	LTE 2600
791 - 862	880 - 960	1710 - 1880	1920 - 2170	2500 - 2690

Table 4.1: Frequency bands (in MHz) of the cellular networks covered by the antennas.

This Section is structured as follows: In the subsequent Section 4.1.1 the characteristics of the prototypical antenna systems are analyzed employing the KPIs from Section 2.3. Next, in Section 4.1.2 the results of the active measurements are shown.

The results of passive measurements, which are used to benchmark the prototypical antenna system on system level, are discussed in Section 4.1.3. The assessment results for both cases are summed up and conclusions drawn in Section 4.1.4.

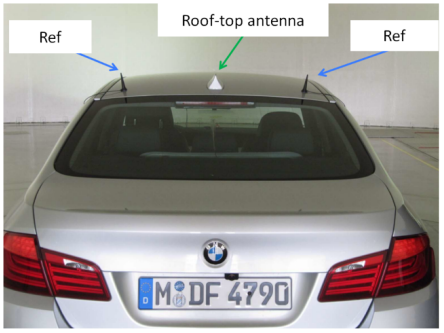

(a) Antenna configuration on vehicle.

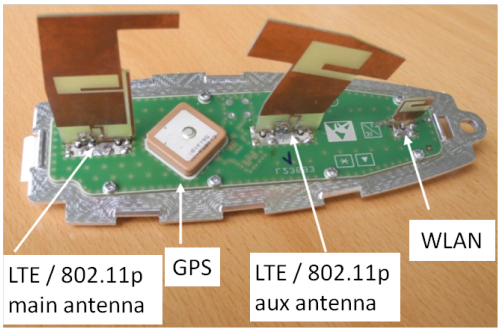

(b) P(I).

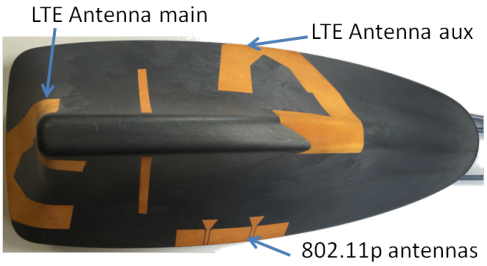

(c) P(II).

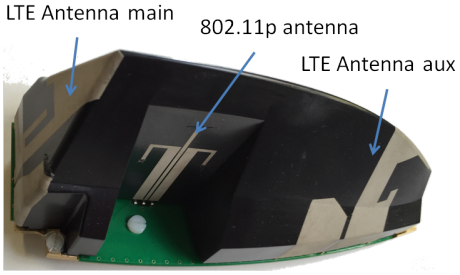

(d) P(III).

Figure 4.1: Analyzed prototypical hybrid antenna systems.

4.1.1 Characteristics of the AUTs

The characteristics of the prototypical antenna systems are summed up for the LTE 800 MHz band in Table 4.3. The KPIs are given separately for the main and aux antenna, where applicable. For more accurately analyzing the antenna gain it is further differentiated in the front and rear region of the vehicle, see Section 2.3. Within these regions it is differentiated between the maximum, minimum and mean value of the antenna gain to determine how well the MIMO system supports SMX transmission in the front and rear of the vehicle. In addition to the determined gain values Table 4.3 also includes the KPIs ρ_{TH} and ρ_{Diff}, which were also introduced in Section 2.3. For the threshold G_{TH} -3 dB is selected, as at this value the antenna gain is reduced by half. For computing ρ_{Diff} the difference of antenna gain between the main and aux antenna G_{δ} is set to 3 dB. The reason for choosing a lower value than determined in [6], which showed that a fallback from SMX to diversity occurs at a gain difference of approx. 6 dB, yields from the gain values being determined on a ground plane. Comparing the radiation pattern measurements of the prototype antenna

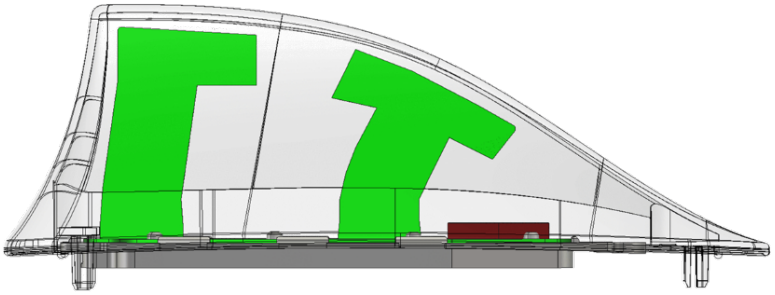

Figure 4.2: Different height for the main and aux antenna in case of P(I) [8].

P(I) on a ground plane and on the vehicle rooftop, reveals significant differences in the yielded pattern, see Appendix A.2. Distortions seen on a ground plane, cf. Figure A.3(a), are increased on the vehicle rooftop, see Figure A.2(b). Thus, if measurements on a ground plane are considered, a high G_δ value potentially does not give accurate results on the antenna performance as deterioration in the pattern is not pronounced as such. Table 4.2 provides a summary of the aforementioned KPIs. In addition the required performance thresholds of the other KPIs are shown. As mentioned previously, the mismatch of both antennas S11 is set to -10 dB, whereas the reference value for the antenna isolation is set to -12 dB. For the mismatch, also referred to as the return loss, -10 dB is a common value from the literature, see [99, pp.962] and [34, pp.101]. An antenna isolation of -12 dB is a conventionally employed value for the design of LTE MIMO antennas, cf. [100, 101]. The targeted radiation efficiency is set to 70 %, as this is a threshold traditionally used in the automotive industry.

G_{TH}	G_δ	S11	S22	S21	RE
-3 dB	3 dB	-10 dB	-10 dB	-12 dB	70 %

Table 4.2: KPI thresholds. All other gain related KPIs are set to 0 dBi or 0 %.

The major difference between the prototype P(I) and the other prototypical systems, cf. Figure 4.1, is that in this case the cellular and 802.11p frequencies are covered by the same printed circuit board (PCB) antenna. Consequently, the prototype uses a diplexer to offer separate ports for the cellular and ad-hoc antennas. The prototypes P(II) and P(III) are manufactured in 3D MID technology [102]. The cellular antennas are placed in both cases in the rear as well as the front region of the antenna housing. The design methodology applied for P(II) was investigated in [97]. The results in Table 4.3 illustrate that in terms of mismatch and isolation prototype P(III) achieves the best values. The main antenna of P(III) shows an antenna mismatch of -12 dB, whereas P(I) and P(II) reveal a higher mismatch of approx. -9 dB. The aux antennas show compared to the main antennas in case of all prototype systems a higher mismatch, which is caused by the smaller integration volume given in the antenna housing. This is most evident for P(I), which due to the shape of the housing and thus the height limitations of the PCB allows only for a smaller aux antenna. This drawback is not only limited to P(I), it is an general difficulty of vehicular antennas comprised of multiple PCBs. The only possibility for employing antennas of similar height is to decrease the spacing between them.

	antenna	region	unit	P(I)	P(II)	P(III)
S11	main		[dB]	-9	-9	-12
S22	aux		[dB]	-6	-7	-8
S21	main-aux		[dB]	-5.5	-9	-10
RE	main		[%]	55	n/a	63
	aux		[%]	46	n/a	71
G_{max}	main	(rear)	[dBi]	-1.3	0.2	1.7
		(front)	[dBi]	-3.3	-2	-0.6
	aux	(front)	[dBi]	-1.8	0.4	1.4
		(rear)	[dBi]	-5.0	-2.6	-3.0
G_{min}	main	(rear)	[dBi]	-3.7	-3.5	-1.4
		(front)	[dBi]	-4.5	-4.3	-4.4
	aux	(front)	[dBi]	-5.2	-4.2	-4.2
		(rear)	[dBi]	-7.3	-5.6	-6.4
G_{mean}	main	(rear)	[dB]	-2.0	-0.8	0.2
		(front)	[dB]	-3.9	-3.4	-2.1
	aux	(front)	[dB]	-2.8	-1	0.1
		(rear)	[dB]	-6.6	-4	-4.5
ρ_{TH}	main	(rear)	[%]	13	7	0
		(front)	[%]	100	74	17
	aux	(front)	[%]	41	11	8
		(rear)	[%]	100	82	92
ρ_{Diff}	main-aux	(rear)	[%]	84	45	92
		(front)	[%]	0	32	17

Table 4.3: Characteristic values of all prototypical LTE antennas.

Although this approach potentially improves the antenna mismatch, it also lowers the isolation between the main and aux antenna. In general, this design trade off is a drawback of PCB antennas, they are not able to make use of the available integration volume as efficiently as possible. P(II) and P(III) are based on laser direct structuring technology [97], which in contrast to PCB antennas offers more flexibility and freedom in the antenna design. Thus both prototype systems are able to exploit the available volume for the integration of the antennas more efficiently. Consequently, such freedom enables a more sophisticated design and potentially better performing antennas. In case of P(II) and P(III) this allows to increase the antenna isolation to 7 dB respectively 9 dB. Improvements are also yielded in regards to the mismatch on the main as well as the aux antenna. P(III) achieves compared to P(I) a 3 dB lower mismatch on the main antenna and 2 dB in case of the aux antenna. Such enhancements also result in a higher radiation efficiency. Comparing again P(III) to P(I) reveals that the main antenna of P(III) achieves a 8 % higher radiation efficiency, while the aux shows an increase of even 15 %. The corresponding radiation efficiency values of P(II) are not given in Table 4.3 as those were not measured at the supplier's end. As illustrated in Section 2.3 the gain related KPIs are applied for a detailed analysis of the antenna systems separately to the front and rear region of the vehicle. To depict the yielded results in Table 4.3 the regions are discussed

separately from one another for all prototypical systems starting with the rear region.

In the rear region P(III) yields, in addition to showing a low antenna mismatch compared to the other prototypical systems, the highest antenna gain values. The maximal gain G_{max} is 1.5 dB higher compared to P(II) and even 3 dB higher in contrast to P(I). Analyzing the performance metrics G_{max}, G_{min} and G_{mean} reveals that the aux antenna yields for all prototypical systems the lowest gain values for the rear of the vehicle. The lowest G_{min} value is obtained for P(I) reaching -7.3 dBi, which is compared to the other prototypes up to 1.7 dB lower. Evaluating G_{min} for the main antenna illustrates similar values around -3.6 dBi for P(I) and P(II). The prototype P(III) achieves about a 2 dB higher value. A similar behavior is seen for the main antenna for the KPI G_{mean}, however the gain value of P(II) is 1 dB higher compared to P(I). The greatest G_{mean} value is seen in case of P(III), which is 1 dB higher than P(II) and consequently 2 dB higher than P(I). The lowest gain value for the aux antenna of -6.6 dBi is determined for P(I). The other prototypical systems yield similar values, which are around -4 dBi. For the rear region it is feasible to conclude that P(III) achieves the highest gain values, whereas the PCB antenna P(I) illustrates overall the lowest values.

Analyzing the KPIs G_{max}, G_{min} and G_{mean} for the front region reveals that the differences between the main and aux antenna are compared to the rear region considerably smaller. It is interesting to note that all prototypical systems yield in this region similar values for G_{min}. The values for both antennas of all prototypes are alternating around -4.5 dBi. The lowest G_{min} values is obtained by the aux antenna of P(I) yielding -5.2 dBi. As all antennas are designed by different institutions or suppliers and are also based on different manufacturing schemes, this similarity is remarkable. Evaluating G_{max} reveals that the highest values are obtained with the prototype P(III). The difference between P(I) and P(III) for both the main and aux antenna varies around 3 dB. The values of P(III) and P(II) differ about 1 dB. A similar behavior is seen for the KPI G_{mean} for the aux antenna, where P(III) shows an increase in gain of approx. 3 dB compared to P(I) and about 1 dB to P(II). Also in case of the main antenna P(III) yields the highest gain value, which is more than 1 dB higher than the values of the other prototype systems.

In summary the results show that in case of all prototypical systems the front region is covered evenly by the main and aux antenna. Thus in trying scenarios, such as in LOS, shown in the following Section, the front region is less subject to any deterioration of the SMX performance. On the other hand the rear region is due to the higher difference in gain values between the main and aux antenna to a higher degree prone to a fallback to diversity transmission schemes. Hence in the design of vehicular MIMO antennas more consideration needs to paid to the rear region.

The prototypical antenna systems are further analyzed with the help of the KPIs threshold crossing rates ρ_{TH} and ρ_{Diff}, which were introduced in Section 2.3. All gain values of the aux antenna of P(I), cf. Figure 4.3, cross the threshold in the rear region. P(II) and P(III) also exceed the threshold substantially by 82 % and 92 % respectively. The low performance seen in all prototypical systems results from the aux antenna being shadowed by the main antenna when trying to cover the rear of

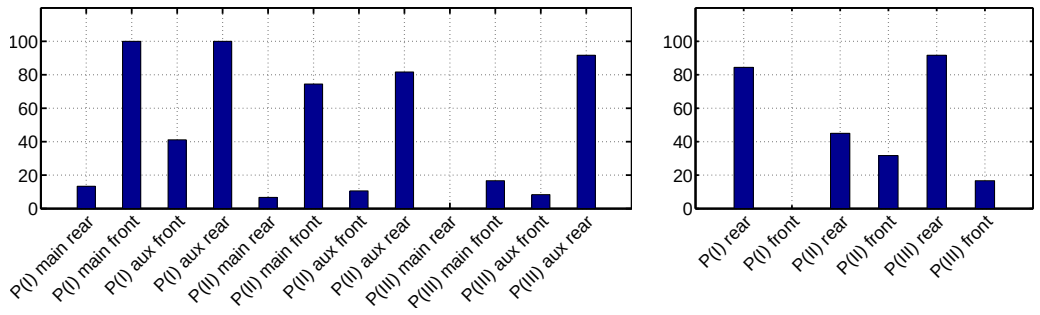

(a) ρ_{TH}. (b) ρ_{Diff}.

Figure 4.3: ρ_{TH} and ρ_{Diff} for all prototypical LTE antennas.

the vehicle. As expected the main antenna covers the rear region of the vehicle very well, as this the region it is primarily intended for. P(I) yields in comparison to the other prototypes a high crossing rate of 13 %. P(II) achieves 7 % and the gain values of P(III) never cross the set threshold. In case of the front region the main antenna of P(II), 74 % of the gain values cross the threshold. Considering that the prototypical system is based on 3D MID technology and thus likely offers increased possibilities to compensate shadowing by the aux antenna, this shows that just an 3D antenna design does not necessarily yield an enhanced performance. The lowest threshold crossing rates are obtained with P(III) yielding only 17 %. A similar behavior is seen for the front region covered by the aux antenna. The highest outages rates for the front region are yielded in case of P(I) resulting in an outage rate of 41 % for the aux antenna, while all values of the main antenna cross the threshold.

In summary the assessment of ρ_{TH} corroborates the previous finding that covering the rear region of the vehicle with aux antenna is very challenging. Avoiding a similar shadowing effect of the main antenna by the aux antenna in the front region is likely achieved with a proper antenna design as shown with P(III). In addition a PCB based antenna is subject to a higher degree of shadowing due to the positioning of the antennas, though in comparison to technologically advanced 3D antennas, it overall shows a fair performance.

Assessing the KPI ρ_{Diff} also confirms that all prototypical antenna systems suffer from an increased antenna gain difference in the rear region of the vehicle, cf. Figure 4.3(b). The highest values are yielded with the prototypes P(I) and P(III) resulting both in values higher than 80 %. About only 40 % of the gain values exceed the threshold in case of P(II), which is due to the overall lower gain values obtained with both antennas, see Appendix A.2. Although this points towards a fair SMX performance, due to the low gain difference between the antennas, a fallback to diversity transmission schemes is likely still occurring as a result of the low gain values per antenna. A similar behavior is seen for P(I), which shows that for the front region the gain differences between the main and aux antenna never exceed the threshold. As seen in Table 4.3 and in Figure 4.3(a) both the main and aux antenna illustrate overall low gain values causing this effect. The lowest ρ_{Diff} values for the

front region of 17 % are obtained with P(III), followed by 32 % obtained with P(II)

S11	S22	S21	mean gain	RE port 1	RE port 2
-14 dB	-15 dB	-40 dB	-1 dBi	57 %	59 %

Table 4.4: Characteristic values of the reference antennas.

The following Sections include the system level assessment of the prototypical systems against one another as well as in comparison to a reference antenna system. As reference two magnet-mount monopole antennas [103] are used, which are aligned longitudinally with the mounting space of the prototype antenna, cf. Figure 4.1(b). However, they are separated by 83 cm, which is almost the full width of the roof resulting in an antenna isolation of -40 dB, see Table 4.4. The mismatch of both antennas is measured with a calibrated vector network analyzer yielding about -14 dB. Antenna gain measurement at 800 MHz on the vehicle rooftop illustrate a mean value of approx. -1 dBi. The normalized radiation pattern is presented in Figure A.2(a) in the Appendix A.2. The reference antennas are denoted 'left' and 'right' according to their position on the vehicle roof in driving direction, cf. Figure 4.1(a). It is seen that the highest gain values are obtained at the angles in the azimuth between approx. 135 ° - 150 ° and around 225 °. Gain drops are obtained at certain angular values reaching up to -4 dBi. Measurements of the radiation efficiency of both antennas result in 57 % and 59 %. In addition to the reference antenna another prototypical system is evaluated in the forthcoming Sections. The antenna system is based on prototype P(I), but offers twice the antenna isolation, thus 10 dB. This is achieved with a phasing line used as decoupling branch at 796 MHz to increase the antenna isolation. The prototype 'P(I) opt' has compared to P(I) an improved antenna mismatch resulting in -9 dB for the main and -8 dB in case of the aux antenna, but also yields approx. 1 dB lower mean gain values, as seen in Table 4.5. This is resulting from the decoupling approach, which deteriorates the radiation pattern of the antenna. Furthermore, it also shows an improved radiation efficiency of 58 % and 55 % for the main and aux antenna respectively. In an ideal scenario all characteristics besides the antenna isolation of P(I) and 'P(I) opt' have to be the same to illustrate just the impact of the isolation on system level. Nevertheless, analyzing and comparing both prototypes gives an indication of the importance of the antenna isolation. To quantify this evaluation of the antenna isolation more accurately also different reference antenna setups are considered in the following Sections.

Non-opt main	Opt main	Non-opt aux	Opt aux
0.2 dBi	-0.3 dBi	-1.3 dBi	-1.4 dBi

Table 4.5: Mean antenna gain of P(I) and 'P(I) opt' for the main and aux antenna.

4.1.2 Active Measurement

As discussed in Section 2.1.2 the evaluation of MIMO antennas is carried out on system level either by performing active or passive measurements. Although it was concluded that passive measurements are better suited to assess the performance of MIMO antennas, active measurements are an essential means to determine the behavior of antenna systems in an operator's network. Using passive measurements does not allow to determine the boundary conditions when a fallback from SMX to diversity transmission is occurring, as no connection is made to an operator's network. Naturally these boundary conditions are complex and also depend on the operator's settings, thus likely vary in case of a different operator. However, active measurements, as shown in the following, give an indication on the requirements of a MIMO antenna. As the goal of the investigation is not the benchmark of different antenna systems only the prototypical systems P(I), cf. Figure 4.1(b), is considered. Antennas not employed for the evaluation, such as the 802.11p or GPS antenna, are always terminated with a 50 Ω impedance. The measurements are carried out at 796 MHz, the center-frequency of the operator's band in the 800 MHz spectrum rolled out in Germany [98]. The employed test track is the one shown and discussed in Section 2.1.1. The offered data rate of the base station is limited to 50 MBit/s in the downlink for using a two antenna configuration. The transmit power of the base station is set to 46 dBm. As in LTE, SMX is only employed in the downlink [32], the following evaluations do not consider the uplink. To avoid cluttering of the results, due to long waiting periods at traffic lights or other unforeseeable incidents, the methodology discussed in Section 2.1.1 is applied. Consequently, measurements are recorded every 10 m. To ensure that altering server loads, do not have an impact on the results, servers dedicated only for this evaluation are used to perform the downloads, see Section 2.1.2. Moreover, is the evaluation, as agreed upon with the operator, conducted in a single user scenario, thus allocating all resources to the measurements. The measurements are carried with the help of a CE device using the setup presented in Figure 2.4 in Section 2.1.1.

The results of the active measurements are presented in Figure 4.4. Histograms for the entire measurement track are shown for the KPIs received signal strength indicator (RSSI), SINR and the throughput in Figures 4.4(a) - 4.4(c). As only the overall performance of P(I) is of interest, it is not differentiated in the main and aux antenna. Comparing the RSSI outcome for both directions in Figure 4.4(a), reveals that the distributions are similar. The calculated mean RSSI and the corresponding variance values, seen in Table 4.6, confirm this as well. Direction I illustrates a mean value of -60 dBm, whereas the opposite Direction II yields -63.5 dBm. Although the mean values are similar, the RSSI values, where the highest occurrence rates are seen, differ. On Direction I the highest rates are seen in the range between -64 dBm and -61 dBm whereas for Direction II these are shifted to higher power values, thus range between -83 dBm and -80 dBm. The SINR distribution in Figure 4.4(b) shows an overall high direction dependent behavior, even though the mean values for both direction are also close in this case, see Table 4.6. Direction I shows compared to Direction II an increased amount of low SINR values below 10 dB and also negatives

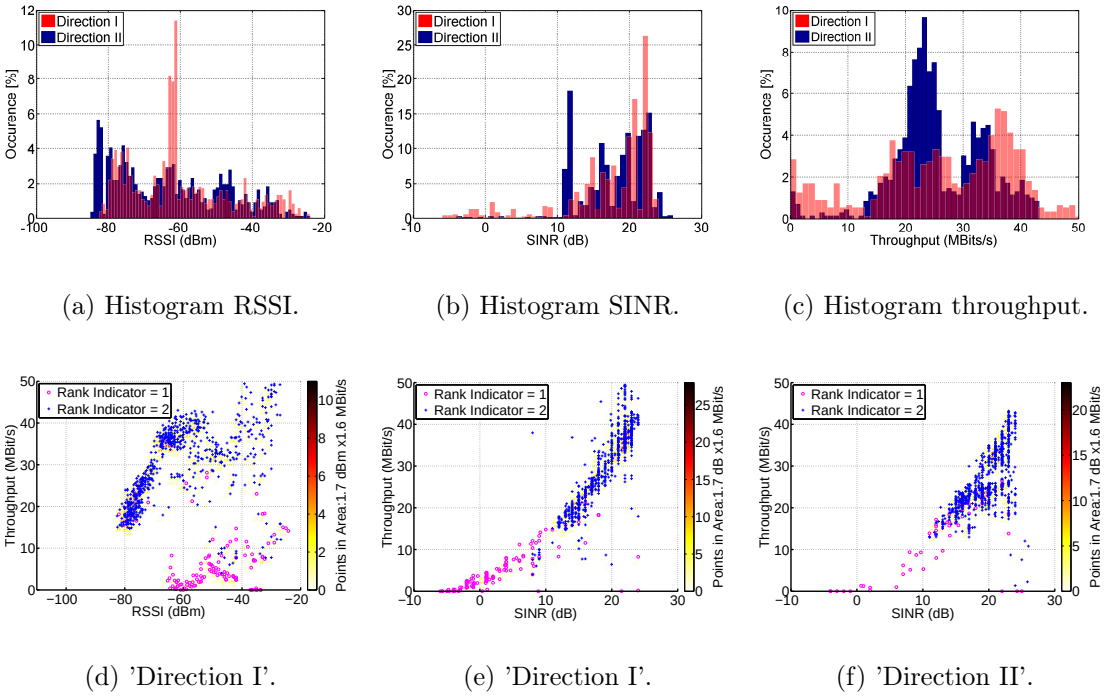

(a) Histogram RSSI. (b) Histogram SINR. (c) Histogram throughput.

(d) 'Direction I'. (e) 'Direction I'. (f) 'Direction II'.

Figure 4.4: Histogram for the mean RSSI, SINR and throughput values for P(I). Scatter plots of RSSI and SINR as a function of the throughput.

values. Consequently, the variance for Direction I is about 2 dB higher compared to Direction II, cf. Table 4.6. The direction dependent behavior becomes even more evident analyzing the throughput distribution presented in Figure 4.4(c). Direction I shows compared to the opposite direction widely spread throughput values resulting in an approximately 4 Mbit/s higher variance, see Table 4.6. Although in Direction I lower throughput values are seen with a high occurrence, throughput values, such as 50 MBit/s, are only seen in this direction. These values are obtained driving towards the base station in a LOS scenario between the vehicle and base station. The primary reason for this behavior results from the low gain deviation between the main and aux antenna in the front region of the vehicle, see the normalized radiation pattern in Figure 4.5.

	Direction I		Direction II	
	mean	variance	mean	variance
RSSI [dBm]	-60	13.9	-63.5	15.2
SINR [dB]	17.3	6.4	17.8	4.5
TP [Mbit/s]	26.3	12.3	25.6	7.9

Table 4.6: Direction dependency of the actively measured KPIs.

To illustrate the relation between the previously discussed KPIs and to further analyze the direction dependent behavior of the antenna system 3D scatter plots are analyzed in the following. The KPIs RSSI and SINR are evaluated as a function of the throughput. Highlighting is used to disclose areas with a high concentration of measurement points. The corresponding coloring illustrates the quantity of data

points in a rectangle of the size specified at the colorbar. Figure 4.4(d) illustrates that only for a certain region, here between -80 dBm and -60 dBm, a relation is seen between the KPIs RSSI and the throughput. Thus for analyzing the performance of the antenna system and to determine direction dependent behavior RSSI is not a suitable KPI. That power related KPIs are not suited to rate the LTE performance, was also established with the help of simulations in [104]. The results for SINR are displayed in Figure 4.4(e) for Direction I and in Figure 4.4(f) for Direction II. In contrast to RSSI, it is seen that the throughput has a relation to the SINR and is increasing with high SINR values. A similar conclusion that SINR compared to the RSSI is a more suited KPI to gauge the link performance is also established in [79]. The authors in [79] established that SINR based vertical handover algorithms offer higher throughput values under any noise level compared to power, RSSI, based algorithms.

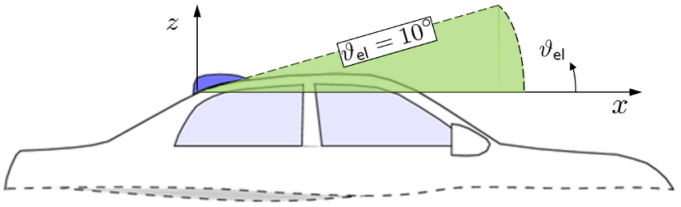

(a) Elevation ϑ for the radiation pattern assessment.

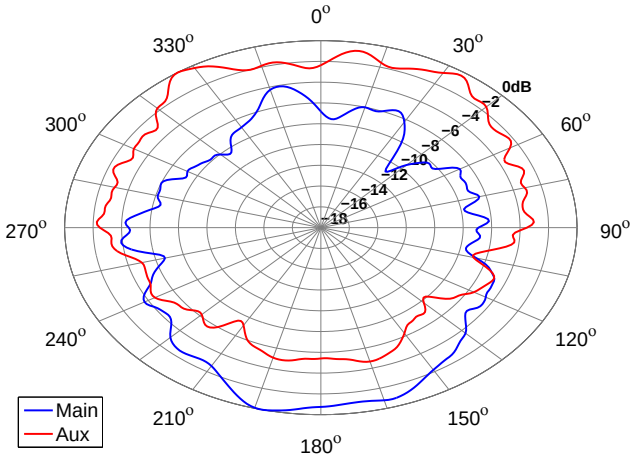

(b) Normalized pattern averaged for ϑ_{el} between $0\,^{\circ} - 10\,^{\circ}$, see Figure 4.5(a).

Figure 4.5: Radiation pattern measurement of P(I) on the vehicle rooftop.

However, both KPIs are suitable means to determine performance degradation of MIMO antenna system. Taking into consideration the rank indicator in the scatter plots, it is revealed that lower throughput values are obtained when the rank indicator has a value of 1 as such diversity is used instead of SMX transmission. This behavior predominantly occurs for Direction I, as seen in the previously discussed histograms.

(a) Direction I.

(b) Direction II.

Figure 4.6: Rank indicator results in an area close by the base station.

In particular this is observed for RSSI values ranging from -30 dBm to -65 dBm and SINR values ranging from -5 dB to 10 dB. Analyzing the rank indicator on the entire measurement track reveals that this performance degradation is occurring predominantly in areas in close vicinity to the base station in an obstructed LOS as wells as a direct LOS scenario. To illustrate that primarily the difference in antenna gain is responsible for this performance deterioration the rank indicator results are shown in an area close to the base station in Figure 4.6. Comparing the rank indicator results for Direction I, Figure 4.6(a) and Direction II, Figure 4.6(b), reveals that a deterioration is seen depending on whether the vehicle is driving towards or away from the base station. When driving in Direction I the rear of the vehicle is primarily pointing towards the base station. For the opposite way, Direction II, the signals are mainly picked up by the front region of the vehicle. Analyzing the radiation pattern measured on the vehicle rooftop, it is shown that this behavior is caused by a gain imbalance of the main and aux antenna. The normalized radiation pattern of P(I) is shown in Figure 4.5(b) and is averaged here between 0 ° and 10 ° in elevation. Averaging is considered due to the increased LOS component of the signal in close proximity to the base station, see [72]. In the non-normalized radiation pattern it is seen that the gain values of the aux antenna alternate between 0 dBi and -8 dBi, whereas the gain values change between 2 dBi and -9 dBi in case of the main antenna. Although the gain values differ overall significantly between the antenna systems the gain difference of the main and aux antenna does not exceed approx. 6 dB. Calculating the gain difference between the main and aux antenna yields for Direction I, in the azimuthal range of 120 ° - 240 ° 5.7 dB. In case of Direction II, thus the azimuthal range of 300 ° - 60 °, this difference results in 3.2 dB. The higher gain difference of 2.5 dB in case of Direction I is the primary reason for the fallback to diversity transmission. The communication links of the main and aux antenna

are to a higher degree imbalanced, which results in diversity being scheduled by the base station instead of SMX. A similar behavior is also seen for Direction II after driving by the base station, cf. Figure 4.6(b), where also the signals are primarily picked up by the rear region of the vehicle. Although the antenna gain difference is an essential KPI for a fallback from SMX transmission to diversity, drops or nulls occurring in the radiation pattern are also key to support SMX. This is, for instance, is seen for Direction I when driving towards the base station, where a fallback to diversity transmission occurs even though the gain differences are not as high. Due to the evaluation of only one antenna system and the dependence on the scheduling occurring in the network it is difficult to pinpoint the exact threshold for the gain differences or the gain drops in the radiation pattern. Nevertheless the evaluation illustrates that differences in the antenna gain and nulls in the radiation pattern are key for the SMX performance of MIMO antenna systems.

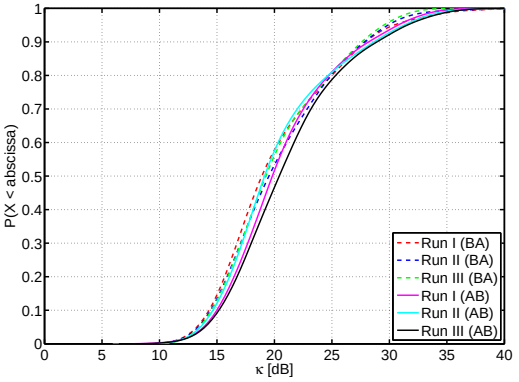

(a) Condition number.

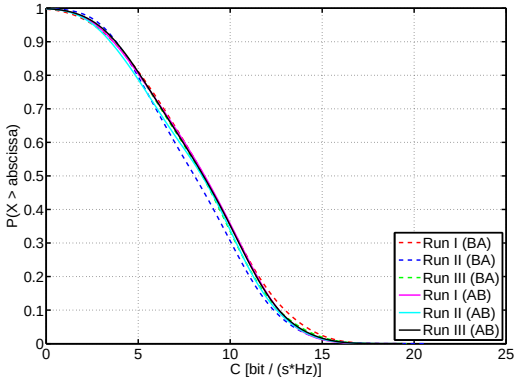

(b) Mutual Information.

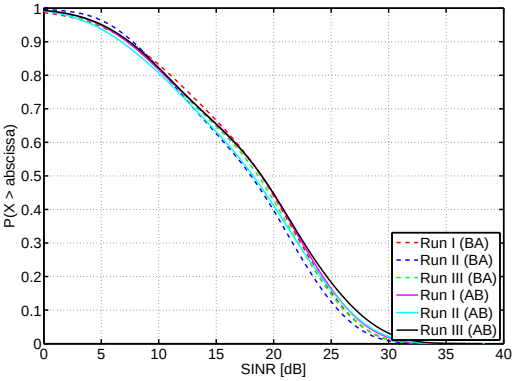

(c) SINR.

Figure 4.7: Reproducibility of the measurements.

4.1.3 Passive Measurements

The prototypical antenna systems are analyzed in this Section on system level with passive measurements. In Section 2.1.2 it was pointed out that the main advantage of passive compared to active measurements is their reproducibility, which results from the methodology being based on the evaluation of pilot symbols broadcasted periodically by the base station [35]. The reproducibility using passive measurements is shown only with the help of prototype antenna P(I). The analyzed KPIs include the mutual information (C), condition number (κ) and SINR as seen in Figure 2.2 in Section 2.1.1. The results in Figure 4.7 are gathered in six consecutive measurement runs, three in each direction. As illustrated in Section 2.1.1, the measurements are conducted at the center frequency of the operators band in the downlink (796 MHz) using a 10 MHz bandwidth. The abbreviations (BA) and (AB) illustrate the chosen driving direction in the test track shown in Figure 2.3, see Section 2.1.1. Considering the cumulative distribution function (CDF) curves of all KPIs and the corresponding percentiles in Table 4.7 reveals that the measurements are very similar showing low deviations from one another. Moreover, are the results also independent of the driving direction. Thus it feasible to conclude that the measurements are reproducible, which was also shown in [27].

Reference Antenna Setups To investigate the impact of antenna isolation on the KPIs κ and C, magnet mount monopole antennas are used as a reference. Antenna separations of $d = \{3, 11, 23, 43, 53, 83\}$cm are evaluated for the reference antenna system for the LOS and nLOS of the track as well as for the entire measurement track. All antenna separations are measured from the center of one monopole to the other. Among these distances 11 cm is the highest realizable antenna spacing in the currently deployed antenna housing in series production. The different reference antenna setups are placed 10 cm in front of the housing of the integrated antennas, cf. Figure 4.8. A distance of at least 10 cm to the roof edges or insets, such as for the regular antenna system, is required according to the specifications of the manufacturer to ensure proper functionality [103]. Only in case of a separation of 83 cm are the reference antennas aligned with the conventional mounting space. This

%ile	KPI	Run I (BA)	Run II (BA)	Run III (BA)	Run I (AB)	Run II (AB)	Run III (AB)
15	κ	15.0	15.1	15.1	15.7	15.2	16.0
	C	12.1	11.6	11.8	11.8	11.8	11.8
	SINR	24.8	24.4	24.9	24.8	24.8	25.7
50	κ	18.7	19.2	19.1	19.5	18.9	20.2
	C	8.4	7.9	8.4	8.5	8.4	8.5
	SINR	18.8	17.8	18.5	18.9	17.8	18.8
90	κ	27.8	27.8	27.4	27.9	28.6	28.7
	C	3.5	3.6	3.6	3.5	3.4	3.7
	SINR	7.2	7.4	6.8	7.0	6.6	7.2

Table 4.7: Corresponding percentiles of the CDFs from Figure 4.7.

is done in order to have a direct reference to the integrated antenna systems for the best case scenario in terms of antenna separation, cf. Figure 4.8. It is not possible to use this position for smaller antenna separations as this is not achievable with the antenna housing being in between. The yielded antenna isolation values for the different separations are presented in Table 4.8. As starting point the antennas are positioned in the middle of the roof and then separated towards the roof edges. The measurements are taken with a calibrated network analyzer[1]. It is seen that for the lowest antenna separation of 3 cm the antenna system yields an isolation of 12.8 dB. An antenna separation of 11 cm, approximately the length of the antenna housing, gives an isolation of 18.5 dB. A further increase in separation does not impact the antenna isolation significantly. For distances between 23 cm and 53 cm the isolation is only increased by approximately 6 dB. As expected the highest antenna isolation, of 40 dB is obtained for the largest separation of 83 cm.

Table 4.8 also includes the mean values for the KPIs κ, C and SINR determined for the different reference antenna setups. As previously stated all three KPIs are evaluated for the LOS, nLOS and entire measurement track. The results show that with increased antenna separation lower κ values and higher C values are yielded. As the SINR values do not give an indication towards the assessment and ranking of the antenna setups, they are not considered further. The KPIs κ and C illustrate that the reference antenna setup with a separation of 83 cm yields a significantly higher performance compared to the other setups. Recalling that for this separation the reference antennas are aligned with the conventional mounting position, cf. Figure 4.8, this also illustrates how essential the placement of the antenna systems on the vehicle rooftop is. Comparing the κ values for all three scenarios, shows that significant changes occur between the antenna separations of 3 cm and 11 cm, see Figure 4.9(a). The lowest κ values are yielded for the nLOS section. Moreover, are the κ values for this section of the measurement track also decreasing more rapidly with an increase of the antenna separation. The κ value drops from 20.4 dB to 15.8 dB for an increase of antenna separation from 3 cm to 11 cm. In contrast to this result κ is reduced by only 2 dB from 24.4 dB to 22.4 dB for the same separation in case of the

[1] Agilent N5230A, Firmware: A.07.50.26

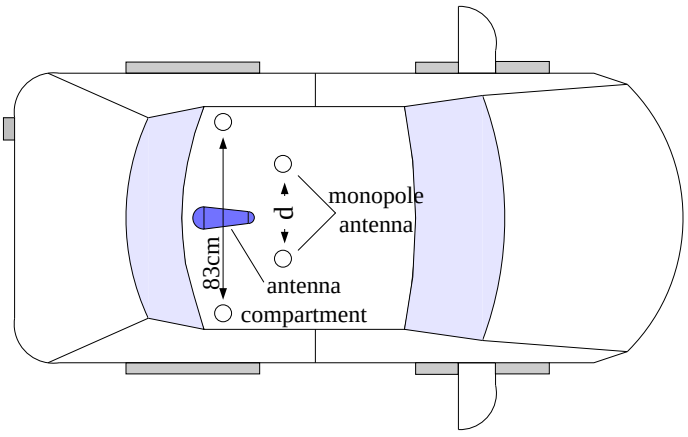

Figure 4.8: Reference antenna setups on the vehicle rooftop.

LOS section. Distances between 11 cm and 43 cm do not show significant changes. Improvements in κ are seen, which are most evident for the LOS section, starting at 53 cm. The highest antenna separation of 83 cm illustrates, as expected, the least correlated channels, yielding similar results for the LOS as well as nLOS scenario. Similar to κ a saturation of the C values occurs for separations between 11 cm and 53 cm. As illustrated for κ, the highest increase of C is seen when increasing the reference antenna setup from 3 cm to 11 cm, see Figure 4.9(b). This increase in separation results in approx. a 1 bit/(s·Hz) higher C value for each considered scenario. Although the reference antenna setups yield the least decorrelated channels, thus the highest κ values for the LOS section, the highest C values are recorded here. The values are approximately 3 bit/(s·Hz) higher for a separation of 53 cm and even approx. 4 bit/(s·Hz) for 83 cm. This is mainly resulting from the increased SINR values, which are recorded in this section of the measurement route. These values are more than 8 dB higher compared to the nLOS section.

Dist. [cm]	κ [dB]			C [bit/(s·Hz)]			SINR [dB]			S21 [dB]
	Entire	LOS	nLOS	Entire	LOS	nLOS	Entire	LOS	nLOS	
3	21.8	24.4	20.4	6.6	7.8	4.6	14.1	17.8	9.2	12.8
11	18.0	22.4	15.8	7.7	8.6	5.7	15.3	18.8	10.8	18.5
23	18.2	22.8	16.2	7.4	8.3	5.2	14.8	18.2	10.0	23.8
43	17.5	21.9	15.5	7.7	8.8	5.6	15.3	19.1	10.6	26.6
53	16.9	20.5	15.3	7.6	9.2	5.4	14.8	19.1	10.0	30.1
83	14.4	14.7	14.3	8.9	11.1	6.3	16.7	21.5	11.5	40

Table 4.8: C, κ, SINR and antenna isolation of the reference antenna.

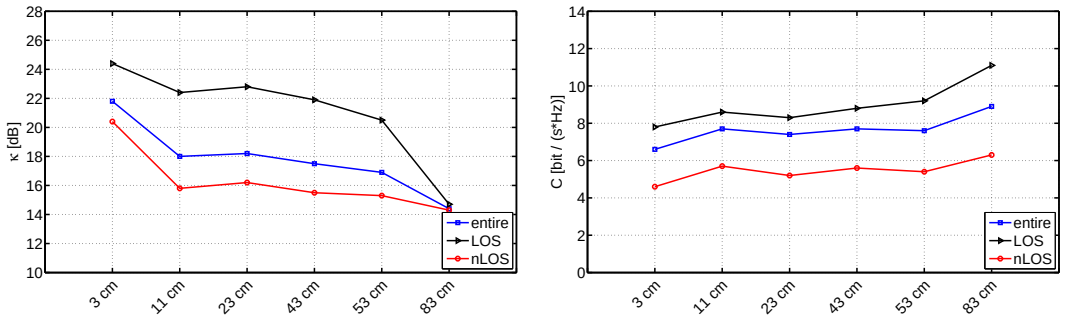

(a) Condition number.

(b) Mutual information.

Figure 4.9: Mean KPI values of the reference antenna setups for different scenarios.

To thoroughly analyze the occurring differences between the reference antenna setups CDF curves, are presented for the aforementioned scenarios in Figure 4.11. As before the SINR values are not considered, thus CDF functions are only shown for the KPIs κ and C. The corresponding percentiles for the two KPIs are shown in Table 4.9 and 4.10 respectively. As suggested in [11] for comparing different CDF curves the following percentiles are used: $15th, 50th, 90th$. The in terms of overall antenna

performance relevant scenario, the complete measurement track, corroborates the previous finding of a saturation area between a separation of 11 cm and 53 cm, see Figure 4.11(a). This is also well visualized analyzing the 15th and 50th percentiles in Table 4.9. To better visualize the yielded percentiles in case of the entire measurement the results of the KPI κ are displayed for the different setups in Figure 4.10(a). The κ value of the reference antenna setup with a separation of 3 cm differs around 4 dB from the other setups. The other setups yield similar results, except the highest separation of 83 cm, which illustrates the highest probability for lower κ values. Considering the necessary effort to separate antenna systems by, for instance, 53 cm compared to 11 cm the yielded performance does not justify the attempt. In case of the nLOS scenario the impact of the antenna separation on the resulting performance is even further reduced. The κ values start to converge above an antenna separation of 11 cm. Although the highest separation of 83 cm still yields the lowest κ values, the other antenna setups differ only to a small degree from this reference configuration. The highest difference is seen for the 90th percentile, which compared to the other values shows a high deviation of 2.5 dB. This is further increased for the LOS scenario of the measurement track yielding a difference of more than 7 dB between the setups 53 cm and 83 cm for the 90th percentile. In case of the LOS scenario the gap between the lowest antenna separation of 3 cm and the remaining distances is also decreased. The least differences are yielded at high percentiles, such as the 90th.

%ile	Scenario	3cm	11cm	23cm	43cm	53cm	83cm
15	entire	17.3	13.2	13.4	12.5	12.5	11.4
	non-LOS	17.2	12.6	13.1	12.0	11.8	11.7
	LOS	19.9	16.7	17.2	16.2	15.8	11.2
50	entire	21.4	16.8	16.8	16.6	16.2	14.0
	non-LOS	20.1	15.4	15.8	15.0	14.9	14.3
	LOS	24.2	22.1	22.3	21.2	20.1	14.1
90	entire	27.1	25.1	25.0	24.3	22.7	17.5
	non-LOS	24.5	19.7	20.3	19.4	19.4	16.9
	LOS	30.5	29.3	29.8	29.3	26.8	19.3

Table 4.9: Percentiles of κ for the discussed reference antenna setups.

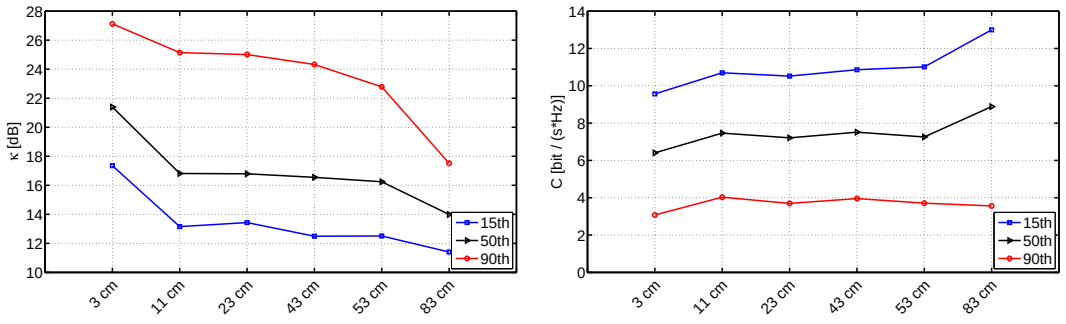

(a) Condition number.

(b) Mutual information.

Figure 4.10: Reference antenna setup percentiles of κ and C for the entire test field.

A similar behavior for the different antenna setups is also seen for the KPI C. Figure 4.11(b) illustrates that the antenna separations of 11 cm, 23 cm, 43 cm and 53 cm yield similar results for the entire measurement track. Thus showing compared to κ also a saturation of the C values, cf. Figure 4.10(b). The highest mutual information is, as expected, obtained for the reference configuration at 83 cm. The 15th percentile shows an increase in C of up to 2 bit/(s·Hz) and the 50th of approx. 1.6 bit/(s·Hz) compared to the saturated values, cf. Table 4.10. As expected the lowest C values are obtained at a separation of 3 cm, which are for all percentiles up to 1 bit/(s·Hz) lower compared to the saturated antenna setups. The nLOS section of the measurement shows compared to the other scenarios the lowest C values, see Figure 4.11(d). Furthermore, the results also illustrate a reduced difference between the C values between the different reference antenna setups. The setup with a separation of 83 cm still yields the highest mutual information values. However, for a low percentiles, such as the 15th, the C is still about 3.6 bit/(s·Hz) lower compared to the entire measurement track. In contrast to the nLOS section, higher mutual information values are yielded for the LOS scenario. Similar results were also obtained in [105], where measurement drives were conducted in an UMTS network. As previously seen for the KPI κ the reference antenna setup separated by 53 cm, deviates from the saturated outcome of the separations 11 cm, 23 cm and 43 cm. Increased C values are especially yielded towards lower percentiles. The mutual information is in case of the LOS section value more than 1 bit/(s·Hz) higher compared to the entire measurement track. Thus the impact of antenna isolation to the performance of the antenna system is especially crucial in the LOS section.

%ile	Scenario	3cm	11cm	23cm	43cm	53cm	83cm
15	entire	9.6	10.7	10.5	10.9	11.0	13.0
	non-LOS	6.3	7.5	6.9	7.3	7.3	9.4
	LOS	10.6	11.6	11.3	11.8	12.7	14.5
50	entire	6.4	7.5	7.2	7.5	7.3	8.9
	non-LOS	4.5	5.4	5.0	5.4	5.0	6.0
	LOS	7.8	8.8	8.5	8.9	9.0	11.0
90	entire	3.1	4.0	3.7	4.0	3.7	3.6
	non-LOS	2.5	3.6	3.2	3.7	3.2	2.7
	LOS	3.9	4.4	4.1	4.9	4.6	6.3

Table 4.10: Percentiles of C for the discussed reference antenna setups.

Prototypical Antenna Systems In the following the prototypical antenna systems are compared to three selected reference antenna setups. These setups include the lowest separation of 3 cm and the highest realizable separation in the current antenna housing 11 cm. Moreover, is also the greatest reference antenna separation of 83 cm included. The characteristics of the investigated prototypical antenna systems were already discussed in Section 4.1.1. Recalling from Section 4.1.1 the antenna systems P(I) and 'P(I) opt' are physically identical antennas with the exception that 'P(I) opt' uses a phasing line as decoupling branch at 796 MHz to reduce antenna decoupling. Comparing the results of the reference antenna setups to the

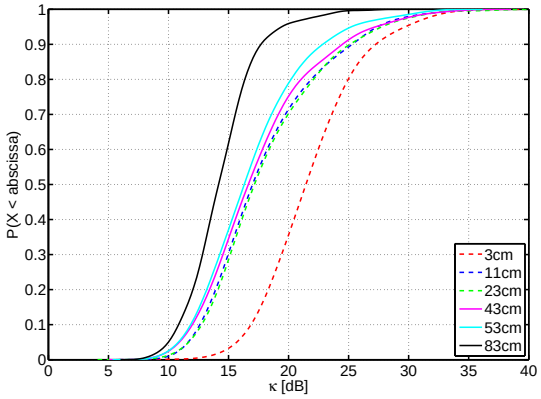

(a) κ, whole track.

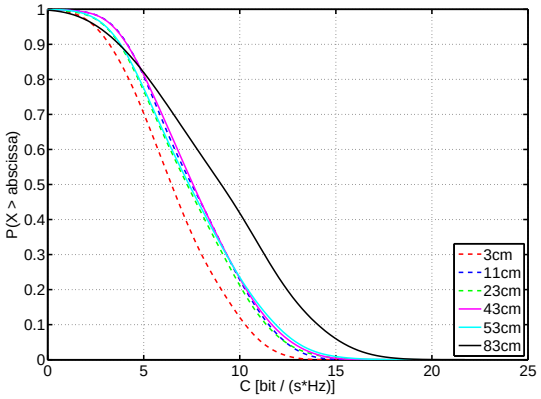

(b) C,whole track.

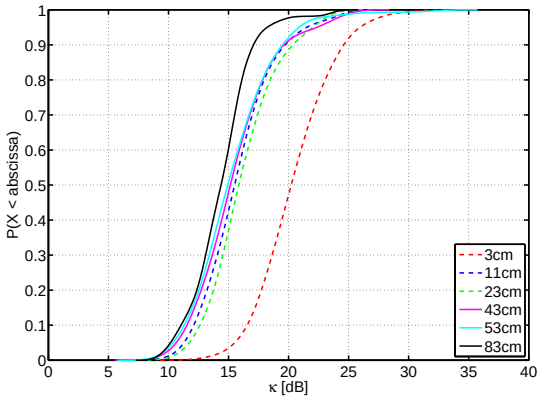

(c) κ, nLOS.

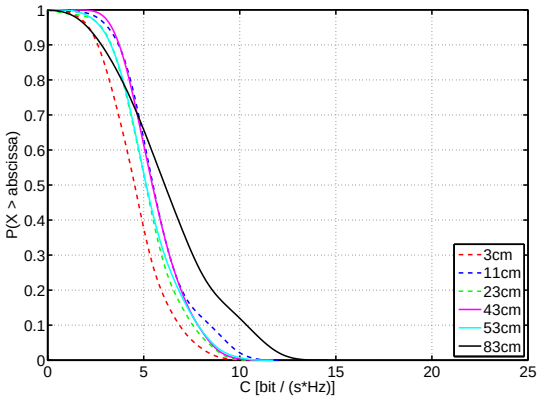

(d) C, nLOS.

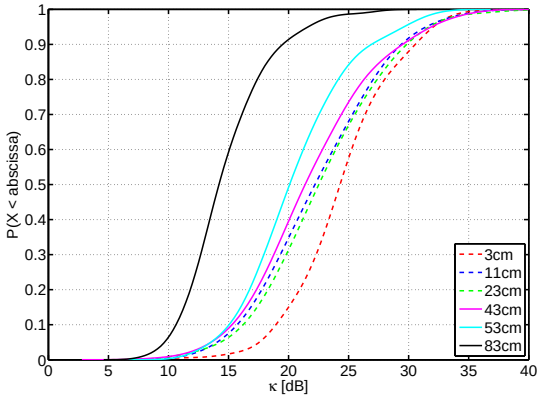

(e) κ, LOS.

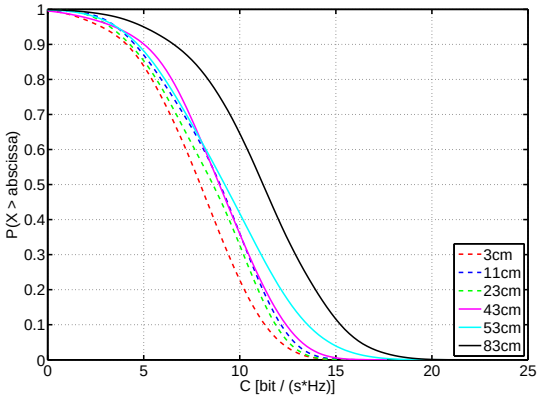

(f) C, LOS.

Figure 4.11: CDF and CCDF curves for the reference antenna setups for the entire measurement track, its nLOS as well as LOS section.

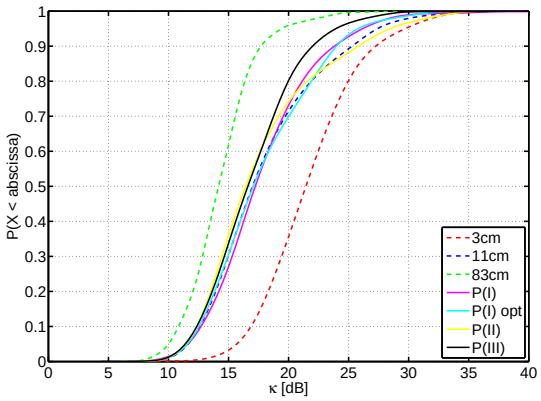

(a) κ, whole track.

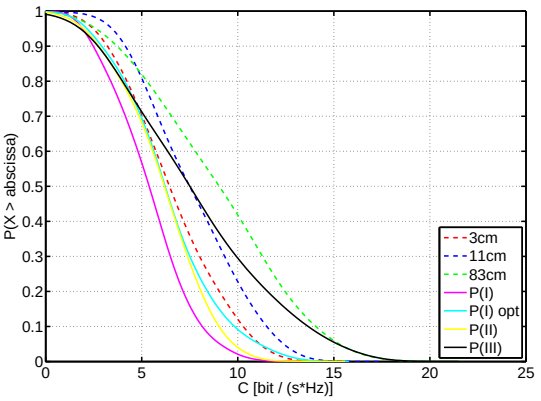

(b) C, whole track.

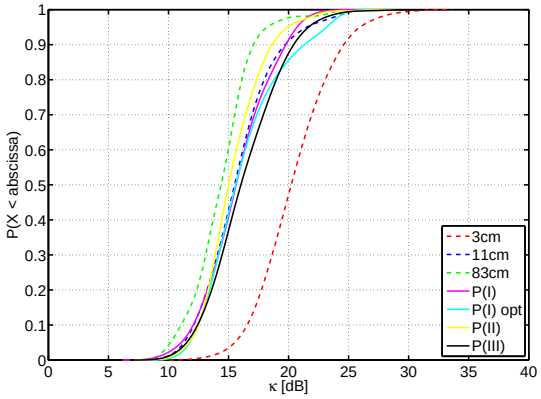

(c) κ, nLOS.

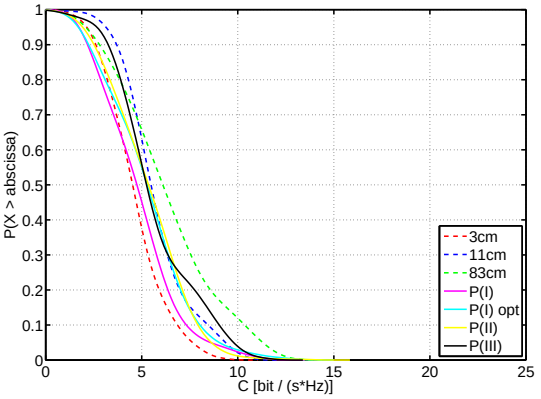

(d) C, nLOS.

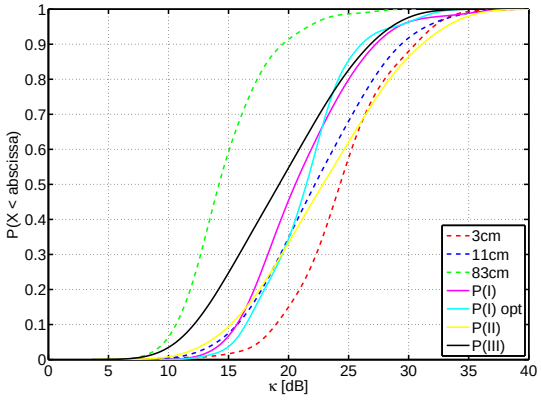

(e) κ, LOS.

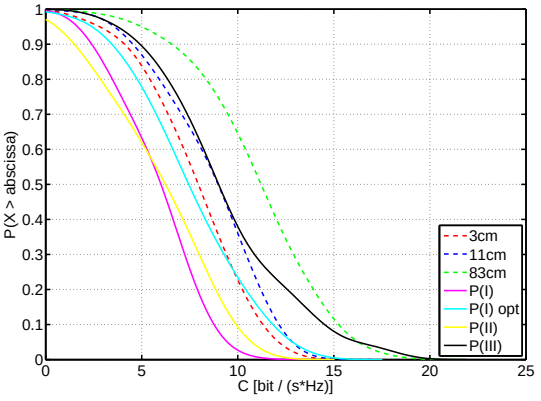

(f) C, LOS.

Figure 4.12: CDF and CCDF curves for the reference antenna setups and the prototypical antennas for the entire measurement track, its nLOS as well as LOS section.

prototype antennas allows to visualize the impact of antenna characteristics on the aforementioned KPIs. The CDF curves for the KPIs κ and C are shown for the different sections of the measurement route in Figure 4.12. Similar to the previous investigation the percentiles, 15th, 50th and 90th, see [11], are evaluated in Table 4.11 for κ and in Table 4.12 for C. To better visualize the obtained percentiles, they are presented for each antenna configuration in Figure 4.13(a) and respectively in Figure 4.13(b). As previously, only the outcome of the entire measurement track is displayed, since this provides an overall assessment taking into consideration all analyzed scenarios. Evaluating the results for κ for the entire measurement track reveals that the differences between all prototype antennas and the reference antenna separation of 11 cm is low for most percentiles. Deviations from this behavior occur for higher percentiles, such as the 90th, except in case of P(II). The yielded κ curves of all prototype antennas are enclosed by the lowest reference antenna separation of 3 cm and the highest of 83 cm. The lowest κ values among all prototypes are yielded by P(III), cf. 90th percentile for the entire measurement track in Table 4.11. P(III) is also the only antenna prototype yielding the lowest differences between the entire measurement track and the nLOS section for the KPI κ, cf. Figure 4.12(c). This becomes even more evident comparing the κ values of the 15th, 50th and 90th percentile of the entire measurement track and the nLOS section in Table 4.11. A similar behavior is also seen for the lowest reference antenna separation of 3 cm. However, this setup illustrates low κ values for high percentiles, such as the 90th. The prototype antenna systems and the reference antenna setups, except the one with a separation of 3 cm, show overall steeply rising curves in case of the entire measurement route and its nLOS section. The deviations between the reference antenna setup with a separation of 83 cm and all other antennas, except the reference system separated by 3 cm, is considerably reduced. This illustrates that the difference in the antenna design and thus the corresponding antenna characteristics do not impact the results to a significant degree. This behavior changes considerably in the LOS section, cf. Figure 4.12(e). The least affected is the reference antenna setup separated by 83 cm. The highest deviation compared to the previously analyzed scenarios is seen in this case for higher percentiles, such as the 50th and the 90th, cf. Table 4.11. The CDF curves for the other reference antenna setups and prototypes run flatter and are shifted towards higher κ values. Compared to the previous scenario the difference in κ values between all antennas and the lowest reference antenna separation of 3 cm is reduced. The differences among the prototypical systems and the reference antenna setups, except the one separated by 3 cm, are in turn increased. The CDF curves are spread further apart, yielding greater differences in the performance of the considered antenna systems. Out of all prototypes P(II) achieves the lowest performance, thus the highest κ, whereas P(III) yields the lowest κ values.

The results for the KPI C are presented for the entire measurement track in Figure 4.12(b). As expected the reference antenna setup with a separation of 83 cm yields also the highest mutual information. However, also P(III) achieves considerable values, matching the C values for percentile below the 10th. As the CDF curves of C, see Figure 4.12(a), have not pointed towards this behavior, these results show that solely the κ values are not sufficient for the benchmark of MIMO antenna systems.

%ile	Scenario	3cm	11cm	83cm	P(I)	P(I) opt	P(II)	P(III)
15	entire	17.4	13.2	11.4	13.2	13.0	12.8	12.8
	non-LOS	17.2	12.6	11.7	12.5	12.8	12.8	13.0
	LOS	19.9	16.7	11.2	16.3	17.0	16.1	12.9
50	entire	21.4	16.8	13.4	16.8	16.8	16.4	16.4
	non-LOS	20.1	15.4	14.3	15.6	15.6	14.8	16.0
	LOS	24.2	22.1	14.1	20.3	21.3	22.6	19.2
90	entire	27.1	25.1	17.5	23.6	23.9	25.6	21.8
	non-LOS	24.5	19.7	16.9	19.7	21.3	18.5	20.2
	LOS	30.5	29.3	19.3	27.0	25.8	31.1	26.8

Table 4.11: Percentiles for κ for the reference antenna setups and prototype antennas.

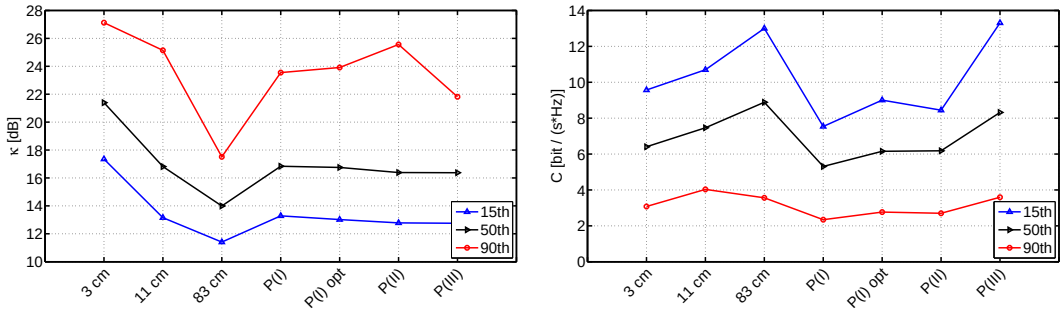

(a) Condition number.

(b) Mutual information.

Figure 4.13: Reference and prototype antenna percentiles for the entire test field.

The C values obtained with the prototype antennas P(I) and P(II) are even lower compared to the smallest reference antenna separation of 3 cm. The lowest results are obtained with the prototype P(I). The optimized version of 'P(I) opt' having a higher antenna isolation yields especially towards lower percentiles, such as the 15th, increased mutual information values of 1.5 bit/(s·Hz). Thus, this illustrates how essential antenna isolation is for enhanced antenna performance in terms of mutual information. Even for higher percentiles, such as the 50th, an improvement of approximately 1 bit/(s·Hz) is seen. The yielded results of P(II) is enclosed between the outcome of P(I) and P(I) opt. Among all prototype antennas the highest C values are recorded with P(III), which are also the closest to the reference antenna separation of 83 cm. This behavior changes in case of the nLOS scenario, shown in Figure 4.12(d). The difference between both antennas is increased to 1 bit/(s·Hz) for percentiles, such as the 15th and 50th, cf. Table 4.12. Furthermore, is the overall distance between the yielded results of the antenna systems reduced. Thus differences in the antenna design and setup are not feasible to be adequately differentiated in this scenario. Compared to the entire measurement track, the lowest mutual information values are obtained with the lowest reference antenna separation of 3 cm. In contrast to the nLOS scenario, the LOS section yields similar results to the outcome of the entire measurement track, cf. Figure 4.12. However, the reference antenna setup with a separation of 83 cm yields significantly higher mutual information values compared to

the other antennas, cf. Table 4.12. Although the yielded C values of P(III) converge to the behavior of this antenna setup, the C value are for percentiles, such as the 50th or 90th, around 2 bit/(s·Hz) lower. Moreover, is the difference in performance between the isolation optimized antenna system 'P(I) opt' and its regular version P(I) revealed more extensively. These difference are increased further towards lower percentiles, such as the 15th, where 'P(I) opt' illustrates a 2.7 bit/(s·Hz) higher C value. Similar to the entire measurement track the prototypes P(I) and P(II) yield the lowest mutual information values, which are once again below the one obtained for the reference antenna separation of 3 cm.

%ile	Scenario	3cm	11cm	83cm	P(I)	P(I) opt	P(II)	P(III)
15	entire	9.6	10.7	12.3	7.5	9.0	8.4	12.3
	non-LOS	6.3	7.5	9.4	6.7	7.4	7.3	8.4
	LOS	10.6	11.6	14.5	8.2	10.9	9.2	13.3
50	entire	6.4	7.5	8.9	5.3	6.2	6.2	7.3
	non-LOS	4.5	5.4	6.0	4.7	5.1	5.2	5.1
	LOS	7.8	8.8	11.0	5.9	7.2	6.2	8.9
90	entire	3.1	4.0	3.6	2.3	2.8	2.7	2.6
	non-LOS	2.5	3.6	2.7	2.1	2.1	2.4	3.2
	LOS	3.9	4.4	6.3	2.3	3.4	1.3	4.7

Table 4.12: Percentiles for C for the reference antenna setups and prototype antennas.

4.1.4 Conclusion

In this Section a methodology to assess cellular MIMO systems was discussed and applied. The assessment was carried out on component level with KPIs relating to the antenna impedance and to the antenna gain. To better quantify the antenna gain related KPIs statistical metrics were introduced. These included the probability of antenna gain difference (ρ_{Diff}) exceeding a certain threshold and the crossing rate (ρ_{TH}) per antenna. Moreover, also the peak values of the antenna gain (G_{max}) and (G_{min}) as well as the (G_{mean}) value were evaluated. To cover direction dependent behavior all aforementioned KPIs were assessed separately for the front and rear region of the vehicle. From the assessed prototypical antennas two systems were based on 3D MID technology and the remaining antenna on a conventional PCB design. The 3D prototypes offering more possibilities in regards to the antenna design achieved an isolation value, which was about twice as high as in the case of the PCB antenna. This is resulting from exploiting the available volume of the antenna housing more efficiently, hence allowing to separate the antennas further compared to the PCB prototype.

The prototypical antenna systems were assessed on systems level conducting active and passive measurements to evaluate their SMX performance. Both measurements were carried out at 796 MHz, the center frequency of the operators frequency band. The active measurements carried out with a prototypical antenna system illustrated that in a LOS scenario with the base station a fallback to diversity transmission potentially

occurs. Analysis into the antenna system revealed that this effect predominately took place in the rear region of the vehicle. In this region a gain difference of around 6 dB was seen between the antennas of the MIMO system. Naturally the exact value for differences in the antenna gain or gain outages, which result in such a performance deterioration, varies depending on the network operator. However, in designing antenna systems, balanced gain values between the antennas of a MIMO system and low crossing rates of reference antenna gain is key for the SMX performance [106]. In order to achieve a low interference between the antennas and consequently a high antenna isolation, the possibility of placing the antennas is limited. Thus to achieve high antenna isolation and to limit the antenna interference they have to be separated as far as possible. Considering the size constraints of the integration volume and the centralization of the antenna systems, this is, however, challenging.

Passive measurements were performed to assess the prototypical antenna systems independent of the current network condition. As performance metrics the condition number (κ) and mutual information (C) were used. The impact of antenna decoupling on system level was investigated by modifying the separation of monopole antennas on the vehicle rooftop. The outcome was compared to the prototypical antenna systems and to a fourth prototypical system, which apart from a decoupling branch was physically identical to an already analyzed prototype. The investigation revealed that distances above an antenna separation of 11 cm, which is approximately a quarter of the wavelength at 800 MHz, yields no significant changes in antenna performance. It was shown that an improved performance is possible, but requires a substantial antenna spacing of, for instance, 83 cm, which is not realizable in the current antenna integration volume. Comparing the prototypical antennas revealed that a singular KPI is unsuitable to benchmark the performance of antenna systems. As such the investigation illustrated that the impact of antenna isolation is better revealed with the achieved mutual information rather than the condition number. The results in this Section showed that using system level KPIs, such as κ and C, are well suited to rank MIMO antenna systems. It is thus concluded that for assessment of future antennas these system level KPIs have to be included in specification sheets in addition to impedance and radiation level KPIs. Focusing on singular KPIs, such as the antenna isolation, are potentially misleading in regards to the overall antenna performance, as seen for the certain reference antenna setups.

4.2 802.11p Antenna Benchmark

In this section the 802.11p antennas, which are part of the previously discussed prototypical systems, are analyzed. Emphasize is put on the evaluation of the diversity efficiency as SMX transmission is not intended for 802.11p communication, see also Section 2.2. On system level the prototype systems are evaluated on the 802.11p test field. The component level evaluation investigates the capability of both antennas of each prototypical system to cover the front as well as the rear region of the vehicle. Consequently, this analysis shows the degree to which the prototype systems are able to compensate the performance deteriorating effects occurring by integrating them on the vehicle rooftop. The analysis conducted here is organized as follows: In the subsequent Section 4.2.1 the prototype systems are analyzed in detail applying the KPIs from Section 2.3. Based on these evaluations measurements are conducted to benchmark the different prototype systems. As all prototype systems apply a different methodology to place 802.11p antennas among the cellular antennas, this evaluations also gives insight into the positioning of such antennas within such a system. The yielded benchmark results of the antenna systems are presented in Section 4.2.2. Due to the high operating frequency of 5.9 GHz evaluations, such as in [10], showed that blind spots for certain angles in the azimuth are occurring, when mounting the antennas on the vehicle. As compensating such blind spots is key for successfully deploying vehicular safety applications a methodology is illustrated in Section 4.2.3 to accomplish compensation without altering the exterior design of the vehicle.

4.2.1 Characteristics of the AUTs

The discussed prototypical antenna systems include two antennas in order to exploit diversity transmissions techniques for 802.11p communication. The position of the 802.11p antennas differ among the prototypes, whereas the cellular antennas are located at similar positions. The major difference between P(I) and the other prototypes, cf. Figure 4.1, is that in this case the cellular and 802.11p frequencies are covered by the same PCB antenna. Consequently, the antenna system uses a diplexer to offer separate ports for the cellular and ad-hoc domain. The cellular antennas of P(II) and P(III) are placed at the rear as well as the front region of the antenna housing. The antenna characteristics of the analyzed prototype systems are summed up in Table 4.13. Analyzing the S-parameters of the prototypes reveals that the antennas are well matched. Among all prototypes P(III) illustrates the highest return loss of -13 dB and -17 dB respectively. All prototypes yield a higher mismatch for their main antenna, which is primarily intended to cover the rear of the vehicle. P(II) and P(III), which are based on 3D MID technology, thus offering increased possibilities for the antenna design, illustrate the lowest mismatch values with -18 dB and -17 dB respectively. However, the conventional PCB based rooftop antenna P(I) yields the highest isolation with 27 dB. This is partially resulting from the applied design methodology in case of P(II) and P(III). P(II), cf. Figure 4.1(c), has the antennas placed adjacent to one another on the right side of the antenna housing. The

antenna feeds are separated by a distance of 2 cm. In case of P(III) the antennas are mounted on opposite sides of the antenna housing at similar longitudinal positions. The lowest antenna separation is approximately 1 cm and the distance between the corresponding feeds is 2 cm. Thus in both cases the antenna separation is compared to P(I) lower, due to the applied design methodology. Although both antennas are in case of P(I) aligned, they are separated by 5 cm, which is the maximum separation given the size constraints of the antenna housing.

	antenna	section	unit	P(I)	P(II)	P(III)
S11	main		[dB]	-17	-15	-13
S22	aux		[dB]	-20	-23	-17
S21	main-aux		[dB]	-27	-18	-17
RE	main		[%]	74	n/a	72
	aux		[%]	79	n/a	72
G_{max}	main	(rear)	[dBi]	4.2	2.8	3.9
		(front)	[dBi]	3.3	1.7	3.3
	aux	(front)	[dBi]	3.5	3.4	3.8
		(rear)	[dBi]	1.2	1.9	3.4
G_{min}	main	(rear)	[dBi]	0.4	-4.8	-3.6
		(front)	[dBi]	-2.7	-19	-3.6
	aux	(front)	[dBi]	-0.6	-9.6	-3.3
		(rear)	[dBi]	-6.9	-10	-4
G_{mean}	main	(rear)	[dB]	2.3	-0.7	0.7
		(front)	[dB]	1.1	-3.5	0.2
	aux	(front)	[dB]	1.7	-0.3	0.8
		(rear)	[dB]	-2.2	-2.5	0.6
ρ_{TH}	main	(rear)	[%]	0	24	6
		(front)	[%]	0	64	8
	aux	(front)	[%]	0	27	3
		(rear)	[%]	43	42	14
ρ_{Diff}	main-aux	(rear)	[%]	88	38	14
		(front)	[%]	3	65	33

Table 4.13: Characteristic values of all prototypical 802.11p antennas at 5.9 GHz.

Comparing the maximum achieved gain G_{max} in Table 4.13 for all prototypes systems for both the rear and front region reveals that P(III) yields the most homogeneous values. The corresponding normalized antenna radiation pattern are shown in Figure A.1 in the Appendix. The values are above 3.3 dBi and do not vary more than 0.5 dB from one another. A low G_{max} value of 1.2 dBi is yielded for the aux antenna of P(I) covering the rear region. A similarly low value is also seen in case of P(II). This is mainly resulting from the previously discussed arrangement of the main and aux antenna. The antennas are in both cases aligned, which does not allow the aux antenna to sufficiently cover the rear region as the main antenna works in this case as a disruptor. The applied design methodology in P(III) with the main and aux antenna on the side bypasses this drawback. A similar effect of the antenna alignment causing deterioration in the pattern is also seen in case of P(II) for the main antenna

covering the front region. The gain drops to 1.7 dBi. Although P(I) has a similar design such a performance deterioration is not seen in this case, which is resulting from the higher separation of the antennas. Similar to G_{max} the lowest variations for G_{min} are seen for P(III); the yielded gain values differ between -3.3 dBi and -4 dBi. In comparison to the other prototypes P(II) shows the most deterioration in the pattern, with a gain as low as -19 dBi. This shows that a close placement of the main and aux antenna, as seen for P(II), potentially causes blind spots in the radiation pattern. This finding is also emphasized by P(I)'s aux antenna, which yields for both the front and rear region values around -10 dBi. However, such an alignment does not necessarily point towards a poor performance, as shown with the results of P(I). Although the antennas are aligned, the prototype yields in contrast to the other prototypes the highest antenna gain values. Only in case of the aux antenna covering the rear, the prototype yields the second highest value. The in terms of overall performance interesting KPI G_{mean} corroborates the aforementioned findings. P(I) is performing best followed by P(III), which shows overall the most balanced values. As previously seen for G_{min} the prototype P(II) shows again performance deficiencies for the aux antenna covering the rear. As indicated from the analysis of G_{min} and G_{max} the main and aux antenna from P(II) perform well in regions they are primarily intended for, that is the rear and respectively the front.

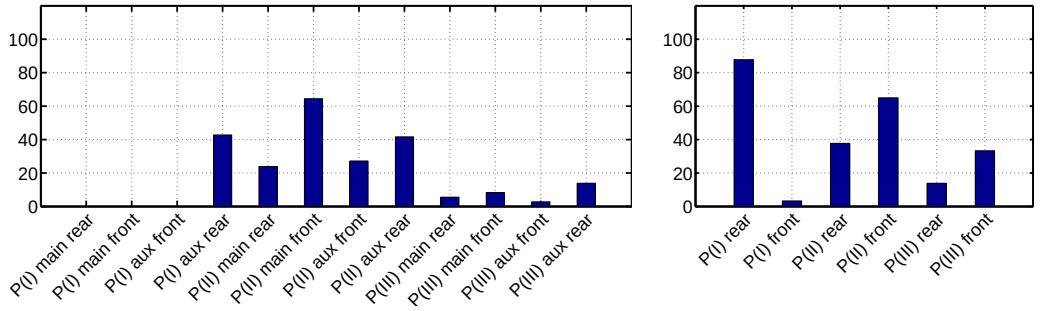

(a) ρ_{TH}. (b) ρ_{Diff}.

Figure 4.14: ρ_{TH} and ρ_{Diff} for all prototypical 802.11p antennas.

To investigate the differences of the prototypes further the yielded results of the KPIs ρ_{TH} and ρ_{Diff} are also depicted in Table 4.13. The threshold 'G_{TH}' is set to -3 dBi and 'G_{δ}' to 3 dB. Higher threshold are not selected as the radiation patterns are obtained on a ground plane, thus do not consider any integrational effects caused by the roof or the antenna housing. Consequently, performance degradation of the pattern incurring in nulls [10] is not included. As such a degradation is not present in the measurements, setting higher thresholds likely results in low values for ρ_{TH} and ρ_{Diff}, which are, however, not the case in reality and falsify the findings. The results illustrate that P(I) and P(III) yield the lowest threshold crossing rates, whereas P(II) yields the highest. This is also well visualized with the bar chart shown in Figure 4.14(a), where for each prototype it is differentiated between the main and aux antenna as well as the region of the vehicle. However, as implied by the previous analysis, the aux antenna of P(I) crosses the threshold approximately half the time

in the rear region. In contrast to P(I) the prototype P(III) shows again an overall balanced performance with the highest level crossing rate reaching only 14 %. P(II) yields crossing rates of approximately one fourth even in regions, where the main and aux antenna are supposed to perform well, thus in the rear and front region. The difference in antenna performance are even better emphasized analyzing the metric ρ_{Diff}, cf. Figure 4.14(b). The previously established difficulty of P(I) covering the rear region well with both the main and aux, is clearly illustrated with the help of this KPI. The difference in antenna gain crosses the pre-determined difference 88 % of the time. The finding that the front region is covered well by P(I) is also be corroborated with ρ_{Diff}. The level crossing rate is as low as 3 %. As expected the highest values are seen for P(II), which yields 38 % and 65 % for the rear and front region respectively. The overall lowest crossing rates are again yielded for P(III). However, applying ρ_{Diff} to the gain values of P(III) also reveals that studying only values, such as G_{max}, G_{min} and G_{mean}, is not sufficient for a complete picture of the antenna performance. The yielded results are with 33 % for the front and with 14 % for the rear region in comparison not high. However, the balanced impression between the main and aux antenna given by the previously discussed KPIs is not able to be verified. Thus a reliable antenna benchmark is only possible when all KPIs are evaluated as a whole.

4.2.2 Benchmark Results

The antenna systems are evaluated in the testbed, described in Section 2.2. The commercial radio Cohda Wireless MK3 [107] is used for both the vehicle and the RSU, which is mounted at the office building on the first floor. The RSU is located in the middle of the measurement route, see Figure 4.16, which is approximately 1.4 km long. The RSU is setup to transmit random packets with an also randomly chosen payload length of 50, 163, 324, 645 or 1100 byte. The randomly varying payload size is resulting from the employed script, which is designed by the manufacturer of the RSU for testing the equipment in different communication scenarios. Approximately 100 packets are sent each second using always the robust modulation scheme quadrature phase-shift keying (QPSK). The transmit power of the RSU is set to 23 dBm, which is also the maximum output power of the radio. The sensitivity of the receiver for successful decoding of the packets is approximately -90 dBm. Consequently, the yielded communication range for each antenna is evaluated according to this threshold. The obtained RSS values are filtered spatially every 10 m to avoid cluttering of the measurements due to a slower traffic flow or for instance waiting periods at traffic lights. Naturally a lower distance than 10 m allows to fulfill the requirements of a stationary channel and thus correct for small scale fading by calculating the mean over the selected distance. However, as the used GPS receiver offers only an accuracy of 10 m, smaller distances are not possible unless high accuracy GPS receivers are considered.

The yielded results of all prototypical systems for both directions is depicted in Figure 4.15. To illustrate the yielded communication range for both directions the measurement is centered around the RSU, which is thus located at 0 m in both

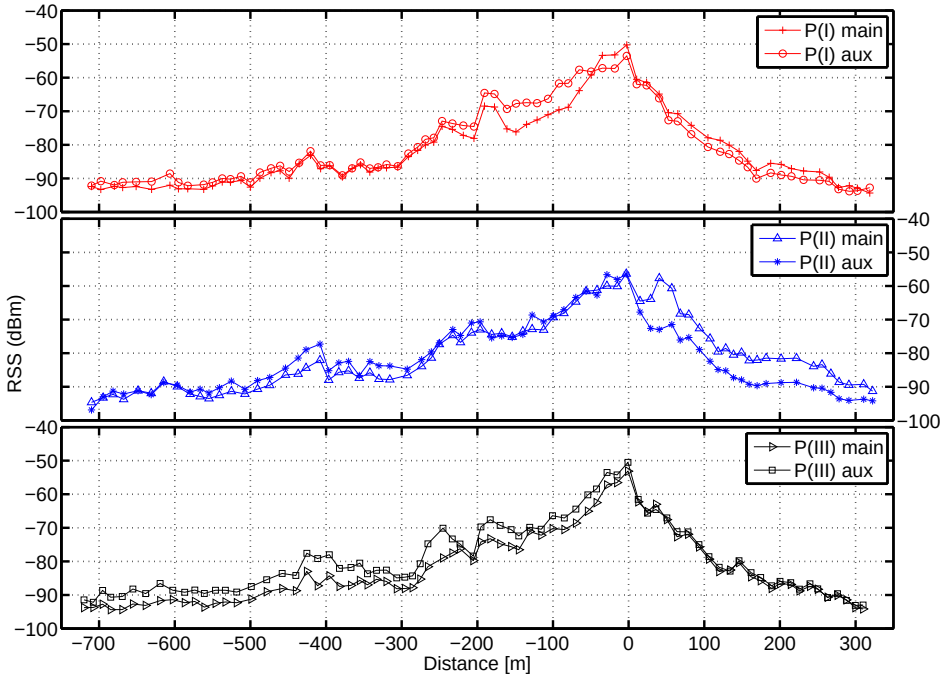

(a) Direction I from Point 'A' to 'B'.

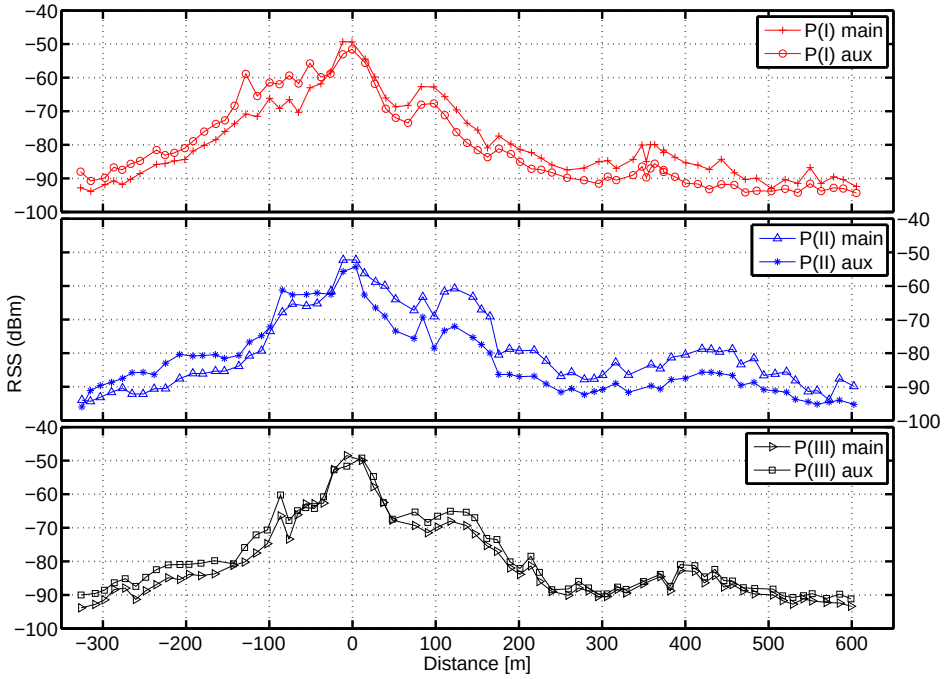

(b) Direction II from Point 'B' to 'A'.

Figure 4.15: RSS measurements for Direction I and II. The RSU is located at 0 m.

Figure 4.16: Measurement testbed used for 802.11p antenna benchmark.

cases. Consequently, the covered range whilst driving towards the RSU is in both directions negative. Although the measurement route is selected in such a way that the RSU is separating the route in two equally long sections, the yielded range differs significantly for both sections. The section in between point 'A' and the RSU is significantly longer compared to the section from the RSU until point 'B'. It is difficult to pinpoint the exact reason for this behavior, as this is potentially resulting from different factors. Probable factors are a suboptimal channel characteristics in between point 'B' and the RSU, deterioration of the RSU antenna radiation pattern by shrubberies and trees in front of the building or shadowing effects of other kind. As, however, the purpose is to characterize and benchmark the prototypical antenna systems and not to investigate the channel characteristics, the main reasons for this behavior are not in the scope of this work. In terms of antenna characterization it is important that the yielded measurements are reproducible and all of the antennas are effected in a similar way by the channel.

As expected the highest RSS values are obtained for Direction I as well as Direction II, cf. Figure 4.15(a) and Figure 4.15(b) respectively, when driving by the RSU. For Direction I the highest values of -50 dBm are yielded for P(I) and P(III). P(II) yields a 6 dB lower value, as both antennas face away from the RSU whilst driving in this direction. The chosen antenna positioning for P(II) is also causing the highest difference $\delta_{D,RSS}$ between the main and aux antenna after passing by the RSU. A difference in signal strength of up to 10 dB is seen between a distance of 0 and 300 m in Figure 4.15(a), which is resulting from the aux antenna being shadowed by the other antennas. Taking into consideration the values from Table 4.13, this behavior is not surprising. The main and aux antenna of P(II) yield the lowest gain values for the rear region of the vehicle. Moreover, is the antenna gain threshold of -3 dBi overall the most frequently exceeded. Compared to the other prototypes P(I) shows the lowest $\delta_{D,RSS}$ values between the main and aux antenna. Discrepancies from this behavior are seen about 200 m before reaching the RSU, where the main antenna shows a sudden drop in signal power of approximately 5 dB. This is resulting from low gain values on the sides of the radiation pattern of the main antenna. The G_{min} values from Table 4.13 are primarily measured in this area. A similar behavior is not occurring after passing the RSU as such low gain values are neither seen for the main

nor for the aux antenna in this region. The design methodology employed for P(III), cf. Figure 4.1(d), is also implied by the yielded RSS results. One antenna, in this case the aux antenna, is facing the RSU without being shadowed by other antennas, whereas the main antenna is pointing away from the RSU. Thus the aux antenna illustrates overall higher RSS values, which are in comparison to the main antenna up to 10 dB higher. After driving by the RSU, prototype P(III) shows the lowest $\delta_{D,RSS}$ values among the analyzed systems. This is resulting from the very balanced values for the KPIs G_{min}, G_{max}, G_{mean} and ρ_{TH} seen in Table 4.13. Consequently, after driving by the RSU both the main and aux antenna are due to their positions among the cellular antennas subject to similar shadowing effects. Due to the similarity of the benchmark results from Table 4.13 prototype P(III) also yields a similar communication ranges with both antennas. Considering a receiver sensitivity of -90 dBm the communication range starts at approx. -500 m and reaches up to 250 m, yielding in total 750 m. The highest communication range of 790 m is obtained with P(II), whereas P(I) achieves only a range of 560 m. The aforementioned maximum communication ranges are also summed up in Table 4.14, as they are one of the essential performance indicators for 802.11p communication.

In comparison to the previous results higher $\delta_{D,RSS}$ values are recorded for Direction II, cf. Figure 4.15(b). The highest $\delta_{D,RSS}$ values are seen for P(II). This is especially evident after driving by the RSU. The power levels of the main and aux antenna vary up to 11 dB, with the main antenna yielding higher gain values. The higher signal values of the main antenna result in a significantly higher range, considering again a receiver sensitivity of -90 dBm. Whilst for the aux antenna such drops occur after a distance of 250 m, it takes about 550 m to see a similar behavior for the main antenna. Considering selection combining as diversity scheme a total range of approximately 850 m is obtained. The poor performance of the aux antenna is resulting from being shadowed by the other antennas, thus having difficulties covering the rear of the vehicle, see Table 4.13. A similar behavior is also seen for P(I), which also has aligned 802.11p antennas. The aux antenna of P(I), which encounters shadowing to an increased degree achieves only a range of 250 m. However, in contrast to P(II) the resulting range of the main antenna is smaller and results in approximately 470 m. In total P(I) yields the second highest range with 720 m. Compared to P(I) and P(II) the value for the performance metric $\delta_{D,RSS}$ is the smallest for prototype P(III). The differences do not exceed 5 dB. Very balanced gain values for the main and aux antenna for the KPIs G_{min}, G_{max} and G_{mean} are the primary reason for the least deviations seen in case of P(III). However, the small difference of the antennas is also the main reason for both antennas being very close to the receiver sensitivity of -90 dBm after covering a distance of approximately 250 m. Nevertheless P(III) yields, also considering selection combining [63] as diversity scheme, a range of 750 m. All communication ranges are also for this Direction summed up in Table 4.14.

Direction	P(I)	P(II)	P(III)
I	560 m	790 m	750 m
II	720 m	850 m	750 m

Table 4.14: Maximal communication range of the prototypical antenna systems.

In order to compare the different prototypes in terms of their achieved diversity efficiency, the results for the main and aux antenna are summed up to obtain the total received power. The results are shown depending on the chosen direction in Figure 4.17. The results for Direction I, see Figure 4.17(a), illustrate that compared to the other prototypical systems P(II) yields the lowest signal strength. This is also seen considering the mean values in Table 4.15. Thus P(II) achieves a lower diversity efficiency compared to the other prototypical systems. Passing by the RSU the obtained power values are even 6 dB lower. The prototype P(I) shows high variation in the signal strength, especially between -500 m and -300 m, yielding low RSS values. This improves in close proximity to the RSU from -200 m to 0 m, where the signal strength is higher compared to the other antennas. In case of Direction II, the prototypical system P(II) is also yielding the lowest RSS values when passing by the RSU, see Figure 4.17(b). At 0 m, the position of the RSU, the signal values is about 4 dB lower. Although the obtained results are lower passing by the RSU, P(II) shows increased power levels driving away from it. Compared to the other antennas the difference is the greatest in the range between 150 m and 250 m. P(III) on the other hand yields values, which are enclosed between the results of prototype P(I) and P(II). It is also the prototype system, which achieves around the RSU the highest power values, see Table 4.15. For P(I) an increased direction dependency is seen for the achieved performance. In between the area of -200 m and -100 m P(I) obtains higher RSS values compared to the other antennas, however after passing by the RSU P(I) performs worst among all prototypes. This is resulting from the gain imbalances of the main and aux antenna in the front and respectively in the rear region of the vehicle, see Table 4.13. Whereas in the front region the mean values of the aux and main antenna do not differ more than 0.6 dB, in the rear region the gain imbalance is approx. 4 dB, cf. G_{mean} in Table 4.13.

Direction	P(I)	P(II)	P(III)
I	-62.7 dB	-65.7 dB	-63.3 dB
II	-60.8 dB	-63.1 dB	-60.0 dB

Table 4.15: Mean total received power of each prototypical system.

To benchmark the prototype antennas further in regards to the probability of supporting high RSS values CDF curves are depicted in Figure 4.18. Direction I, Figure 4.18(a), shows compared to Direction II, Figure 4.18(b), less spread RSS values for the main and aux antenna of each prototypical system. The results for P(II) vary for higher percentiles, such as the 90th, less in contrast to lower percentiles, for instance, the 15th, cf. Table 4.16. A further spread of the RSS values between the main and aux antenna is seen for P(III), which, however, starts converging towards higher RSS values. The opposite behavior is seen in case of P(I). For higher percentiles the results of the main and aux antenna vary to an insignificantly low degree, whereas starting at approximately -83 dBm the results begin to diverge. Considering selection combining as diversity scheme using either the main or aux antenna of all prototypical antennas potentially yields similar results, as the outcome of both antennas in the prototypical systems are comparable. This behavior is also seen for Direction II, which is also illustrated by the CDF in Figure 4.18(c) showing

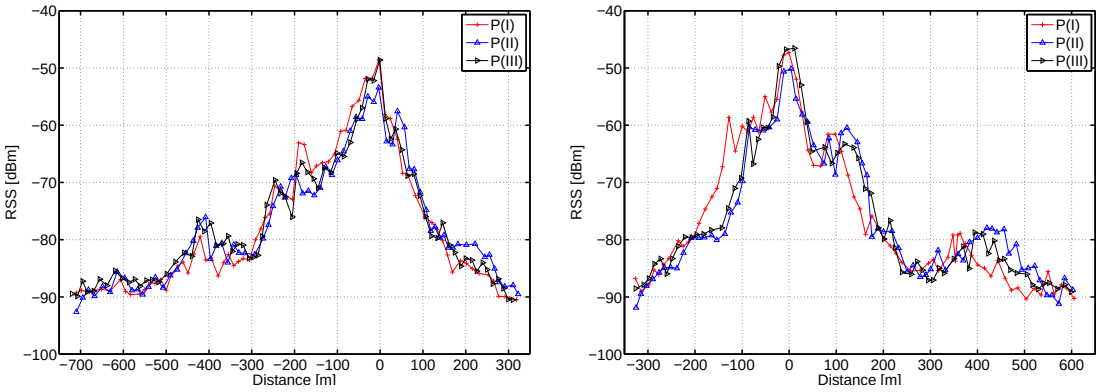

(a) Direction I.

(b) Direction II.

Figure 4.17: Total received power and communication range of each prototype.

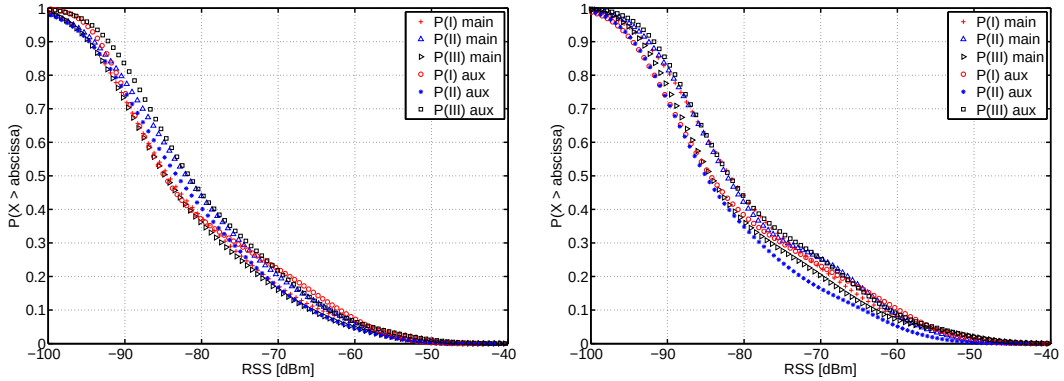

(a) Direction I.

(b) Direction II.

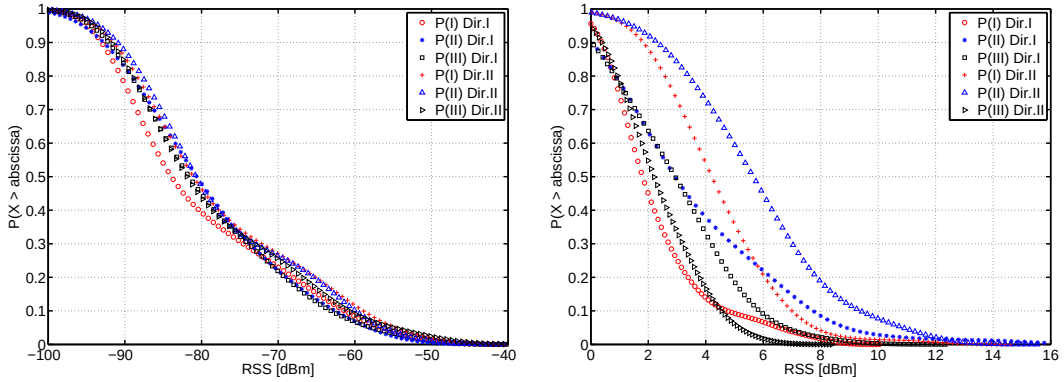

(c) Maximum of main and aux antenna per prototype.

(d) Difference of main and aux antenna per prototype.

Figure 4.18: CDFs of the RSS values of the 802.11p prototypical antennas.

the maximum value of the main and aux antenna of each prototype depending on the driving direction. As indicated the results of the prototypes are not widely spread, thus similar RSS values are to be expected. P(I) shows the highest direction dependency compared to the other prototypical systems. Taking into consideration a diversity scheme being based on the sum of both signal powers, this changes. In case of Direction II prototype P(II) yielding the highest difference between its main and aux, results in the worst performance. As this difference is substantially smaller in case of the other prototypes, see Table 4.16, these systems show a higher performance. Differences in the antenna performance applying another diversity scheme is also underlined with Figure 4.18(d). The overall highest difference in RSS values is seen for P(II), making it unsuitable for diversity schemes based on the sum of the signal power. On the other hand P(III) shows the smallest difference in RSS values between the antennas, thus allowing a similar performance even for diversity schemes based on the sum of the signals [63].

%ile	Dir.	P(I) m.	P(II) m.	P(III) m.	P(I) a.	P(II) a.	P(III) a.
15	I	-69.1	-67.5	-70.0	-65.4	-69.3	-66.6
	II	-66.2	-64.5	-67.4	-64.4	-69.6	-64.6
50	I	-84.8	-82.1	-84.9	-85.0	-83.4	-81.8
	II	-82.7	-82.8	-85.5	-84.8	-85.9	-82.7
90	I	-94.7	-94.6	-95.0	-93.6	-94.7	-92.2
	II	-93.4	-93.2	-94.5	-95.1	-95.0	-92.8

Table 4.16: Percentiles for *RSS* in dB from Figure 4.18(a) and Figure 4.18(b).

4.2.3 Radiation Pattern Optimization

As stated in the beginning of this Section aiming towards an omni-directional radiation pattern for 802.11p systems is key for the antenna performance. Resulting from the integration of antenna systems in a housing on the vehicle rooftop, also called radome in the following, this is challenging. The antenna housing deteriorates the radiation pattern to a significant degree [28]. However, as the exterior of the vehicle is subject to design considerations, changing the shape of the antenna housing to compensate for such losses is difficult to accomplish. Consequently, investigations into a methodology to turn the destructive interference into a constructive one without altering the design of the antenna housing is key. The investigations described in the following illustrate a methodology to compensate nulls in the radiation pattern by changing the thickness of the antenna housing. This is shown with the help of simulations and measurements. Moreover, is it illustrated that geometrically simplified shapes allow to analyze the behavior of an antenna housing design fitting the exterior of the vehicle to save simulation time and to simplify such investigations.

The radiation patter measurements are carried out in a semi-anechoic chamber, where the antenna under test is placed on a turn table, see Figure 4.19(a). A circular ground with a diameter of 1 m having rounded edges is used to mount the RX, cf. Figure 4.19(b). The Figure shows the original antenna radome covering the RX,

which in this case is a monopole antenna. As the focus of the investigation is to analyze the radome behavior for 802.11p communication a monopole being only resonant at 5.9 GHz is used. The RX is placed in the middle of the ground having a distance of 1 cm to the rear of the radome profile. This position is chosen as it is realizable without significant changes in the current antenna module layout, which is currently in series production. For the transmit antenna (TX) a horn antenna is used. The distance between the TX and RX is set to 7 m. For determining the power loss between the TX and RX for each angular step, the TX is connected to a signal generator and the RX to a spectrum analyzer. The losses occurring on both cables are calibrated out in this way. For the TX the power is increased until on a reference antenna system, located at the same place as the RX, a received power of 0 dBm is measured. The compensation of the losses is performed for each degree step of the turn table. The gain of RX is then determined using the three antenna method and the Friis formula for free space [28]. For the third antenna a dipole is used. To ensure accurate measurements the metallic floor of the semi-anechoic chamber, cf. Figure 4.19(a), as well as the doors of the chamber, fitted with a ferrite coating, are covered with absorbers. In order to guarantee that the LOS component of the antennas is predominantly recorded rather than a reflection component, five received power values are averaged for each azimuthal degree step. The obtained radiation patterns shown in this work are all normalized. For the following investigation four radome prototypes are used. As a reference the radome being currently in series production for sedan type vehicles is employed, where the wall thickness varies between 2 mm and 12 mm. Two prototypes in the style of the original radome are manufactured having the same geometrical size and shape, however with uniform wall thicknesses. The corresponding wall thicknesses are set to 0.9 mm and 2 mm. The employed material for all prototypes is PC-ABS having a dielectric constant of 2.9 at 1 MHz and a dissipation factor of 0.0054 [28]. To visualize to which degree the impact of geometrically complex shape of the antenna radome is probable to be approximated with more simplified shapes two more prototypes are prepared. Cuboids with the dimensions 150 mm x 50 mm x 50 mm (length x width x height) and wall thicknesses of 0.9 mm and 2 mm are manufactured. The material of the cuboids is the same as for the previously mentioned prototypes.

All of the following patterns are gathered for the horizontal plane. In each pattern 0° degrees shows the obtained gain when the front of the radomes is facing the TX antenna. For the radome displayed in Figure 4.19(b) this is, for instance, the pointy front, which when mounted on the car faces towards driving direction. Figure 4.20(a) shows the antenna gain obtained for a monopole antenna when placed in the middle of the ground. It is differentiated between a reference measurement (Ref.), where the gain is obtained without a radome and the result with a radome, which is currently in series production for sedan type vehicles, cf. Figure 4.19(b). The dashed lines illustrate the results obtained from simulations as described in Section 2.2.2, whereas the solid lines display the measurement results obtained in the semi-anechoic chamber. The radiation pattern obtained from simulations shows the expected omni-directional radiation pattern with a gain of -5 dB. The measurements deviate around 1 dB from the pattern obtained by simulations. Even though the results are gathered in a semi-

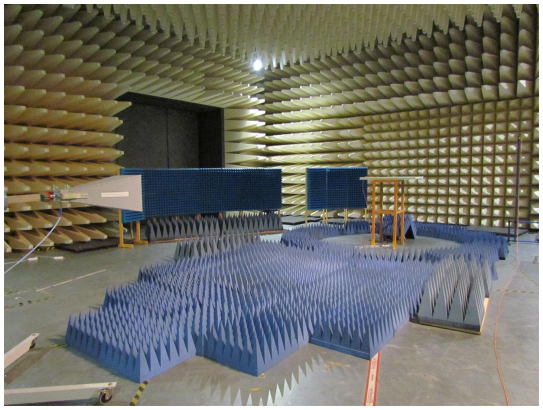

(a) Setup with the TX (horn) and RX (monopole).

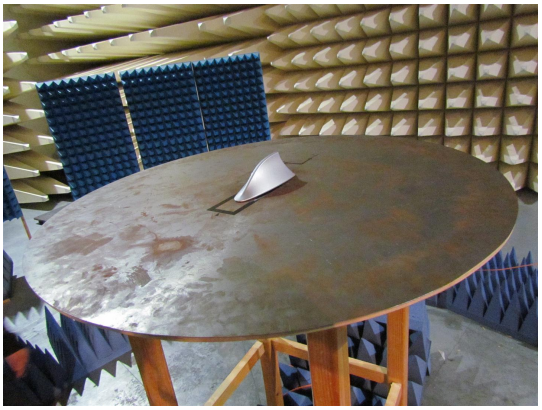

(b) Original radome placed on a circular ground with a diameter of 1 m.

Figure 4.19: Measurement setup in the semi-anechoic chamber.

anechoic chamber fitted with absorbers on the metallic ground and ferrite covered doors the results prove to be reliable for qualitative comparison with simulations. The results of the original radome illustrate for both the simulations and measurements a shape similar to a butterfly in the area between 270° and 90°. The lowest gain value is seen in both cases at 0°. In the area around 0°, which is the driving direction of a potential vehicle, the RSS values are subject to be substantially reduced. Interestingly, however, is the amplifying effect of the radome around 45° and 315°. This is resulting from the constructive interference from the electromagnetic waves radiated from the antennas and the reflected components at the walls of the antenna housing. In comparison to the front, the rear section of the pattern between 260° and 110° is influenced the least by the radome. The results thus illustrate that the radome works depending on the direction as a dielectric lens amplifying or reducing the antenna directivity at certain directions. The difference between the reference and the radome measurements is the greatest between 0° and 310°. The deviations at these particular locations and also in other locations is caused by three factors: (1) inaccurate positioning of the monopole inside the radome, (2) deficiencies in the computer-aided design model, (3) an air gap within the original antenna radome. The antenna radome is positioned on the circular ground alongside markings, which is why the antenna position of the simulation and measurement do not match. Concerning (2) and (3): The computer-aided design model and the radome used for measurements do not exactly match mainly due to air gaps in the structure and markings on the inside walls of the series radome.

In Figure 4.20(b) the measurements illustrate the deliberate use of the dielectric lens effect of the radome prototypes. Two prototypes are evaluated one with a wall thickness of 0.9 mm and the other with 2 mm. As before, dashed lines are used for the simulation results and solid lines for the measurements. The results show that the null occurring in the radiation pattern of the original radome at 0°, cf. Figure 4.20(a), is compensated successfully. The gain peaks, resulting in the butterfly alike shape,

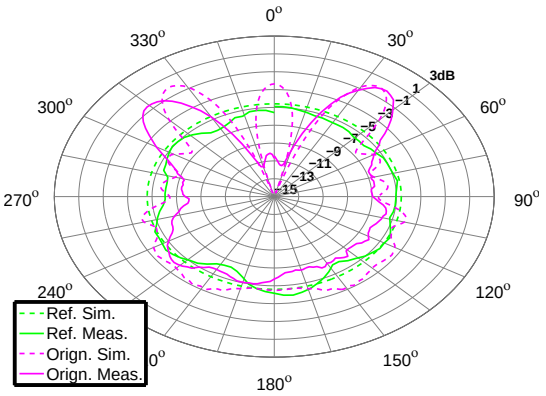

(a) With / without original antenna housing.

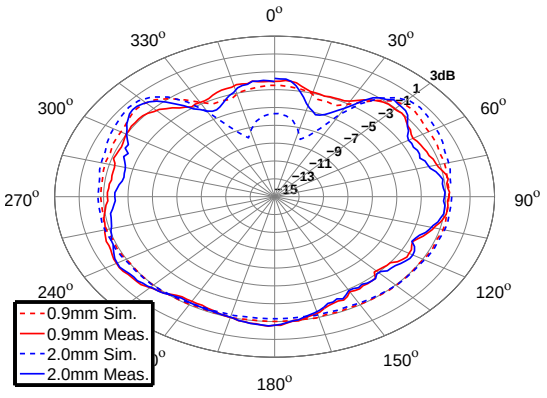

(b) Original radome prototypes.

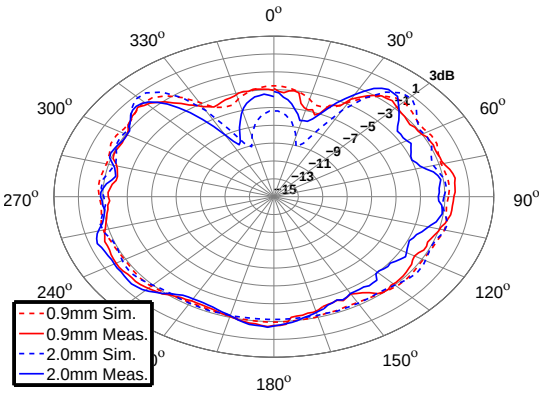

(c) Cuboid radome prototypes.

Figure 4.20: Radiation pattern of a 802.11p monopole with various housings.

cf. Figure 4.20(a), are reduced to such a degree that a more congruently distributed radiation pattern is yielded. The gain is higher for the prototype with a lower wall thickness, in this case 0.9 mm. The null between 15° and 30° and at around 330° is in this cases even better compensated, up to 2 dB higher. Moreover, it is seen that for the rear part of the pattern a variation of the wall thickness has a negligible impact. The deviation between the measurements and the simulations is in comparison to the results of the original radome substantially lower, see Figure 4.20(a). This is resulting from: (1) the computer-aided design model of the radome, where no air gaps are present, (2) uniform inner walls without small cavities for identification markings in the series antenna housing. However, the results are also in this case subject to inaccurate positioning on the ground plane, which is primarily seen for the radome with a wall thickness of 2 mm between 330° and 30°.

The impact of a geometrically simplified radome shapes, a cuboid in this case, on the radiation pattern is visualized in Figure 4.20(c). As seen in the previously discussed radome prototype the nulls in the pattern are compensated. It is also seen that the lower wall thickness increases the antenna gain up to 5 dB for both the simulations

and measurements. In contrast to the previously discussed results, the measurement and simulation outcome match better in this case. These results also confirm the finding that the deviation between the simulation and measurements yield from the positioning inaccuracy. More precise results are likely to be obtained by carrying the measurements out in a more suitable environments as in a fully anechoic chamber and and a more sophisticated positioning methodology.

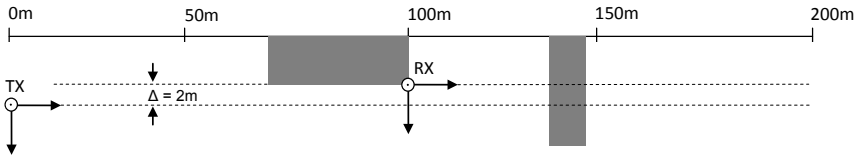

(a) Simulation track.

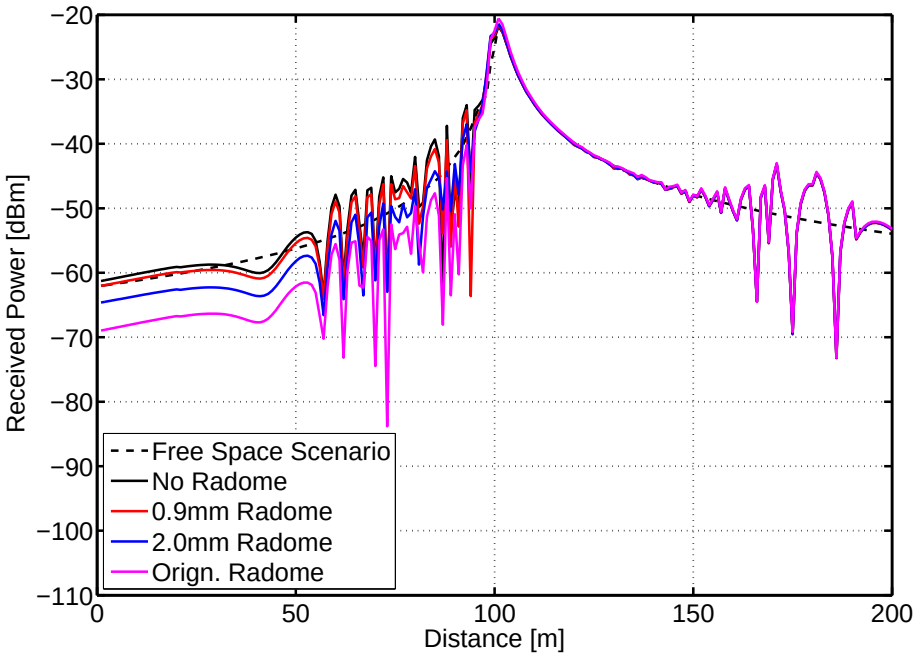

(b) Results.

Figure 4.21: System level simulations.

To illustrate the impact of compensation the performance deterioration of the antenna radome on system level a 'virtual test drive' scenario is performed. As described in Section 2.2.2, the scenario is implemented in FEKO [70] and computed using hybrid solving methods. Recalling from Section 2.2.2 the implemented hybrid solver combines a method of moments approach with the uniform theory of diffraction (UTD) [71] to calculate the system level performance in virtual drive tests. The scenario, as seen in Figure 4.21(a), consists of a single 200 m long lane with buildings alongside the route. The buildings are assumed to be ideal conducting surfaces, the worst case setting for V2V and V2I communication, see also Figure 2.7 from Section 2.2.1. The first building is 30 m long and is starting at 70 m. The receiver, in

this case a RSU, is located 100 m away from the starting position with a distance of 2 m to the lane. Both the vehicle and the RSU antenna are positioned at a height of 1.5 m. For the vehicle, the antenna radiation patterns are imported from CST Microwave Studio [68]. In case of the RSU an omni-directional radiation pattern with a gain of 0 dBi is assumed. The output power of the RSU is set to 30 dBm.

Four different scenarios are considered for the investigation: (1) antenna without a radome, (2) orign. radome, (3) radome wall thickness 0.9 mm, (4) radome wall thickness 2 mm. The free space case is only evaluated for scenario (1). The obtained results are presented in Figure 4.21(b), where the received power is plotted as a function of the distance. To analyze the results, it is feasible to divide each scenario in four phases each with a length of 50 m. In the first phase ($dist. < 50$) the simulated vehicle has not yet reached the buildings. The radome with a wall thickness of 0.9 mm illustrates the highest RSS values in this phase. The RSS values are 9 dB higher compared to the series radome. Throughout all phases this radome prototype shows also the best match with the case of not using an antenna radome. The second phase ($50m < dist. < 100m$) visualizes the impact of the first building. The reflections from the building cause multiple spikes, which impact the obtained RSS values with the orign. radome the most. In phase three ($100m < dist. < 150m$) no reflections of either of the buildings is detected, all curves overlap. In the fourth phase ($150m < dist. < 200m$) spikes are seen, which are resulting from the second building. The curves of all the radomes overlap as the variation of the radome thickness has a negligible impact on the rear of the radiation pattern.

4.2.4 Conclusion

Antenna systems designed for 802.11p communication thus working at 5.9 GHz are subject to performance deteriorating resulting e.g. from vehicle rooftop and the antenna housing. The benchmark methodology introduced in Section 2.3 to quantize the antenna performance was applied to the three prototypical systems. The majority of the analyzed KPIs related to the antenna gain, since an omni-directional pattern without any nulls is key for any safety applications using 802.11p communication. Naturally also KPIs focusing on the antenna impedance were analyzed. However, due to the high operating frequency at only 5.9 GHz and thus a narrow band antenna design, these KPIs are not as crucial as for cellular systems. The required thresholds were shown to be met by all prototype antennas. Thus concluding that putting an emphasize on impedance related KPIs in specifications sheets for 802.11p antenna system benchmark is not a suitable approach.

In case of KPIs relating to the antenna gain, high variations were seen for the different antenna systems. To better quantify these variations statistical metrics were applied, describing the probability of the antenna gain dropping below a threshold ρ_{TH} or the difference of the main and aux antenna exceeding a threshold ρ_{Diff}. Due to the use of diversity instead of SMX transmission techniques, the focus was put on ρ_{TH} thus evaluating the main and aux antenna separately. Requiring two antennas instead of one is mainly resulting from trying to compensate the integration challenges of

antenna systems. These integration difficulties do not allow to cover the front and rear region of a vehicle efficiently by one antenna. Consequently, the gain related performance metrics were applied separately to both regions. The prototypical systems were analyzed each providing a different solution for positioning the 802.11p antennas among the cellular antennas to minimize the caused interaction. Each prototype system offered similar positions for the cellular antennas, which were in the rear and front of the antenna housing shaped similarly to a 'shark fin'. The 802.11p antennas were located either adjacent to one another on one side, each on one side or integrated in the cellular antennas. The results showed that the prototype, which had the 802.11p antennas positioned one on each side, yielded overall a higher performance. The performance metrics based on the antenna gain showed the least deviations between the antennas for this prototype. The antenna design with co-located cellular and ad-hoc antennas also yielded low deviations for the gain performance metrics.

To assess the prototypical antennas on system level measurements were carried out in an urban setting. The employed V2I communication scenario, yielded a higher difference in the measured signal values depending on the driving direction. The highest direction dependency on the RSS values was seen for the setting, where both antennas are adjacent to one another. It was also the antenna setup were the signal values between the main and aux antenna differed most significantly. Although in some case the RSS values were higher compared to the other prototypes or a higher communication range was yielded, this design solution proved to have the most blind spots in the pattern. Taking into consideration that safety application in a vehicular scenario require, independent of the direction in the azimuth a reliable and robust link, a design methodology with frequent blind spots is unsuitable. Consequently, also the system level evaluations showed that the positioning 802.11p antennas each on one side is an advisable way to accomplish the least blind spots and to achieve a high diversity efficiency. It is thus concluded that locating cellular and 802.11p antenna systems alternating within the antenna housing with the cellular antennas in the front and rear is a feasible antenna design methodology for hybrid antenna systems. Due to the small difference in signal values such a design methodology yields similar results independent of the applied diversity transmission scheme, such as for maximal-ratio or selection combining.

Lastly this Section presented a straightforward realizable methodology to compensate the impact of the antenna housing (radome) without changing its design. The typically undesired dielectric lens effect of the housing is deliberately used by altering its wall thickness to eliminate nulls in the radiation pattern. It was shown that simplified shapes, such as cuboids, are feasible to be used to design suitable antenna housings for 802.11p communication. This saves computation resources and time, thus lowers the expenses in the design phase. The impact of compensation nulls in the radiation pattern on the yielded system level performance was also discussed. The yielded results illustrated that drops in the received power are compensated and a higher power level in this case of 9 dB is reached, not even considering the spikes in the RSS results.

Chapter 5

Assessment of Service Delivery in Hybrid Networks

In this Chapter the service delivery in the vehicular environment is assessed for safety as well as infotainment applications. Safety applications, such as LHWs, rely on the participation and cooperation of different vehicles, thus function properly, if vehicles are able to exchange messages reliably. Consequently, in this case one of the key aspects is the dissemination of the corresponding messages and the yielded communication range. On the other hand infotainment applications, such as video or audio streaming applications, are user-centric, thus do not require any cooperation with other parties. Optimization of one's own connection is in general performed without consideration of others. Both application domains are investigated in Chapter, with the first part focusing on infotainment applications and the second on the evaluation of the service delivery for safety applications. For infotainment applications the emphasize is put on achieving an increased QoS compared to the use of only one access network, which is in current vehicle models the case. Improvements in the achieved QoS are evaluated in regards to a reliable connection with few or even no drops occurring in the communication link and an overall high throughput. Thus the investigated handover algorithms and KPIs aim towards an overall high mean throughput by performing handovers only, if an additional value is probable to be yielded. Such an additional value likely includes off-loading of the current traffic to save transmission costs, use network resources more efficiently as well as to obtain a dependable link.

The Section on safety applications focuses on the message dissemination using hybrid radio networks. As safety applications are of a cooperative nature [13, 14], they depend on the collaboration of all vehicles in a given scenario. Thus it is analyzed to which degree a reliable distribution of safety messages is ensured in the case that vehicles are equipped with different radios. It is shown that hybrid radios are able to overcome the drawbacks of ad-hoc and cellular networks and increase the range of safety applications. Besides technical advantages it is also established that their use also allows to use the available network resource in the cellular network more efficiently.

5.1 Infotainment Applications

The Section on infotainment applications is structured as follows. In Section 5.1.1 the simulation environment and the modeling of the access networks is described. The emphasize of the investigation is to illustrate the additional value of using KPIs from external sources to increase the yielded QoS. As such the focus is on the yielded performance of different multi-criteria algorithms being able to incorporate KPIs from different sources. The evaluations are carried out using MATLAB with abstracted model of the access networks to focus primarily on the potential of external KPIs for dependable communication. The simulation results of three multi-criteria and one basic reference network selection algorithm are presented in Section 5.1.2. The outcome of the algorithms are rated in regards to the yielded throughput and outages in the communication link. Moreover, is the reduction in transmission costs assessed, for a combined use of different access networks for a data download application. Lastly the obtained findings are verified by measurements in Section 5.1.3, which are carried out in the hybrid testsite discussed in Section 2.2.

5.1.1 Simulation Setup

The simulation is conducted with abstracted models of the access networks, which in this case includes WLAN 802.11g, UMTS and LTE. The characteristic values for the implemented models are displayed in Table 5.1. The parameters taken from [108] include at the side of the transmitter the transmit power, the operating frequency and bandwidth as well as the receiver sensitivity at the vehicle. The cellular networks UMTS and LTE are selected, as in urban scenarios these networks are primarily used for data connections. Selecting 802.11g results from the deployed WLAN AP in the hybrid testsite using also the same standard. Due to the focus on infotainment applications 802.11p access networks are not taken into consideration.

	802.11g	UMTS	LTE
Frequency [MHz]	2400	2150	800, 2600
Bandwidth [MHz]	20	5	5
Transmit Power [dBm]	20	46	46
Receiver Sensitivity [dBm]	-96	-106.4	-106.5

Table 5.1: Radio parameters of the modeled access networks.

For the simulations the channel is modeled using large and small scale fading. Large scale fading is modeled for each radio access network according to the Okumura-Hata model with the COST 231 extension [109] assuming an urban environment. Rayleigh fading is used to model small scale fading [110]. Further included inputs are the RSS, throughput, latency, network load, energy consumption and the SINR. The SINR is calculated according to Eq. (5.1), where RSS is the signal strength, P_N the noise power of the receiver and P_I the interference, see also [17]. For the interference a static value of -90 dBm is considered. The noise power is determined with Eq. (5.2),

where k is the Boltzmann's constant, T the noise temperature of the receiver and B the applied bandwidth, see [108, p. 245].

$$\text{SINR} = \frac{RSS}{P_N + P_I} \qquad (5.1) \qquad P_I = kTB \qquad (5.2)$$

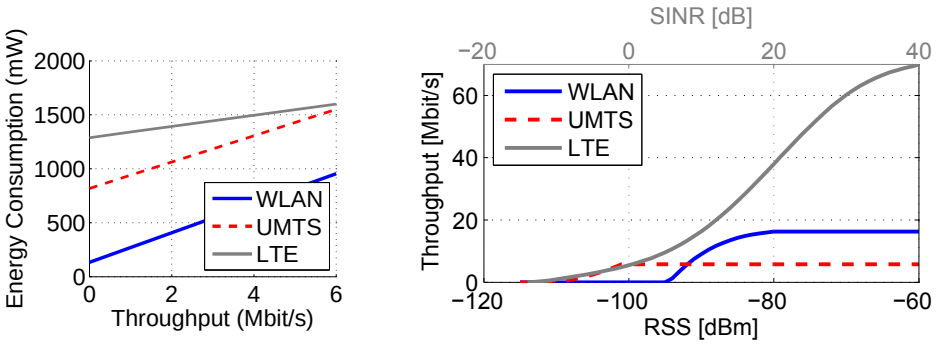

(a) (b)

Figure 5.1: Energy consumption shown exemplary until 6 Mbit/s [111]. Throughput model for WLAN and UMTS based on RSS [81] and for LTE on SINR [112].

Analytical models proposed in [81] are used to estimate the throughput for both UMTS and 802.11g, see Figure 5.1(b). According to this empirical approach, a relation between the RSS and throughput is defined. The results show a maximum achievable throughput of 16 Mbit/s for WLAN and 6 Mbit/s for UMTS. As illustrated in Figure 5.1(b) the throughput values for UMTS are saturated above a RSS value of -100 dBm, whereas this threshold is shifted to -80 dBm in case of WLAN. The throughput modeling for LTE is based on simulation results presented in [112]. It is dependent upon the SINR, which in turn is determined by the RSS value. A simplified model is implemented for the load of the radio access networks. The radio resources of the access networks are modeled with regards to the overall achievable throughput. The maximum achievable throughput per user is calculated according to Eq. (5.3). The achievable throughput is calculated subject to the network load given in percent and the maximum supported throughput. The network resources are distributed equally among all users within the range of the base stations and APs.

$$throughput_{achievable} := max(throughput) \cdot (1 - \frac{load}{100}) \qquad (5.3)$$

According to measurements performed in LTE live test networks [113] a constant average round trip time of 35 ms is considered for the simulations. The mean end-to-end latency for UMTS was determined in the CoCar project to be 150 ms [1]. According to [114] a mean latency value of 10 ms is suitable for WLAN APs. Additional latency constituted by signaling in core networks or the Internet or changes to these values by, for instance, additional traffic caused by other user, is not taken

into consideration. The energy consumption is modeled according to [111], where all of the aforementioned access networks have a linear relation to the throughput, cf. Figure 5.1(a). Here, a section of up to 6 Mbit/s of the energy consumption models is shown for the access networks.

For the simulation a characteristic scenario is designed, where several radio access networks are co-deployed. The investigated simulation scenario is presented in Figure 5.2. It is an exemplary scenario, where the street names are chosen for illustration purposes. In the simulation area four different radio access networks are considered: LTE 800 MHz and 2.6 GHz, UMTS and WLAN. On the 4.2 km long trajectory, five WLAN APs are located, which have a range of about 180 m. To investigate the extent to which external information improve the perceived QoS, WLAN AP #3 is assigned a network load of 95 %, neglecting collisions on MAC layer. The cell sizes of the cellular networks depict approximately 4.8 km for the LTE 800 MHz cell, 2.1 km for the UMTS cells and 1.7 km for the LTE 2600 MHz cell. The velocity of the mobile node used in the scenario is set to 10 km/h. A higher velocity is not chosen, since the mobile node is not likely to stay long enough in the range of an AP to be able to make a connection. Such low or even lower speeds are probable to be found in a traffic congestion or longer waiting periods at traffic lights. The considered external KPIs are based on coverage and user experience maps, containing information on the throughput of previous connections made to a radio access network. In case the achieved throughput, when connected to a network, falls below an assumed threshold of 4 Mbit/s the radio access network is considered to be unsuitable for future connections in the location, where this deterioration occurred. In the beginning of the simulation scenario the mobile node has no information on any of the radio access networks. Thus on a simulation run the vehicle gathers information on the available radio access networks and their performance characteristics, such as the throughput. This data is collected by monitoring the active connection and passively scanning other available access networks. The initially collected information is then validated on a second and a third drive on the previously presented route. Further runs are not necessary as the results do not vary after the third. Furthermore, for the transmission cost analysis a generic cost metric (CM) per amount of data transmitted is introduced, subject to the used access network: 1 MB of data transmitted via WLAN costs 2 CM, whereas for 1 MB via UMTS and LTE costs 8 CM.

5.1.2 Simulation Results

The previously discussed scenario is used to evaluate the performance of four different handover algorithms. These include a reference signal power based algorithm [80], a Fuzzy algorithm [81] and two AHP based algorithm [19], see Section 3.1.2. The primary difference between both AHP algorithms is that one incorporates only local KPIs, whereas the other also considers external KPIs. For both algorithms the bucket threshold is set to 30, see algorithm on page 31, which proved to be a suitable threshold in analyzing the implemented algorithm. Recalling from Section 3.1.2 the bucket threshold defines the consecutive times an alternate network has to be better

rated compared to the network currently connected to. A balanced and optimized weight profile is defined for both the local and external AHP algorithm. The KPIs RSS, SINR, delay, energy consumption and costs of the local AHP algorithm are prioritized equally, assigning each a weight of 0.2, cf. Table 5.2.

	RSS	SINR	Delay	Costs	Energy	CPU	TP	Ex.
Fuzzy	0.2	0	0	0	0.4	0.1	0.3	0
AHP local	0.2	0.2	0.2	0.2	0.2	0	0	0
AHP ex.	0.1	0.1	0.1	0.1	0.1	0	0	0.5

Table 5.2: Weight profile of the considered network selection algorithms.

In case of the external AHP the weights are assigned equally between local and external KPIs. Thus as there are five local KPIs the weights are set to the same value of 0.1. As for the external values only one KPI, the user experience map on the network performance, is considered and consequently assigned a weight of 0.5. The KPI weights of the Fuzzy algorithm are taken from [81] and presented in Table 5.2. For the RSS based algorithm the handover threshold T_{HO} and hysteresis margin H are set to -73 dBm and respectively 3 dB, according to [80]. The overall throughput over distance and the handover decisions represented by network IDs are depicted for all aforementioned algorithms in Figure 5.3. The ripples in the throughput plots are caused by the modeled Rayleigh fading [110]. Comparing the throughput outcome of the four algorithms, see Table 5.3, illustrates that the AHP external yields the highest average of 15.9 Mbit/s. The RSS based algorithm achieves a throughput value of 9.4 Mbit/s, the Fuzzy algorithm 14.1 Mbit/s and the local AHP 15.2 Mbit/s. The overall lowest throughput value and fluctuation in network selection is seen for the RSS algorithm, since it performs a high quantity of handovers, cf. Table 5.3 at locations where the access networks have similar RSS values. This especially becomes evident around 2.1 km and 2.6 km. The number of handovers, which is also depicted in Figure 5.3, is the lowest for the AHP algorithm with external KPIs. This is resulting from the user experience map, where handovers to networks resulting in an unstable connection are not performed. The Fuzzy or AHP local algorithm perform a higher number of handovers. Although the RSS algorithm performs more handovers in total, with a tendency to a ping-pong effect in the network selection, it generates

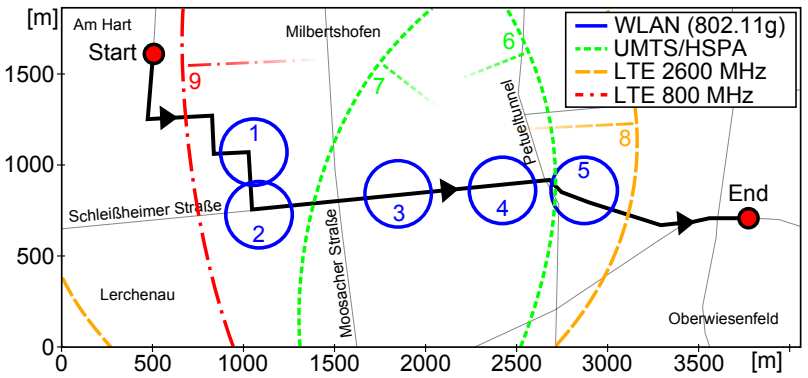

Figure 5.2: Simulation scenario for the investigation of different VHDAs.

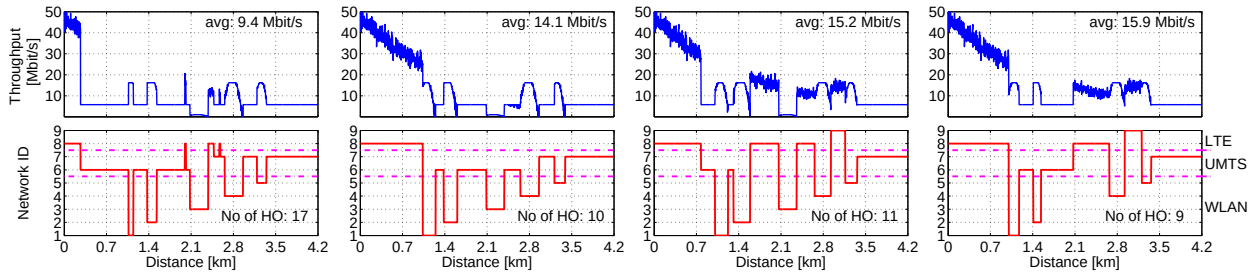

(a) RSS algorithm. (b) Fuzzy algorithm. (c) AHP local. (d) AHP coop.

Figure 5.3: Throughput and network selection of the handover algorithms.

less throughput drops in comparison to the AHP local or Fuzzy algorithm. This is caused by the prolonged use of the WLAN AP. In case of the Fuzzy algorithm this is resulting from prioritizing the energy consumption about twice as high compared to other KPIs, such as the RSS values. Thus more energy efficient WLAN APs are preferably used rather than better performing cellular networks. The same behavior is occurring for the AHP local, where this is caused by parameters, such as transmission costs and latency. The combination of the two aforementioned KPIs outweighs the others indicating even in areas close to the coverage edge of the access networks that the current connection is still the better choice. With the advent of external information, the AHP algorithm achieves better timed handovers at the cell edges leading to an overall improved throughput performance and the highest average of 15.9 Mbit/s. In comparison to the local AHP algorithm the external AHP algorithm decides not to connect to the overloaded WLAN network (network #3) at a distance of 2.1 km but rather connects to the LTE 2600 MHz cell (network #8). This is primarily caused by the external information taking the user experience map of the radio access networks into consideration. This map indicates that a lower throughput level is potentially achieved connecting to the UMTS networks #6 and #7, since the mobile node is closer to their cell edge.

	RSS	Fuzzy	AHP local	AHP ex.
Number of Handover	17	10	11	9
Mean Throughput [Mbit/s]	9.4	14.1	15.2	15.9

Table 5.3: Performance of the analyzed algorithms.

To evaluate the additional value of external KPIs in regards to transmission cost efficiency an algorithm called *intelligent data planning* (IDP) is designed. The IDP aims at minimizing the arising data transmission costs of pre-defined FTP file-downloads of a certain size. Based on the navigation route it takes into account external KPIs, such as the networks load and coverage of radio access networks. In a first step it evaluates the available access networks on the chosen navigation route. In order to save transmission cost it forces the network selection to transmission cost efficient WLAN networks, which are on the route. In addition based on the network load the IDP excludes WLAN networks, which have a high network load, in this case network #3. As in this preliminary analysis it is only distinguished between overloaded WLAN APs and such carrying no load, a further threshold is

currently not applied. Taking these inputs into consideration prior to the start of the transmission the IDP predicts the amount of data able to be received using only WLAN networks. If this is smaller than the requested amount of data, the remainder is downloaded after passing the last AP using cellular networks. A suitable cellular radio network is chosen for the download of the remaining data by employing the external AHP algorithm. Performing a download prior to the first AP is also a possibility, but is not implemented in this version of the IDP.

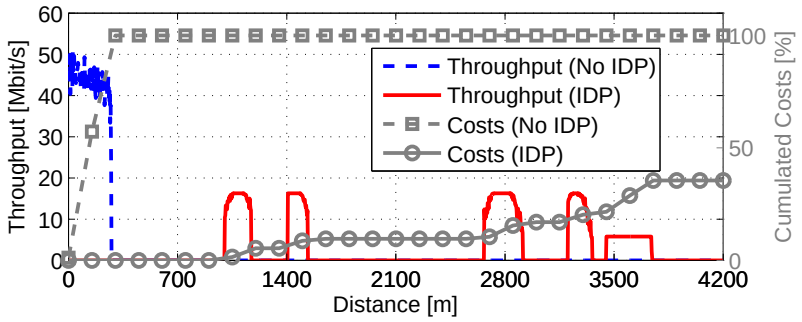

Figure 5.4: Transmission cost optimization using external KPIs.

In order to evaluate the gain of the IDP the previously presented scenario is used, where a file of 500 MB is downloaded to a mobile node driving at a velocity of 10 km/h. In Figure 5.4 the aggregated costs using IDP are compared to the situation where no IDP is applied. It is shown that all of the data is transmitted via the LTE access network in case the IDP is not enabled, which leads to transmission costs of 4000 CM. The LTE network is used as the AHP local algorithm is determining that it is the most suited access network in that area. In the case of IDP, most of the data is transmitted via WLAN APs, being in terms of transmission costs the cheapest radio access networks. Only a small amount is transmitted via the more expensive UMTS network. The overall transmission costs result in 1421 CM, which is a cost reduction of 65 %. Although IDP is a suitable means to save transmission costs, it also elongates the necessary time for completing a download application. Thus a trade-off is done between the elapsed time to download a file and the occurring transmission costs. As such this approach is suitable only for applications, where the file transfer is feasible to be stretched out in time, for instance a video file for the rear seat entertainment system. Using the IDP for on-demand services or streaming applications is not feasible. In addition as the IDP potentially alters the user experience, it is only a good approach to save transmission cost, if the user agrees to it and has a financial benefit. With the help of the abstracted models of the access it is only feasible to establish the potential of the proposed approach. However, for accurately quantifying the additional benefits of this approach and to perform optimization it is suggested to use a network simulator with an integrated mobility modeling environment.

5.1.3 Evaluation by Measurements

To corroborate the findings from the simulations, measurements are carried out in a hybrid testbed, see Figure 5.5. For the evaluation the access networks LTE at 2.6 GHz and WLAN 802.11g at 2.4 GHz are used. As seen in Figure 5.5 five WLAN AP are employed for the evaluation, which are mounted at an office building. In [78] it is determined that in case of WLAN 802.11b at 2.4 GHz a range up to 610 m is feasible to yielded. Depending on the propagation conditions it is differentiated in a LOS and nLOS scenario. In order to relate the measurements to locations in the testbed, reference positions P, E1, E2, E3 and E4 are used. These positions are, as seen in Figure 5.5, either the parking lot (P) or street corners (E1, E2, E3, E4). The different network selection algorithms are implemented on a vehicle ECU comprising modems for LTE and WLAN. The evaluated network selection algorithms include a (RSS) based algorithm and two multi-criteria algorithms. The considered KPIs of the algorithms are presented in Table 5.4. Besides the RSS algorithm, two multi-criteria algorithms AHP algorithms are considered. As seen for the simulations it is again differentiated between a local and external AHP. The RSS based algorithm, see Section 3.1.2 for more details, forces a network re-selection based on whether the RSS value drops below a threshold of -73 dBm. Thus once a connection is made to a certain network, a handover only occurs in case that the current network signal strength falls below this threshold, even if higher RSS values are obtained with an alternative network. Other KPIs for network selection or exclusion of networks are not taken into consideration. Among the network selection algorithms only the RSS algorithm is working actively, thus it controls whether a connection is made to the LTE or WLAN network. The results of the local and external AHP algorithm are calculated after the measurements based on the recorded KPIs during the assessment of the RSS algorithm to illustrate the potential of both multi-criteria algorithms.

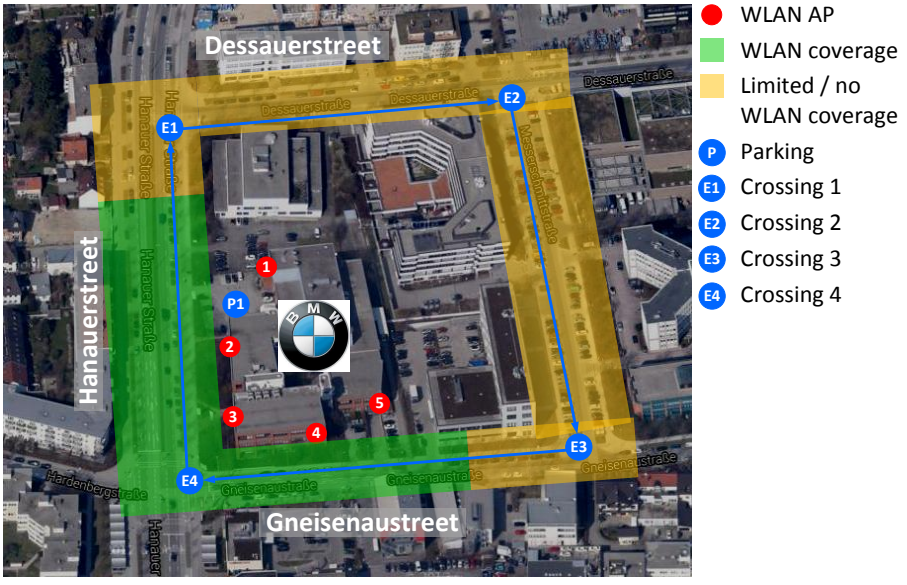

Figure 5.5: Testbed highlighting the WLAN coverage and measurements positions.

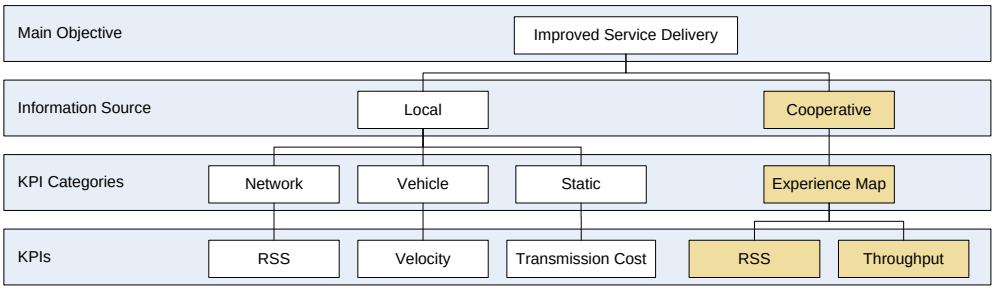

Figure 5.6: Designed AHP algorithm for the measurements.

The structure of the implemented AHP algorithms for the measurements is shown in Figure 5.6. Due to the availability of certain KPIs using the same inputs as for the previously discusses simulations is not possible. The AHP external is taking both local and external KPIs into account to determine the most suitable network. The external parameters include, in this case, an experience map on the throughput and a map of the yielded RSS values. The throughput is recorded for a download application separately for the WLAN and LTE network. To allow for comparability between the yielded throughput values of the access networks a throughput limit of 1 Mbit/s is set for the download application. The obtained mean throughout values are thus available subject to the location in the hybrid testbed. An RSS experience map is obtained in a similar way, however in this case the values are gathered by passively scanning the access networks without causing any additional traffic to both networks. Beside the aforementioned external KPIs also locally gathered KPIs are included in both AHP algorithms. These are differentiated in network, vehicular and static KPIs. The network KPIs include the currently measured RSS value for both access networks, whereas the vehicle parameter consists of the velocity. The transmission costs is considered to be the only constant value. The corresponding weights for the KPIs of all network algorithms is presented in Table 5.4. As no other KPI rather than the RSS values are taken into consideration, theses values are assigned a weight of one in the RSS based algorithm. Recalling from Section 5.1.2 the sum of all weights has to be equal to one. The AHP local is configured in such a way that the RSS values have the highest weight, as this KPI is the only one giving an indication on the network performance and availability. As such it is assigned a weight of 0.5, whereas the vehicle velocity and the transmission costs are given each a weight of 0.25. In case of the AHP external (ex.) the highest weights are set for the external KPIs. Thus the externally stored RSS values have a weight of 0.3 and the external throughput (TP) values are assigned a weight of 0.25. The RSS ex. are given a marginally higher weight, as they are obtained passively by scanning the networks and thus are not subject to potential momentarily outages due to other

	RSS	Velocity	Costs	RSS ex.	TP ex.
RSS	1	n.a.	n.a.	n.a.	n.a.
AHP local	0.5	0.25	0.25	n.a.	n.a.
AHP ex.	0.15	0.15	0.15	0.3	0.25

Table 5.4: Weight profile of the AHP algorithms.

users. The remaining KPIs are each assigned the same weight of 0.15, see Table 5.4.

The yielded results of the three algorithms are presented in Figure 5.7. The first plot shows the network selection between LTE and WLAN depending on the employed handover algorithm. The outcome illustrates that the RSS based algorithm performs a network selection only once, whereas both AHP algorithms perform two selections. The RSS algorithm switches once from WLAN to LTE and remains afterwards with the LTE network. Even though the signal strength of the WLAN APs is compared to the LTE access network higher after passing by the street corner E3, see Figure 5.5. This is resulting from the underlying metric of the algorithm, which only triggers a handover, if the current network strength falls below the predefined threshold of -73 dBm. With the help of multi-criteria approaches, such as AHP ex. and AHP local such shortcomings for network selection are overcome. The outcome of both algorithms shows that a switch to WLAN occurs once the RSS values begin to deteriorate. In addition both algorithms switch back to the WLAN network when the RSS values improve and surpass the values of the LTE network. Comparing the handover of both algorithms in more detail reveals that the AHP local switches later to the LTE network than the AHP ex. algorithm. Moreover, in the section of the measurement route between the points P and E1 the network ratings between the WLAN and LTE network are clearly separated in case of the AHP ex. algorithm. The local AHP rates both networks closer to one another. A handover to LTE does, however, not occur, due to the implemented bucket concept. As the threshold is set to 30, see also AHP algorithm shown on page 31, an alternative network has to yield 30 times a better rating compared to the current network. This specific threshold was selected, as it proved to be suitable in the performed simulations in Section 5.1.2. Around the position E1 both multi-criteria algorithms switch to the LTE network, as the WLAN coverage is weak and in some cases even not available. Due to the external KPIs the AHP ex. performs a handover earlier to the WLAN network at around position E3. This is resulting from the external KPIs RSS and TP from previous drives. With the help of these KPIs the WLAN coverage area is detected earlier.

To quantify the additional value of using multi-criteria algorithms Figure 5.8 illustrates the savings in regards to the transmission costs and transmitted data. For the RSS based algorithm equal amounts of data, 40 MB in this case, are transmitted via both access networks, cf. Figure 5.8(a). The AHP local algorithm enables to transmit around 70 % of the data via the access network WLAN and thus only about 30 % over LTE. The AHP ex. on the other hand increases the usage of WLAN further by 6 %. Comparably to the results in Section 5.1.2 these are not significantly higher values, but this already shows the potential of using external data. Consequently, higher difference are feasible to be seen for an optimized algorithm. The transmission cost savings in Figure 5.8(b) illustrate a similar picture. The RSS algorithm achieves transmission cost savings of approx. 40 %, the AHP local and AHP ex. yield 53 % and respectively 57 %.

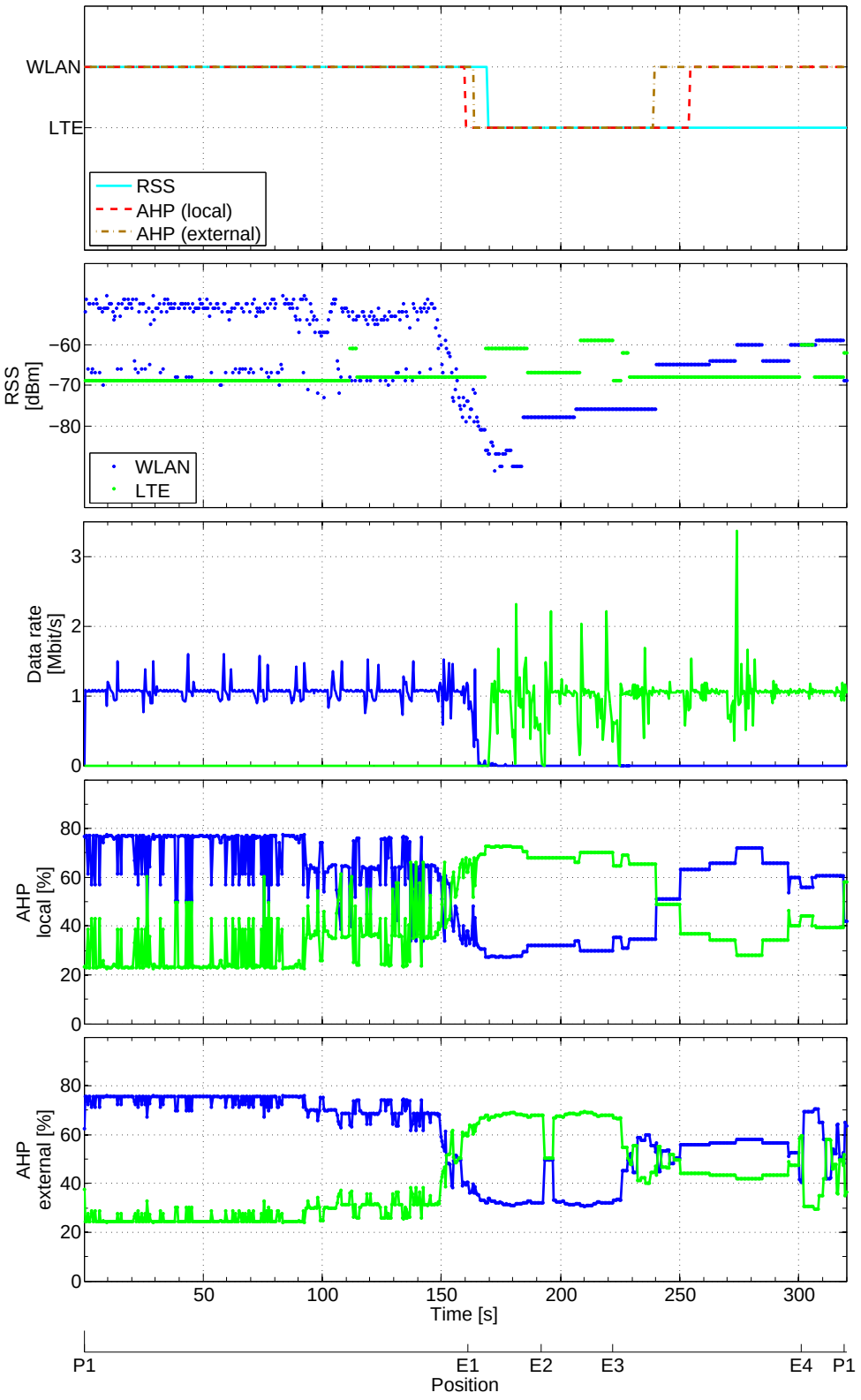

Figure 5.7: Results of the RSS and AHP based network algorithms.

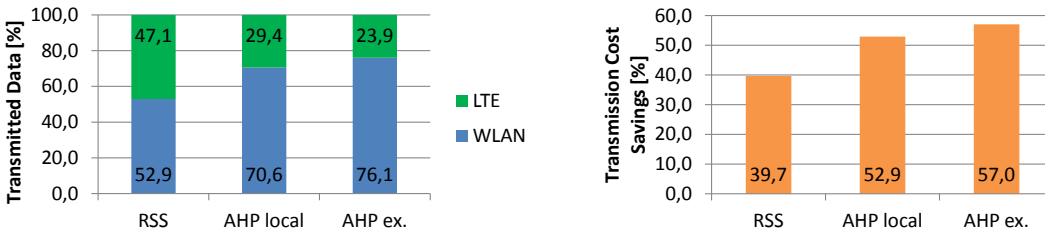

(a) Transmitted data.

(b) Transmission costs.

Figure 5.8: Yielded savings of transmission time and costs using multi-criteria algorithms.

5.1.4 Conclusion

This section illustrated that external KPIs, such as the network coverage, network load and experience maps have a significant impact on the context aware handover decision in hybrid access networks. Evaluations performed with simulations illustrated that the overall yielded QoS is improved and thus throughput drops are avoided. As these evaluations were carried out with the help of abstracted models of the radio networks, exactly quantifying the yielded additional value is not possible. However, the results showed that even for this simplified scenario the comparison between the multi-criteria algorithms clearly illustrated the benefit of including such KPIs in the algorithms. An analysis of the transmission costs by simulations using a file transfer application established that the overall costs were reduced by 65 % resulting from the use of WLAN APs instead of cellular networks. Naturally such an attempt requires a trade-off between the yielded savings and the overall transmission time. However, the introduced approach to rate the different KPIs allows to adapt to such trade-off demands by changing the weights of the included KPIs. As such applications and user profiles are suitable to be defined to adjust the connection according to the current vehicular context. Measurements conducted in a hybrid testsite corroborated these findings and also showed that with the help of external data networks, such as WLAN, are identified earlier and thus handovers are feasible to be performed sooner. Considering the dynamic vehicular environment this enables to exploit alternate networks with potentially lower transmission cost more efficiently.

5.2 Safety Applications

In contrast to infotainment applications the focus for safety applications is not on achieving overall constant throughput values or switching to alternate networks to save transmission cost, but rather on using available access networks to efficiently disseminate safety messages. Thus in this Section it is evaluated to which degree hybrid radio access improves the service delivery of latency stringent safety messages. As in the near feature vehicles of different OEMs potentially offer either cellular or ad-hoc radios and not necessarily both, an important variable of this investigation is the service delivery in regards to the vehicular radio (LTE, 802.11p or hybrid). This Section is organized as follows: The employed simulation environment is discussed in Section 5.2.1. Analytical models of the radio access networks describing the message delivery as a function of the transmission delay and a mobility model of an urban scenario are discussed. Those models are imported in MATLAB, where the service delivery is analyzed. The yielded results are presented in Section 5.2.2. The evaluation emphasizes on the on-time delivery of safety messages as a function of the distance. Thus the latency requirements are lowered with increasing distance from the location, where the incident causing the safety message occurred. Furthermore, is the additional value of using 802.11p RSUs analyzed to use network resources more efficiently.

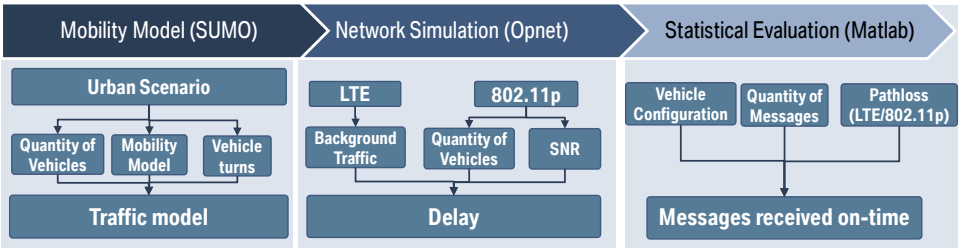

Figure 5.9: Overview of the employed simulation platforms.

5.2.1 Simulation Setup

The simulation environment used for this investigation consists of three different tools (1) SUMO[1], (2) OPNET[2] and (3) MATLAB[3], cf. Figure 5.9. The mobility model is created using the open source application SUMO [115], which enables to investigate microscopic, multi-modal traffic scenarios. Assuming that hybrid communication infrastructure, mainly in terms of 802.11p RSUs, is potentially deployed in urban scenarios first, the assessment is only carried out in such an environment. Besides the availability of network infrastructure an urban scenario proves to be more complex for collisions, since it offers multiple cross-roads, a higher traffic density as well as higher variations of vehicle speeds. In [93] it is proposed to consider 369 vehicles for a high traffic scenario in an urban environment. As this number already excels the

[1]SUMO 0.17.0, Institute of Transportation Systems at the German Aerospace Center
[2]OPNET Modeler 17.5, Riverbed Technology Inc.
[3]MATLAB R2010b SP1, The MathWorks, Inc.

capacity and resources the networks simulator OPNET is able to allocate, OPNET is only used to gather functional dependencies of the access networks and not for the assessment of the service delivery. Thus, after performing assessments for both radio access networks, in this case LTE and 802.11p, further investigations are carried out in MATLAB. Functional dependencies obtained from OPNET describing parameters influencing the transmission delay are then imported to MATLAB. In case of LTE a functional dependency between the delay and the base load is established. For 802.11p the delay is described as a function of the SNR and the quantity of vehicles in the communication range. Those dependencies together with the respective path loss models are implemented in MATLAB, cf. Figure 5.9. With these implementations the service delivery performance of each access network is evaluated in pre-defined time frames. During the evaluations the type of radio equipment deployed in a vehicle is varied. The following vehicle configuration are considered: (1) Equipped with a LTE radio, (2) Equipped with a 802.11p radio or (3) Equipped with LTE and 802.11p radios (hybrid). To ensure statistical reliability the simulations are run 50 times for each radio equipment configuration. In the following the configuration of the mobility model created in SUMO and the simulation environment developed in MATLAB are illustrated. The functional dependencies for the radio access networks obtained with OPNET are discussed afterwards.

Mobility Model The investigated urban scenario is based on a Manhattan grid, which is suggested in [93] for such an evaluation. For the spacing between the streets, it is assumed that from a bird's eye view the horizontal and vertical distance are both 200 m, resulting in a scenario of 1 km^2 in size, see Figure 5.10. To allow overtaking two lanes are implemented for each direction. To differentiate the path loss of 802.11p in a LOS and nLOS scenario 25 buildings are considered in the model.

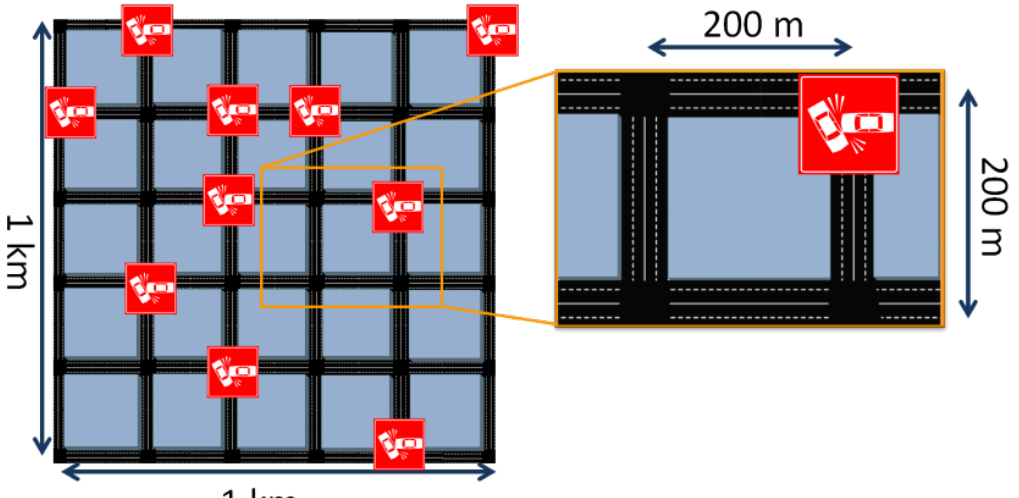

Figure 5.10: Urban scenario implemented in SUMO [115].

Each vehicle is assigned a random trajectory to ensure reproducibility of the results. The trajectories are implemented in such a way that all vehicles remain in the scenario. The probabilities upon which vehicles take turns or drive straight are set according to [116]. In [116] measurement drives were carried out in the city of Vienna and based

on the navigation options probabilities for the driving directions were calculated. The measurements yielded the following probabilities: (1) keeping straight: 26 %, (2) left turn: 33 %, (3) right turn: 41 %. To not complicate the considered mobility scenario u-turns are excluded. The speed limit of the vehicles is set to 60 $\frac{\text{km}}{\text{h}}$. However, due to the chosen high traffic scenario and due to the traffic lights the vehicles do not exceed a speed of 40 $\frac{\text{km}}{\text{h}}$. The current speed, acceleration and deceleration of vehicles are calculated according to the mobility model developed by Krauss [117]. The mobility model ensures that vehicles stop on-time at traffic lights at intersections, and keep a safety distance between one another to avoid rear end collisions.

MATLAB Configuration One LTE base station working at 800 MHz with one sector is considered for the simulations, more sectors are not defined as the scenario is only 1 km^2 in size. The base station is placed in the middle of the scenario and its height is set to 30 m. The Okumura-Hata path loss model [118] is used to determine whether the received signal power drops below the receiver sensitivity. It is assumed that all safety messages exchanged via LTE are routed through the OEM backend. To focus on the service delivery it is assumed that all vehicles are from the same OEM or that they are connected to a backend operator offering the same service for all. Consequently, this enables to distribute the messages to all vehicles in the scenario having a LTE radio. Vehicles with hybrid radio modules, thus with LTE and 802.11p radios, are able to forward safety messages they receive via LTE over 802.11p. Therefore enabling to reach vehicles being equipped with only 802.11p radio modules. To concentrate on the potential of hybrid radios to extent the dependability and range of safety application only one hop is considered between 802.11p vehicles. Thus one hybrid or 802.11p only vehicle is not able to re-transmit messages it has received over 802.11p any further. For 802.11p communication the corresponding radio access modules are either integrated in the vehicles or mounted as RSUs at the traffic lights. The configuration of the 802.11p radio modules is the same for both the vehicles and RSUs.

Considering the results in Figure 5.11 the envisioned range of 802.11p communication of 1000 m [119] is only met in case of a free space propagation model. As, however, free space propagation is not suited as a path loss model for urban areas, the WINNER-II model [120] is implemented. The WINNER-II model is according to [120] applicable for frequencies between 2 GHz and 6 GHz and especially suited in version B1 for urban micro cell scenarios. To be standard compliant a 802.11p receiver needs to have a receiver sensitivity of at least -89 dBm. A practical receiver likely has a better sensitivity, however in the following evaluation the case of a mere standard compliant receiver is considered. The obtained results considering a receiver sensitivity of -89 dBm illustrate a communication range of 570 m. Taking integrational aspects into consideration, see Section 2.2, this range is further decreased by 60 %, yielding a range of 230 m when setting the transmit power at the RSU to 23 dBm [16].

To verify the results measurements are conducted in an urban area using a vehicle as a transmitter and a RSU as a receiver. The RSU is mounted on the same height as the antenna on the vehicle. For the evaluation automotive qualified equipment is

used for both the transmitter and receiver. In the scenario the vehicle and RSU are both located at the starting point 'A' and the vehicle is moving away from the RSU. The transmit power at the RSU is set to 23 dBm and quadrature phase-shift keying is employed as modulation scheme [121]. Packets of the size of 200 byte are transmitted. The measurement route as well as the results are displayed in Figure 5.12. The results match well the outcome of the implemented path loss model, which also includes losses arising from the integration of 802.11p radio hardware in the vehicle. The ripples seen on the curve for the received power are caused by small scale fading. The aforementioned communication range of 802.11p of 230 m is thus corroborated. The path loss implemented in MATLAB is used to determine, if the received signal power is falling below the receiver sensitivity. Furthermore, it is employed to calculate the SNR, which is computed under the assumption of white noise at the receiver. To differentiate the path loss for nLOS conditions from LOS conditions the WINNER-II path loss is modified according to [120]. A nLOS condition is encountered, if a building is accounted between transmitter and receiver.

Network Infrastructure The functional dependencies of the transmission delay of safety messages for access networks LTE and 802.11p are derived in the following. The yielded models are implemented in MATLAB together with the mobility model. For the access network LTE a model is established, where the resulting end-to-end transmission delay is calculated subject to the current network load. To simplify the evaluation the LTE base station is configured with only one sector and the modulation scheme is set to 64 quadrature amplitude modulation. Between the base station and vehicle only unicast transmissions are considered. Broadcast transmissions are not part of this work as broadcasting mechanisms, such as evolved eMBMS, are, to the knowledge of the author, currently not deployed in LTE live networks. For the end-to-end delay in 802.11p a functional dependency is established between the SNR of the communication link and the quantity of vehicles in the proximity of the vehicle

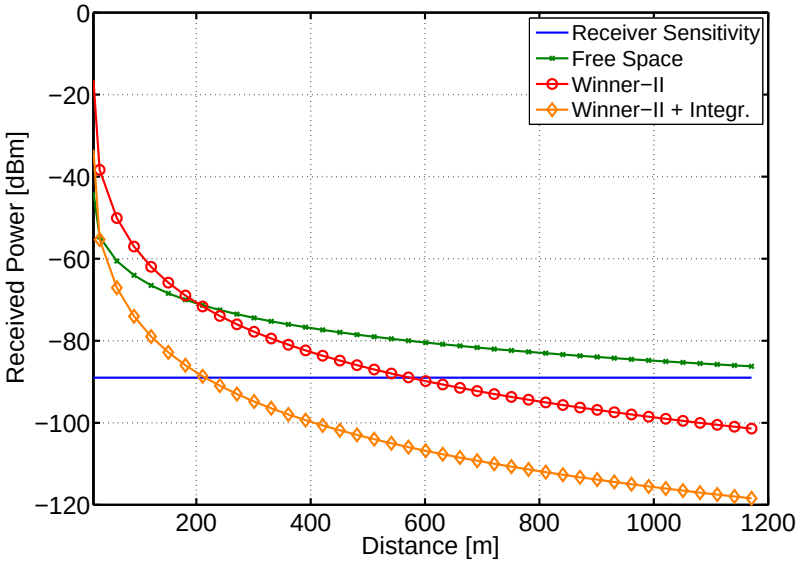

Figure 5.11: Range of 802.11p communication for different propagation models.

(a) Measurement track. Transmitter is located at 'A'.

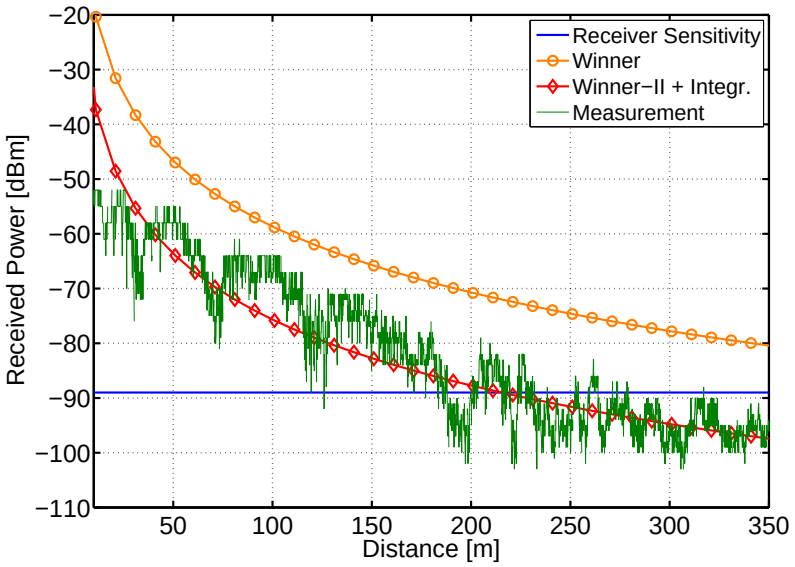

(b) Simulation and measurement results.

Figure 5.12: Verification of the implemented 802.11p WINNER-II path loss model.

reporting the traffic incident.

For the LTE network the functional dependency between the base load and the end-to-end delay is investigated with a simplified scenario with three users A, B and C. All users are located nearby the base station to achieve the highest throughput. User A is running a video conferencing applications while users B and C try to exchange a safety message. Delays occurring by processing the safety message in the OEM backend are not taken into consideration. To evaluate the end-to-end delay also for high throughput values user A runs multiple instances of the same application in parallel with each having a throughput demand of 9 Mbit/s. The resulting delay occurring in the transmission of the safety messages between users B and C is presented in Figure 5.13. Due to scheduling occurring in the base station and the core network as well as re-transmission of packets the obtained delay results differ from one another, especially at high network loads. This becomes significantly

evident at a throughput value of approx. 60 Mbit/s. It is seen that the required end-to-end delay of 100 ms for safety messages is not supported for a network load higher than 55 Mbit/s. To obtain a functional dependency between the end-to-end delay and the network load the median value is calculated for each throughput increment. An exponential regression function[4] Eq. (5.4) is fitted to the median values to obtain a functional dependency between the end-to-end delay $Delay_{\text{median}}$ and the network load $\Delta_{\text{base load}}$ in the LTE network. This functional dependency is used for further processing to calculate the delay for any given network load.

$$Delay_{\text{median}} = 2{,}03 \cdot 10^{-2} \cdot \mathrm{e}^{4{,}69 \cdot 10^{-2} \cdot \Delta_{\text{base load}}} \tag{5.4}$$

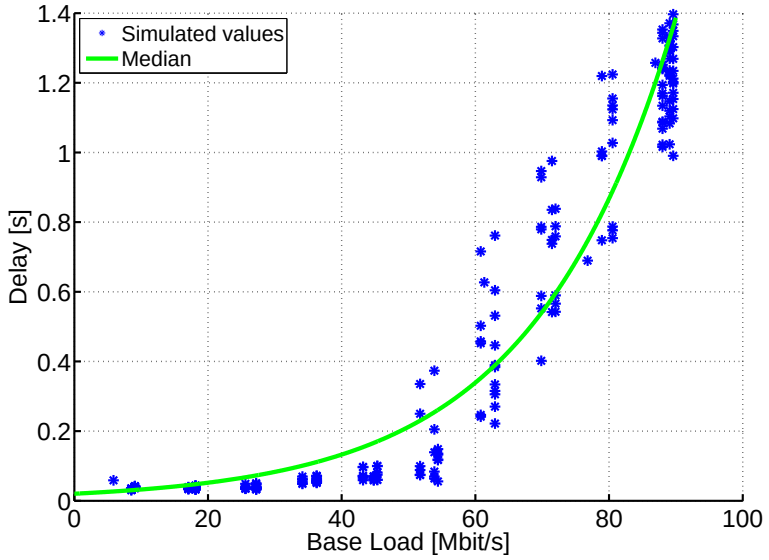

Figure 5.13: Modeling of the end-to-end transmission delay in the LTE network.

Currently there is no 802.11p radio module implemented in OPNET. As, however, the 802.11p standard is based on a 802.11a radio module, it is modified to realize a 802.11p implementation. An extensive investigation into the 802.11p receivers is given in [122]. The following parameters are set in OPNET, see [61]: (1) transmit power 23 dBm, (2) -89 dBm receiver sensitivity, (3) bit rate of 6 Mbit/s, (4) modulation scheme QPSK, (5) coding rate 1/2. Moreover, is the channel scanning on the mac layer of the 802.11a module deactivated and a necessary wildcard-BSS-ID assigned [123]. Further details on modifying the 802.11a radio module is found in [123]. For 802.11p communication a transmit power of 23 dBm is defined for non-safety applications, whereas this threshold is raised to 33 dBm in case of safety applications, see [121]. In the following distances up to 600 m and latency values up to 800 ms are evaluated for the on-time notification of vehicles. As, however, the latency threshold for safety applications is 100 ms, a transmit of 23 dBm is chosen for the entire evaluation to cover safety as well as non-safety applications.

[4]For finding a fit for the simulated values 'Curve Fitting Toolbox 3.0' from 'The MathWorks, Inc.' is used.

Also in case of 802.11p are functional dependencies between relevant KPIs gathered in OPNET and imported to MATLAB. In the investigated scenario two vehicles are exchanging DENMs, while being surrounded by randomly located vehicles of varying quantity. The vehicles are located within an area, which is twice as large as the communication range of 802.11p. The area is thus defined by a circle with a radius of approximately 230 m. All vehicles located in this area, except the transmitter and receiver of a DENM, are exchanging CAMs with a frequency of 10 Hz. As propagation model the previously investigated WINNER-II model is employed. The delay subject to the SNR and the quantity of vehicles is analyzed at the receiving vehicle and presented in Figure 5.14. In case of $N_{Veh} = 50$, cf. Figure 5.14(a), all of the vehicles obtain the message on-time within the defined time frame of 100 ms. This drops to a probability of 90 % for a quantity of $N_{Veh} = 100$ vehicles. A similar effect is seen for the SNR values, cf. Figure 5.14. For $N_{Veh} = 50$ the given delay threshold of 100 ms is not exceeded. In case of $N_{Veh} = 100$ delays higher than 100 ms are only accounted for SNR values lower than 3 dB. The functional dependency relating to the delay, SNR and the quantity of vehicles is shown in Eq. 5.5. The expression is obtained by employing a multivariate linear regression, thus fitting the values for SNR and the vehicle quantity on a plane.

$$\begin{aligned} \log(Delay[s]) = \quad & -5{,}82 + 0{,}81 \cdot \log(N_{Veh}) \\ & + 8{,}66 \cdot 10^{-2} \cdot \log(SNR) \\ & - 0{,}27 \cdot \log(SNR) \cdot \log(N_{Veh}) \end{aligned} \tag{5.5}$$

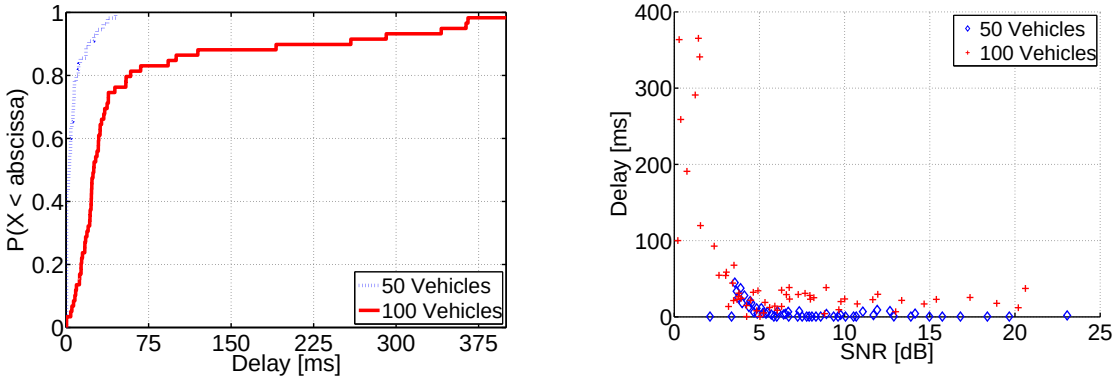

(a) CDF of the delay.

(b) SNR distribution.

Figure 5.14: Modeling of the end-to-end transmission delay for 802.11p radios.

5.2.2 Simulation Results

With the described simulation environment the additional value of a hybrid communication system for the delivery of safety messages is analyzed in this Section. The on-time delivery of safety messages is investigated for 50 DENM events occurring in random locations within the urban scenario, cf. Figure 5.10. The time frames in which the messages have to be received depend on the distance between the

receiving and transmitting vehicle. With increasing distance the time thresholds are incremented, as the recipients have higher reaction times. As the distances define the range, where the message bears relevance for the recipient vehicles, from here on it is denoted as the relevance range. The lowest relevance range of 150 m is resulting from a worst case calculation in an urban scenario. Assuming an icy road deceleration of $1\,\mathrm{m/s}^2$ and a vehicle driving at a 60 km/h, it requires at least a distance of 150 m to prevent a rear-end collision [124]. The corresponding delay of 100 ms is chosen, as it is a defined value for safety messages in the literature, cf. [125]. To the best knowledge of the author correlations between the transmission delay and relevance range are not defined in the literature for vehicles outside the area of stringent delay requirements. Thus, a relevance range of up to 600 m around the vehicle reporting the traffic incident is assumed, while incrementing the ranges by 150 m. Further distances than 600 m are not considered as it is assumed that in an urban scenario time crucial safety messages are not relevant anymore above this point. For the corresponding delay two different scenarios are considered. For the first the delay is incremented by 50 ms and for the second by 100 ms. The resulting delays subject to the relevance range are shown in Table 5.5 and visualized in Figure 5.15. A threshold of 50 m for the lowest range displayed is chosen, as for this range the probability of at least one vehicle being in the relevance range is 85 %. In the following it is investigated how well the aforementioned boundaries are met for vehicles equipped with different radio modules and for varying network loads in the LTE network. Variations in the radio module configuration affect all the vehicles in the scenario. For instance, in case of a 50 % penetration of LTE and 802.11p radio modules, the vehicle transmitting the safety message has a 50 % probability of being equipped with either a LTE or 802.11p radio module. Thus the probability of the radio module configuration of the transmitting vehicle is the same as of all other vehicles in the scenario.

	Relevance Range [m]			
	[50;150[	[150;300[	[300;450[	[450;600]
TH(I) [ms]	100	200	300	400
TH(II) [ms]	100	150	200	250

Table 5.5: Relevance range and corresponding delay in the considered scenarios.

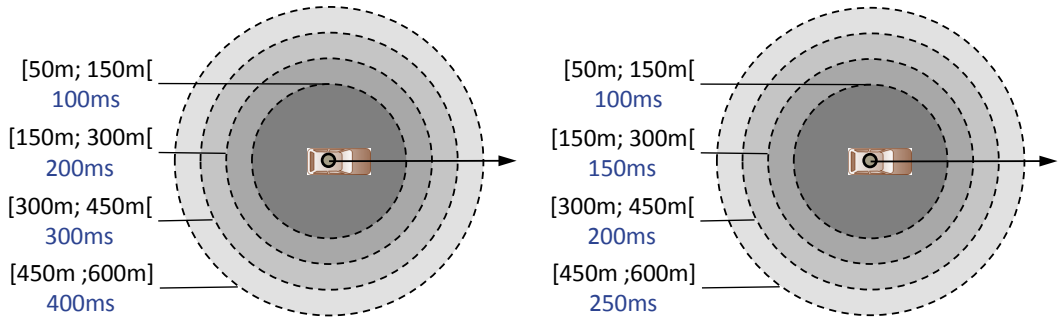

(a) TH(I). (b) TH(II).

Figure 5.15: Visualization of relevance ranges and delays from Table 5.5.

LTE and 802.11p Radio Modules The results for on-time notified vehicles as a function of the relevance range and the vehicle radio module is displayed in Figure 5.16. The investigation is carried out for three different base loads in the LTE network: {20, 40, 45} Mbit/s. Figures 5.16(a) - 5.16(c) illustrate the on-time message delivery for TH(I), whereas Figures 5.16(d) - 5.16(f) for TH(II). Vehicles are equipped with either a 802.11p or a LTE radio module, thus vehicles equipped with both radios are not considered yet. The penetration of the radio module equipment of the vehicles is varied in steps of 5 % starting with all vehicles being equipped with only 802.11p modules. With each step the amount of vehicles having a LTE module is thus increased by 5 %, whereas the amount of 802.11p only equipped vehicles is decreased by 5 %.

The results for TH(I) and a base load of 20 Mbit/s, shown in Figure 5.16(a), illustrate that both access networks are apt to deliver the safety messages to other vehicles on-time. The service delivery of 802.11p radio modules is decreasing starting at approximately 250 m, which is resulting from its low communication range compared to LTE radios. Consequently, to deliver safety message to the vehicles on-time an increase of the penetration of LTE radios is necessary. At approximately 50 % of LTE as well as 802.11p radios about half the vehicles in the scenario are reached on-time. This is resulting from the same odds of vehicles being equipped with either one radio module. Thus potentially 50 % of the affected vehicle do not receive the message, as they lack the radio module necessary to receive the message. Comparing these results to the outcome for TH(II) for the same base load of 20 Mbit/s, seen in Figure 5.16(d), reveals no significant difference.

Increasing the base load to 40 Mbit/s illustrates that two reception areas begin to appear, see Figure 5.16(b) for TH(I). In the first reception area until 250 m the results are up to a penetration of 20 % of LTE radios comparable to the previously discussed results in Figure 5.16(a). However, for an increased penetration of LTE radios a communication gap starts to form. Equipping all vehicles in the scenario with LTE radios results in no on-time notified vehicle in this area. This is only improved with an increased relevance range, as this corresponds to more relaxed delay requirements. Still even at the high relevance ranges above 450 m the high base load of 40 Mbit/s does not allow that all vehicles in the scenario receive the message on-time. As the base load in the LTE network does not effect the 802.11p communication, no changes compared to Figure 5.16(b), are seen for a low LTE penetration thus a high 802.11p radio penetration at increased relevance ranges. To improve the number of on-time notified vehicles in this area, it is essential to enhance the communication range limitations of 802.11p radios.

In contrast to the results of TH(I), the outcome for TH(II), see Figure 5.16(e), illustrates an increased communication gap. The areas, where either 802.11p or LTE radios are able to transmit the messages are clearly separated. Thus for a high 802.11p radio penetration and up to a relevance range of 250 m, all effected vehicles with ad-hoc radios are able to reliably distribute and receive safety messages. Using LTE radios allows only to reach half of the vehicles in the scenario even at the highest relevance range. As the results for base load of 45 Mbit/s for TH(I), see Figure 5.16(c),

are similar to the previously discussed outcome, they are not discussed here again. In case of TH(II), however, for the same base load of 45 Mbit/s, see Figure 5.16(f), the ability of using LTE for the distribution of safety messages is significantly impaired. For the highest relevance range of 600 m and a corresponding latency threshold of 250 ms, cf. Table 5.5, about 20 % of the vehicles receive the safety message on-time. This corroborates the previous findings that the capability of the LTE network to disseminate safety messages depends considerably on the base load. For high base loads using a best effort QoS prioritization is not sufficient for safety applications, as seen in the previously discussed results. The major drawback of 802.11p radios is the limited communication range restricting the message dissemination significantly.

Hybrid Radio Modules Equipping vehicles with hybrid radios, see Figure 5.17, significantly reduces the communication gaps, which were seen in the previous results. The following setting is applied to the simulations: The vehicles having a 802.11p or a LTE radio module are of the same amount, the remainder is equipped with hybrid radio modules. Thus in case of 20 % hybrid equipped vehicles, 40 % of the remaining vehicles are equipped with LTE and the rest with 802.11p radio modules. The results for a base load of 20 Mbit/s in case of using TH(I), see Figure 5.17(a), and for TH(II), see Figure 5.17(d), illustrate that the previously seen communication gaps are overcome. In a relevance range up to 250 m even at low penetration rates of hybrid radios, such as 10 %, almost all vehicles are notified on-time. This is mainly resulting from the ability of hybrid radios to forward messages, which were received over LTE, using 802.11p. Thus 802.11p radio modules work in this case as a bridge to communicate between vehicle having only one radio module. The peak seen in case of TH(II) in Figure 5.17(d) for low relevance ranges, such as 50 m, where only about 90 % of the vehicles receive the safety message on-time, results from statistical fluctuations. In small relevance ranges it is probable that only a few or only one vehicle is located, which, such as in this case, potentially has only one specific radio module. Consequently, even a high hybrid radio penetration does not have an impact on the results.

For a base load of 40 Mbit/s, considering the results of TH(I), Figure 5.17(b), illustrates that to compensate the increased delays of the LTE network a high penetration of hybrid radio modules is necessary. At the range limits of 802.11p radios, which is around 250 m, a drop in the on-time notified vehicles is seen. Even though no transmission gaps occur due to the applied forwarding scheme of hybrid radio modules. For relevance ranges higher than 250 m the yielded results are again similar to the ones yielded at smaller ranges than 250 m. Increasing the hybrid configuration by approx. 10 % yields in addition 10 % on-time notified vehicles. This trend changes, if more stringent delay constraints, as seen for TH(II), are applied. Even though the results in Figure 5.17(e) are up to a relevance range of 250 m similar to the previously discussed outcome, this changes substantially for higher relevance ranges. At approx. 300 m even a full hybrid penetration only yields about 60 % timely notified vehicles. An increased relevance range does not improve the results, as the delay introduced by the base load is still to high. As similar results are yielded for TH(I) in case of a 45 Mbit/s base load, cf. Figure 5.17(c), they are

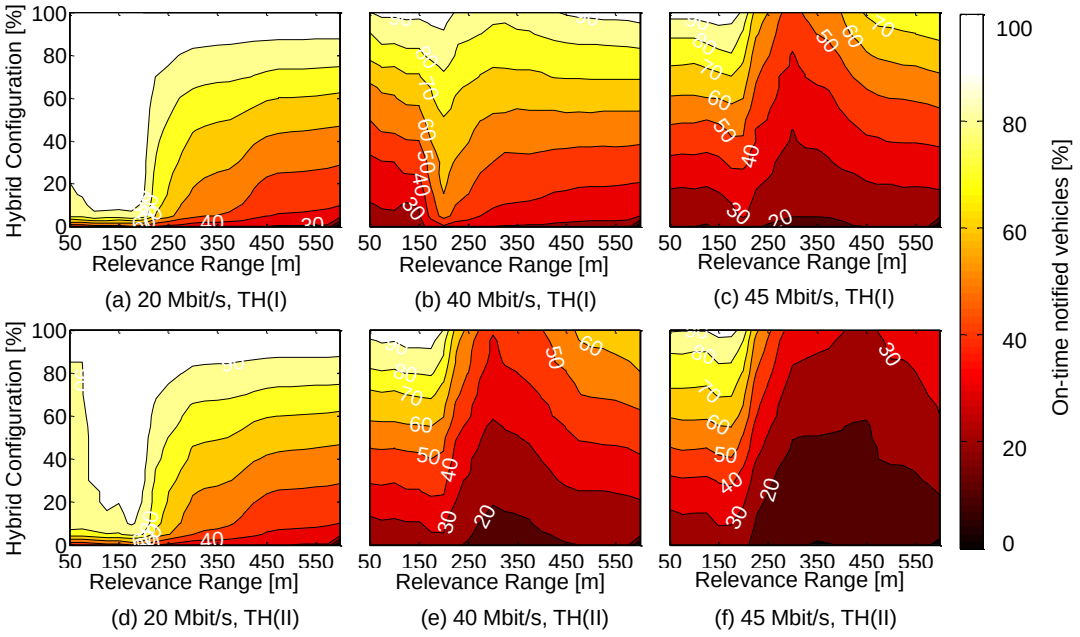

Figure 5.16: On-time notified vehicles using LTE and 802.11p radio modules. The following radio distribution applies: 802.11p = 100 % − LTE. Thus, for instance, at a 20 % penetration of 802.11p radios, 80 % are equipped with LTE radios.

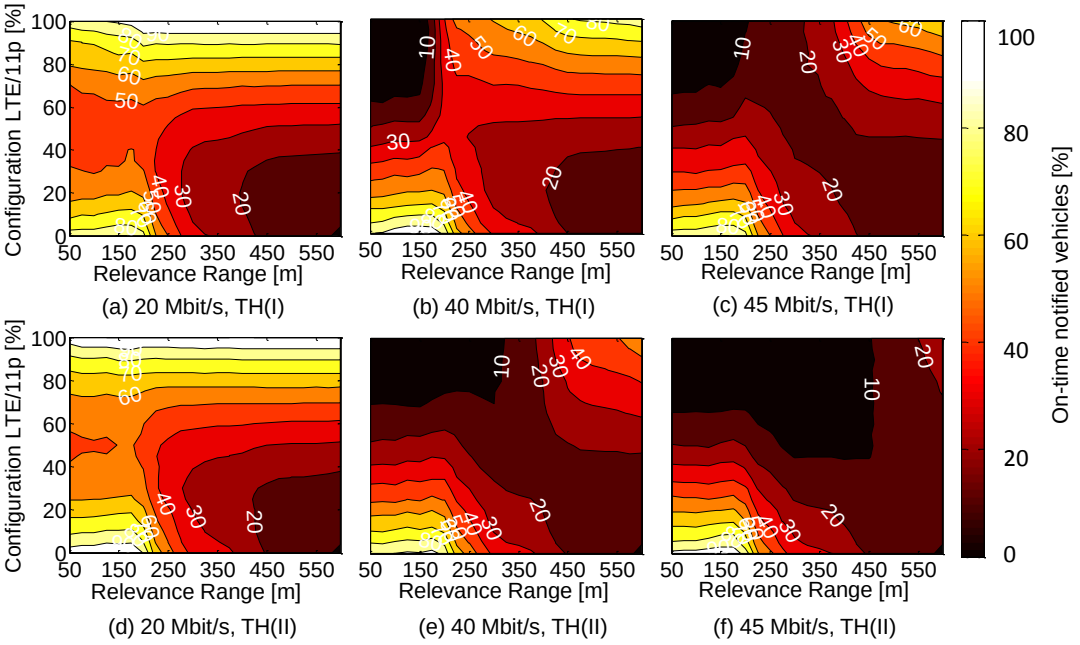

Figure 5.17: On-time notified vehicles using LTE, 802.11p and hybrid radio modules. The penetration of LTE and 802.11p is always the same, the remainder is equipped with hybrid radios. Thus, for instance, at a 20 % penetration of hybrid radios, 40 % are equipped with LTE radios and also 40 % with 802.11p radios.

not discussed here. Changes are, however, seen in case of the TH(II) for the same base load. Figure 5.17(f) illustrates that compared to the previous results starting at 250 % not more than 40 % of the vehicles are reached on-time even at a full hybrid penetration. Consequently, establishing that also in case of hybrid radio modules, which by forwarding offer an approach to disseminate safety messages more reliably, the base load is still the performance determining factor in the LTE network.

Base Load in the LTE Network In Figure 5.18(a) the dissemination of safety messages is investigated as a function of the base load in the LTE network. A relevance range of 500 m with a delay constraint of 400 ms is considered, which is the highest transmission delay from the previous investigation. The yielded results show that the cellular communication is substantially depending on the base traffic occurring in the network. For a traffic of up to 20 Mbit/s even a penetration of 20 % is enough to notify up to 70 % of the effected vehicles on-time. It is also interesting to note that the on-time notified vehicles have a constant offset, depending on the radio penetration. At a penetration close to 80 % approximately all the vehicles obtain the safety message within the required time frame. The break-point, where the base traffic prolongs the reception of the messages is reached at 40 Mbit/s. Above a base load of 40 Mbit/s only up to 50 % of the vehicles are reached on-time. Not considering any QoS prioritization of the safety related vehicular messages, a base load of about 30 Mbit/s is the limit to ensure a reliable service delivery.

To better visualize the functional dependencies between the service delivery and the base load three operating points {0, 30, 45} Mbit/s of the base load are investigated, cf. Figure 5.18(b). The greatest increase of on-time notified vehicles throughout the relevance range is seen for a base load of 0 Mbit/s. At a penetration of 5 % more than 60 % of the vehicles in the scenario are notified on-time. For 30 Mbit/s still up to 50 % of the vehicles are reached. In case of a base load of 45 Mbit/s this is reduced to 25 %. To analyze the impact of the base load on the transmission delay further, another operating point at a hybrid radio penetration rate of 40 % is considered. For this penetration approx. 75 % of the vehicles are notified on-time, when no base load is taken into consideration. A further increase in penetration, in this case 60 %, yields only 25 % more on-time notified vehicle. Thus all vehicles in the relevance range of 500 m. Considering a base load of 30 Mbit/s the safety messages are received by 65 % of the vehicles in the relevance range. A base load of 45 Mbits/s results in 38 %. Considering even a full penetration of hybrid radios such a high base load does not allow to notify all vehicles on-time, only up to 60 % are reached. All three results show that the base load is the most decisive factor for proper distribution and reception of safety messages transmitted over LTE. Even a full penetration of vehicles with hybrid radios does not enable an on-time delivery of the messages, if the base load is too high. Besides decreasing the system efficiency a high base load results in an additional consumption of network resources, as the safety messages, which are not useful anymore, are still received by the vehicles. An analysis of using available cellular network resources more efficiently by deploying 802.11p based road infrastructure is presented in the following.

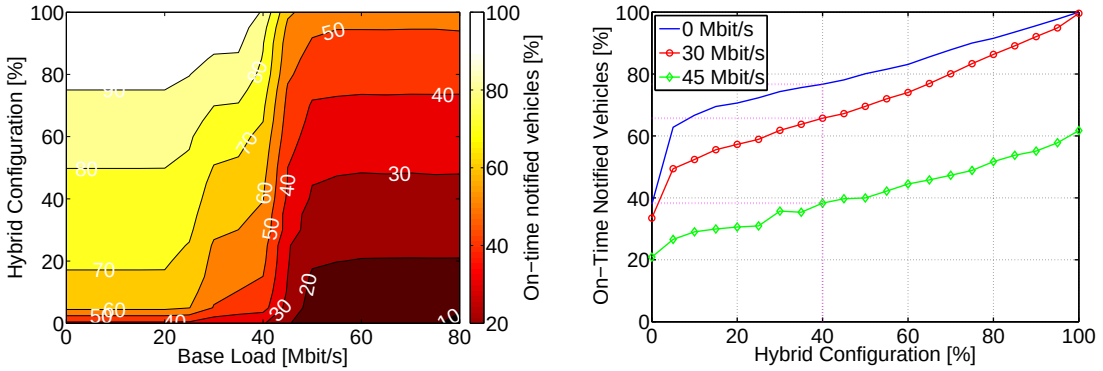

(a) Base load.

(b) Base load operating points.

Figure 5.18: On-time notification of vehicle for operating points from Fig. 5.18(a).

Network Resources To illustrate that using hybrid radios allows to lower the usage of network resources a transmission costs model is assumed as a metric to calculate the savings in the ongoing transmissions. The transmission costs from a vehicle to the backend via LTE is allocated 0.02 cost units (cu). Communication between vehicles using 802.11p and broadcasting via 802.11p from RSUs is assumed to be free of charge. The compensation of the RSU operators for broadcasting messages over 802.11p, which they receive over LTE, is set to 0.04 cu per event. This also covers the expenses of notifying the OEM backend on the radio configuration of the vehicles in the range of the RSU. To illustrate the resulting additional benefit of using RSUs the results are normalized to the case that the vehicles in the scenario are only equipped with LTE radio modules. For the investigation the penetration of hybrid radios is set to 40 % and the base load in the LTE network is assumed to be zero. The results for the arising transmission savings is shown in Figure 5.19. Equipping only a quantity of 40 % of the vehicles with hybrid radios lowers the transmission savings to 55 %, which equals 29 cu. These savings are lowered further by broadcasting messages with the help of RSUs. In the scenario each intersection is potentially able to be equipped with one RSU. As the distance between the intersections is set to 200 m, the RSU are thus also separated by 200 m from each other. With each increment in the number of RSUs, they are placed randomly at the intersection in the scenario.

The results in Figure 5.19 illustrate that the impact of the RSUs on the transmission savings is negligibly small for up to 5 units, which is resulting from their random placement. Thus, if a vehicle transmits a safety message and no RSU is nearby, no transmission savings are yielded. However, starting at 5 RSUs the number of transmissions start to decrease, going down to 38 % for 16 RSUs. Increasing the number of RSUs further up to 25 does not bring additional savings. This is resulting from the higher transmission costs, which were assumed when using RSU to broadcast safety messages rather than unicast transmissions triggered by the OEM backend. Thus the savings encountered by omitting LTE unicast transmissions are compensated with the use of RSUs, where the transmission costs are twice as high. Furthermore, vehicles being in the range of, for instance, two RSUs are notified by both, which

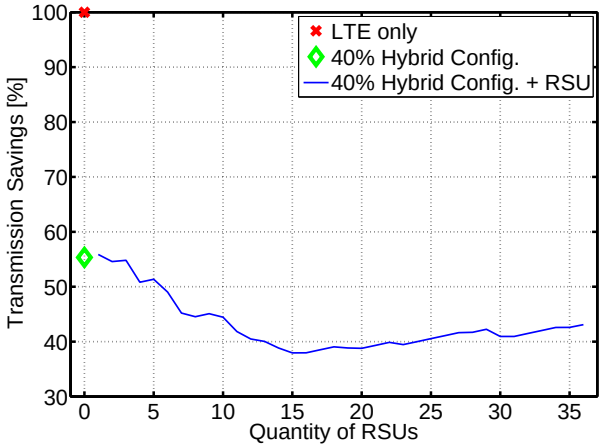

Figure 5.19: Transmission savings using RSUs.

increases the reliability of message reception but also does not allow additional savings. This effect of more transmissions due to RSUs is especially evident for more than 25 RSUs. The transmission savings of 43 % requiring to equip each intersection with RSUs, in this case 36, are still significantly lower compared to not using any RSUs. This shows that a well evaluated approach is necessary, when deploying RSUs. The deployment needs to provide on the one hand necessary redundancy of the safety messages to ensure reliability. On the other hand the use of RSUs has to decrease the demand on the already limited cellular resources.

5.2.3 Conclusion

The evaluation of hybrid radio access for safety applications illustrated that the combination cellular with ad-hoc radio systems significantly enhances the service delivery of safety messages. Consequently, the drawbacks of the radio networks is overcome, which is for 802.11p the limited communication range and in case of LTE the base load in the network, which increases the transmission delay. For small relevance ranges it was shown that 802.11p radio modules are suitable to distribute safety messages to all effected vehicles in the scenario, even in case of high latency thresholds, such as 100 ms. However, this requires an almost full penetration of 802.11p radios in the scenario. For 802.11p radios a relevance range of 250 m was measured in an urban V2I scenario using a prototypical antenna system and a transmit power of 23 dBm. A higher range is feasible to be yielded in case the performance deteriorating effects resulting from integrating the antenna on the vehicle rooftop are compensated, thus when the antenna system is adapted to characteristics of the vehicle. In addition mounting the RSU antenna on a more exposed higher position is also likely to increase the range.

Due to the reduced relevance range of 250 m, higher ranges are only feasible to be covered with LTE radios in case no hybrid radios are considered. Although LTE is designed in contrast to other cellular networks, such as UMTS, to fulfill the stringent delay requirements of safety applications, the investigation showed that this ability

is subject to the base load in the network. Low base loads, such as 20 Mbit/s, allow the on-time dissemination of safety messages. However, increasing the base load to 45 Mbit/s illustrated that messages even with more relaxed latency requirements, such as 400 ms, are only received on-time by a fraction of the vehicles in the scenario. Furthermore, the investigation showed that in this case a communications gap starts appearing at approx. 250 m, where a reliable delivery of safety messages is not possible. Equipping vehicles with hybrid radios enables the service delivery even at high base loads, as messages received over LTE are potentially forwarded using 802.11p. Consequently, hybrid radios enlarge the relevance range of 802.11p radios, which in turn improves the message dissemination even with stringent delay requirements.

Evaluating the efficiency of hybrid radios for selected operating points showed that even low penetrations of these radios are able to yield such service delivery improvements. The assessment also showed that hybrid radios are also beneficial in regards to lowering the amount of data transmitted through the network. Transmission savings around 45 % are obtained by just using one hop forwarding of messages received over LTE for the assumed model. An even further increase in the transmission savings are yielded with the help of 802.11p RSUs, which increased the savings to 62 %. Although data packets of safety messages are compared to the infotainment case small, offloading some of the traffic from cellular to ad-hoc enables to lower the impact that such applications have on the cellular network. In addition to using available network resources more efficiently by employing forwarding the reduced amount of cellular connections is also worthwhile to achieve transmission cost savings. As such this enables to lower the hurdles in deploying safety systems relying on a cellular infrastructure.

Chapter 6

Conclusion

This thesis discussed the use of hybrid radio access incorporating the corresponding antenna systems and the yielded merits for infotainment as well as safety applications. The investigation for hybrid antenna systems focused in the cellular domain on the access network LTE and in the ad-hoc domain on 802.11p systems. For the antenna systems it was established that due to the different application requirements the necessary KPIs to assess their suitability for the access networks is dissimilar. In case of cellular MIMO systems, for instance used for LTE, KPIs have to be applied describing the capability to support SMX transmission schemes. On the contrary KPIs for diversity transmission schemes have to be considered for 802.11p communication, as the primary focus is here a reliable communication rather than achieving high data rates. To better illustrate the obtained results for both the cellular and ad-hoc domain, the conclusions are drawn here separately starting with the cellular antennas.

In the cellular domain, see Chapter 4.1, different prototypical antenna systems and a reference antenna system consisting of two magnet-mount monopole antennas were analyzed. The analysis of the reference antenna system, which was longitudinally aligned with the conventional antenna mounting space on the vehicle rooftop, was used to investigate the impact of antenna isolation on system level KPIs. The assessment showed that the KPIs mutual information and channel condition number are apt to assess the SMX capabilities of different antenna isolation values. The channel condition number was interpreted in this work as the noise enhancement of a zero-forcing receiver. The evaluation was carried out performing active probing and passive listening measurements in a live LTE network conducting drive tests on a 9 km long track in Munich bearing different channel conditions. For a reference antenna spacing between 11 cm and 43 cm, measuring at the center frequency of the operator's band (796 MHz), which equals a wavelength of approx. 38 cm, no significant changes were seen. The condition number fluctuated in this region around 18 dB for the entire measurement track, 22 dB for the LOS and 16 dB in case of the nLOS scenario. A similar behavior was seen for the mutual information, yielding significant changes between an antenna spacing of 3 cm and 11 cm. Overall no significant changes were seen between a spacing 11 cm and 53 cm. A considerable impact was illustrated comparing the highest separation of 83 cm and the second highest of 53 cm. In

the saturated area between 11 cm and 53 cm the mutual information values varied between 7.5 bit/(s·Hz) for the entire measurement track, around 8.5 bit/(s·Hz) for the LOS section and around 5.5 bit/(s·Hz) for the nLOS section. The lowest values for the condition number and highest mutual information values were naturally obtained for the highest antenna separation of 83 cm, which is almost the full width of the roof. The mutual information was increased up to 2 bit/(s·Hz), whereas the condition number was decreased up to approx. 6 dB.

From the reference antenna evaluation it is concluded that the current antenna integration volume having a length of approx. 10 cm is sufficient to exploit the SMX capabilities of 4G communication systems, such as LTE. However, exploiting the available volume efficiently is only possible with antenna systems manufactured in 3D MID technology. Conventional antenna systems based on PCBs are limited by the given unevenly distributed height of the current antenna housing design, thus do not allow to fully exploit the available volume. This was also corroborated assessing different prototypical antenna systems and comparing them to selected reference antenna separations. The prototypical PCB antenna system yielded the lowest antenna isolation of approx. 5 dB and also highest return loss of -6 dB for the aux antenna. The prototypical systems based on 3D MID technology yielded overall mismatch values being about 2 dB lower, but achieved a twice as high antenna isolation reaching up to 10 dB. Moreover, due to the alignment of the PCB antennas and thus a shadowing of the main and aux antenna the prototypical system was subject to frequent gain drops in the radiation pattern. Analyzing different MIMO systems also revealed that the front of the vehicle is in contrast to the rear to a higher degree subject to variations in the antenna gain. All prototypical antennas, although designed by different supplier or institutions, illustrated a similar minimum gain value of approx. -4.4 dBi for the main antenna covering the front. Active measurements conducted in a live LTE network showed that gain differences of approximately 6 dB in the rear caused a fallback to diversity transmission. Such a fallback was predominately registered in a LOS scenario with the base station. The exact value of the gain difference is subject to the parametrization of the operator and is consequently likely to change performing measurements in another network. To gauge the probability of such fallbacks a statistical metric ρ_{TH} analyzing gain outages and a metric ρ_{Diff} determining occurrences for gain differences were introduced. Further applied KPIs to evaluate the antenna performance included the antenna impedance and radiation values as well as antenna gain related metric, such as G_{mean}, G_{min} and G_{max}.

On component level the same KPIs were also applied to the performance assessment of 802.11p antenna systems. However, due to the high operating frequency at 5.9 GHz and the requirements of an omni-directional antenna pattern the priority of the KPIs is different compared to cellular antennas. The evaluation on component level illustrated that all prototypical antenna systems yield results for impedance related KPIs well below the required the threshold in antenna specification sheets, which is -10 dB for the return loss and -12 dB for the antenna isolation. Thus in contrast to cellular antennas the emphasize on impedance values is not of such a high priority. However, antenna gain related KPIs are all the more important, especially ρ_{TH}.

Assessing different prototypical antenna systems revealed that the highest outage rates, in the considered channel scenario, were found for the 2D PCB prototypical system and the 3D MID sample having adjacent located 802.11p antennas. The alignment of the antennas in case of the 2D prototype caused blind spots in the radiation pattern as the antennas shadowed one another in the front and respectively in the rear of the vehicle. Another disadvantage is the yielded communication range, which due to the unevenly distributed integration volume for the main and aux antenna shows an increased direction dependent behavior. Thus depending on the driving direction a maximum range of 560 m or 720 m was yielded at a transmit power of 23 dBm at the RSU. An advantage is, however, resulting from the size constraints of the given integration volume of the antenna housing. In order to exploit the available volume as efficiently as possible the 802.11p antennas are integrated in the same PCBs as are the cellular antennas. This necessity reduces the interaction between the antennas. The lowest interaction between the antennas and the longest communication range was determined for the 3D MID prototypical system with the 802.11p antennas one on each side of the antenna housing. The measurements showed that the least direction dependent behavior is found for this prototypical system yielding in both directions 750 m. Among the analyzed systems this antenna prototype was also the one illustrating overall the lowest gain outages in the radiation pattern. Moreover, due to the small difference in signal power values between the individual antennas such a design methodology is also well suited for different diversity combining techniques, such as for maximal-ratio or selection combining.

To compensate the performance deteriorating effects of the antenna housing and thus to increase the communication range of antenna systems a methodology was evaluated to compensate these effects. It was found that by using an antenna housing with a homogeneous wall thickness the destructive interference was turned into constructive interference. Improvements in the antenna gain of up to 10 dB were seen in areas, where previously nulls were present. By system level simulations it was shown that such a compensation potentially improves the RSS values of up to a level of magnitude of 10 dB considering a V2I scenario. Moreover, it was illustrated that for investigating different sizes of antenna housings or thicknesses geometrically simplified shapes are feasible to be used, which proved to have a similar impact on the antenna radiation pattern.

In the second part of this thesis hybrid radio access was analyzed for infotainment and safety applications. It was discussed that infotainment applications are user-centric as their functionality is not subject to other parties. Thus research was conducted into improving the achieved QoS by avoiding momentarily connection outages. This was achieved by distributing the traffic over different access networks, hence elongating the transmission time, but saving network resources and transmission costs on the other hand. In scenarios, such as in a traffic congestion, where the base load of the cellular network is potentially high, such an off-loading approach is also likely to reduce the transmission time as well as lower the arising costs. To determine the most suited access network in the performed evaluations, inputs were considered from the vehicle control units, such as the velocity, values from the network and KPIs from external sources from the Internet. Especially the values from external

sources, such as network coverage maps and signal values from past connections, proved to be very beneficial. Using the aforementioned KPIs it was shown that only networks offering good QoS were selected. This reduced the number of handovers and yielded the overall highest mean data rate. Considering a download application using cellular and WLAN access networks it was shown that up to 2/3 of the transmission costs are potentially saved. A further advantage of the employed algorithm is that according to user preferences or application demands weights of the KPIs are able to be changed. Thus forcing or even avoiding frequent network re-selections. The measurements conducted in a hybrid testsite also corroborated the findings increasing the transmitted data and lowering the transmission cost by using alternate networks.

Safety applications are on the contrary to infotainment applications of a cooperative nature, thus have to work dependably for anyone and not just satisfy the needs of an individual. Consequently, the conducted analysis focused on the service delivery in a given scenario. The evaluations were carried out in an urban environment equipping vehicles with different radio modules to assess their standalone and combined impact on the achieved service delivery. With the help of simulations and measurements it was shown that the range of 802.11p communication results in approximately 230 m. It was discussed that this reduction in the communication range yields from integrational impairments, such as the roof shape or the antenna housing. Thus making 802.11p communication due to range limitations only suitable for the immediate surrounding of a vehicle to distribute safety messages. LTE on the other hand was proven to be unsuited for the immediate surrounding of such a vehicle in case the base load of the networks is too high. The simulation results in the considered scenario showed that a performance deterioration of the LTE network occurs at a base station loads of 40 Mbit/s. It was found that 802.11p radio system are only able to partially fill this communication gap, due to their own range limitations. Hence a coverage gap between 230 m and 450 m was created, where potentially no vehicular safety application work. Using hybrid radio access, this gap was substantially reduced and the quantity of on-time notified vehicles increased. It was shown that a substantial amount of traffic incidents are prevented when using hybrid radios, even at penetration rates of hybrid radios, such as 40 %. In a scenario with a high base load of 33 Mbit/s more than 65 % of traffic incidents were prevented with a hybrid radio penetration of 40 %. Comparing the impact of safety applications on the cellular network resources by using hybrid radios, it was established that up to 55 % of the cellular transmission were able to be saved. This is primarily resulting from employing forwarding of messages over 802.11p, which are received via LTE, thus reducing the number of LTE connections. Further savings in transmissions were achieved by taking into consideration 802.11p based RSUs. In this case the saving were increased up to 62 %. As the reliability of LTE for vehicular safety applications depends on the base load in the network, QoS prioritization or reserving of network resources for vehicular applications are potentially feasible to be considered. Also new broadcasting schemes, such as eMBMS offered by LTE, are a worthwhile to be analyze for an improved service delivery even in high base loads.

6.1 Outlook

This thesis established an assessment methodology for hybrid antenna systems and evaluated the service delivery exploiting the benefits of the combined use of cellular and ad-hoc radios. For future work in the area of vehicular antenna systems it is suggested that network simulation based approaches are carried out to visualize the impact of antenna characteristics on the system performance. Thus to identify thresholds for the KPIs, which were introduced in this work for vehicular antennas, and consequently to illustrate the impact of singular KPIs on the overall performance. In order to verify selected results with drive tests, it is proposed to use models of existing environments for these investigations. As such this allows to perform precise investigations on, for instance, antenna gain imbalances, which as shown in this work, resulted in a fallback to diversity transmission. In addition conducting the investigation for various settings of an operator's network is worthwhile to enable generalizing the results. The aforementioned evaluations require a network simulator offering accurate models of the access networks and allowing the integration of various mobility scenarios. Moreover to analyze ad-hoc as well as cellular systems the network simulator needs to support active probing as well as passive listening measurements.

In the area of infotainment applications it is suggested to design and verify strategies to incorporate external performance indicator in vertical handover decision algorithms with help of simulations and measurements. It is suggested to focus the evaluation on the optimization of the KPI weights with special regards to external inputs. As network selection algorithms potentially allow to use available resources more efficiently, it is worthwhile to focus on data intensive application with relaxed delay requirements. Consequently the resulting benefits in terms of QoS improvements like a high overall throughput or prevented outages are feasible to be determined quantitatively using such end-to-end network simulations.

For vehicular safety applications it is feasible to evaluate to which degree QoS prioritization in LTE enables to improve the dissemination of safety messages in high base load scenarios. Moreover an interesting approach worth analyzing is the impact of eMBMS on the service delivery. Another research area of interest is to analyze with simulations the partitioning of a MDE in hybrid radio networks to quantitatively compare different approaches. Lastly it is proposed to investigate clustering based approaches for messages dissemination. In this case a methodology needs to be identified feasible for hybrid radio networks and at the same time to keep the occurring signaling overhead as small as possible.

Appendix A

Radiation Patterns

A.1 802.11p Antennas

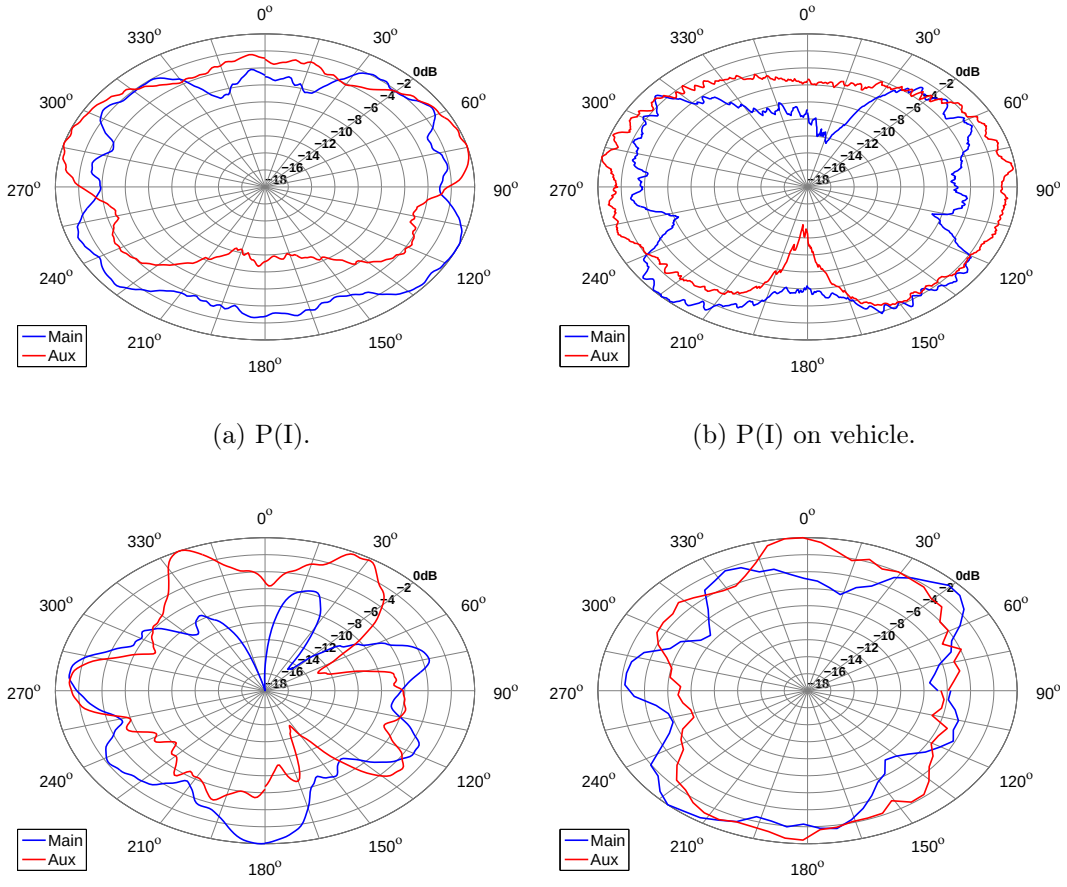

(a) P(I).

(b) P(I) on vehicle.

(c) P(II).

(d) P(III).

Figure A.1: 802.11p antennas measured on a ground plane and on the vehicle.

A.2 Cellular Antennas

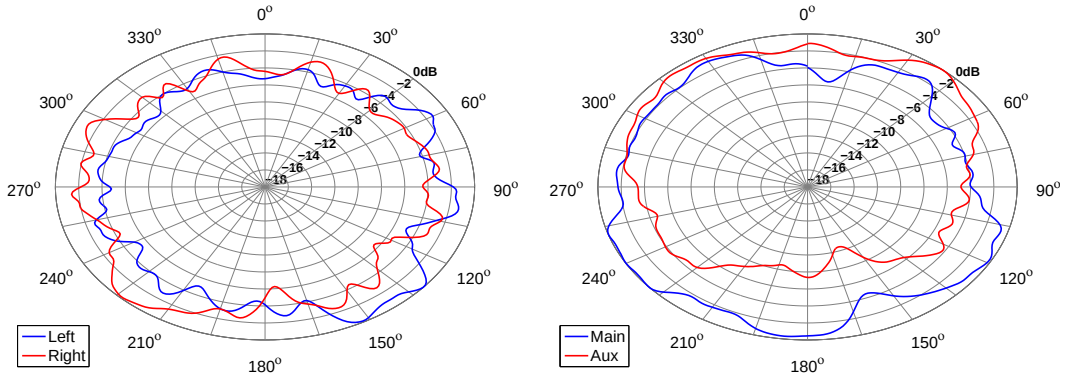

(a) Reference antenna. (b) P(I).

Figure A.2: LTE reference and P(I) antenna measured on the vehicle at 800 MHz .

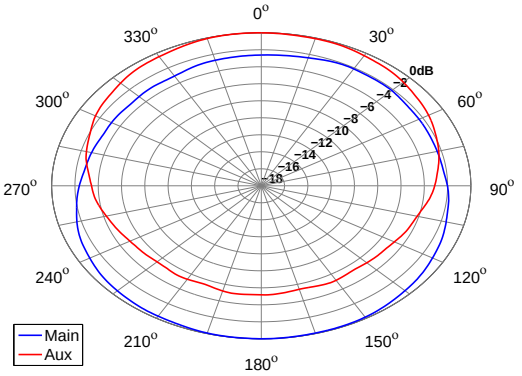

(a) P(I).

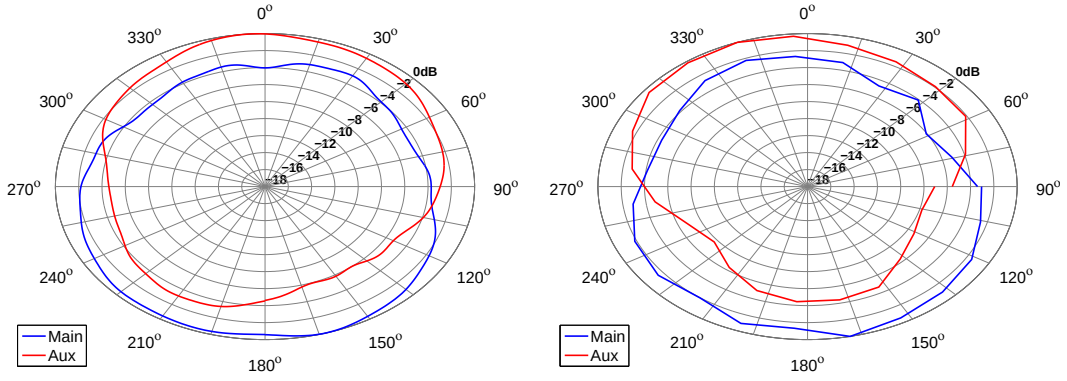

(b) P(II). (c) P(III).

Figure A.3: Prototypical antennas measured on a ground plane at 800 MHz.

List of Figures

List of Tables

List of Acronyms

3GPP	3rd Generation Partnership Project
AHP	Analytical Hierarchy Process
AP	Access Point
C	Mutual Information
CAM	Cooperative Awareness Message
CCDF	Complementary Cumulative Distribution Function
CDF	Cumulative Distribution Function
CE	Consumer Electronic
CPU	Central Processing Unit
DENM	Decentralized Environmental Notification Message
ECU	Electronic Control Unit
ED	Eigenvalue Dispersion
eMBMS	Evolved Multimedia Broadcast Multicast Service
ETSI	European Telecommunications Standards Institute
FCD	Floating Car Data
FEKO	FEldberechnung für Körper mit beliebiger Oberfläche
GPS	Global Positioning System
GSM	Global System for Mobile Communications
IEEE	Institute of Electrical and Electronics Engineers
ITS	Intelligent Transportation systems
KPI	Key Performance Indicators
LHW	Local Hazard Warning
LOS	Line of Sight
LTE	Long Term Evolution
MATLAB	MATrix LABoratory
MDE	Message Dissemination Entity
MID	Molded Interconnect Devices
MIMO	Multiple Input Multiple Output
nLOS	Non Line Of Sight
OEM	Original Equipment Manufacturer
OPNET	Opnet Wireless Modeler
P(I)	Prototype I
P(II)	Prototype II
P(III)	Prototype III
PCB	Printed Circuit Board
POI	Point of Interest

RF	Radio Frequency
RRM	Radio Resource Management
RSS	Received Signal Strength
RSSI	Received Signal Strength Indicator
RSU	Road Side Unit
RX	Receive Antenna
SIM	Subscriber Identity Module
SINR	Signal-to-Interference-plus-Noise Ratio
SISO	Single Input and Single Output
SMX	Spatial Multiplexing
SNR	Signal-to-Noise Ratio
SUMO	Simulation of Urban MObility
TP	Throughput
TX	Transmit Antenna
UMTS	Universal Mobile Telecommunications System
V2I	Vehicle to Infrastructure
V2V	Vehicle to Vehicle
V2X	Vehicle to Infrastructure and Vehicle Communication
VHDA	Vertical Handover Decision Algorithm
WLAN	Wireless Local Area Network
WWDW	Wrong Way Driver Warning
QoS	Quality of Service

Bibliography

[1] *AKTIV - Adaptive und kooperative Technologien für den intelligenten Verkehr*, http://www.aktiv-online.org, Accessed: October 13, 2014.

[2] *simTD, Sichere Intelligente Mobilität, Testfeld Deutschland*, http://www.simtd.de, Accessed: October 13, 2014.

[3] C. F. Mecklenbräuker, A. F. Molisch, J. Karedal, F. Tufvesson, A. Paier, L. Bernado, T. Zemen, O. Klemp, and N. Czink, "Vehicular Channel Characterization and its Implications for Wireless System Design and Performance," *Proceedings of the IEEE*, vol. 99, no. 7, pp. 1189–1212, 2011.

[4] *Converge - COmmunication Network VEhicle Road Global Extension*, http://www.converge-online.de, Accessed: October 13, 2014.

[5] H. Tazi, "Integration of Numerical Simulation Approaches in the Virtual Development of Automotive Antenna Systems," Ph.D. dissertation, Technical University of Munich, 2012.

[6] L. Ekiz, A. Thiel, O. Klemp, and C. F. Mecklenbräuker, "MIMO Performance Evaluation of Automotive Qualified LTE Antennas," in *IEEE 7th European Conference on Antennas and Propagation*, 2013, pp. 1412–1416.

[7] A. Posselt, L. Ekiz, O. Klemp, B. Geck, and C. F. Mecklenbräuker, "System Level Evaluation for Vehicular MIMO Antennas in Simulated and Measured Channels," in *8th European Conference on Antennas and Propagation*, 2014.

[8] A. Thiel, L. Ekiz, O. Klemp, and M. Schultz, "Automotive Grade MIMO Antenna Setup and Performance Evaluation for LTE-Communications," in *International Workshop on Antenna Technology*. IEEE, 2013, pp. 171–174.

[9] A. Kwoczek, Z. Raida, J. Lacik, M. Pokorny, J. Puskely, and P. Vagner, "Influence of Car Panorama Glass Roofs on Car2Car Communication," in *IEEE Vehicular Networking Conference*. IEEE, 2011, pp. 246–251.

[10] O. Klemp, "Performance Considerations for Automotive Antenna Equipment in Vehicle-to-Vehicle Communications," in *URSI International Symposium on Electromagnetic Theory*. IEEE, 2010, pp. 934–937.

[11] L. Reichardt, "Methodik für den Entwurf von kapazitätsoptimierten Mehrantennensystemen am Fahrzeug," Ph.D. dissertation, Karlsruhe Institute of Technology, 2013.

[12] G. Karagiannis, O. Altintas, E. Ekici, G. Heijenk, B. Jarupan, K. Lin, and T. Weil, "Vehicular Networking: A Survey and Tutorial on Requirements, Architectures, Challenges, Standards and Solutions," *Communications Surveys & Tutorials, IEEE*, vol. 13, no. 4, pp. 584–616, 2011.

[13] CONVERGE Consortium, *Deliverable D1.1 - Operational Requirements and Role Models*, 1st ed., July 2013.

[14] ——, *Deliverable D3 - Functional Requirements and Architecture Options*, 1st ed., September 2013.

[15] L. Bernado, S. Rührup, D. Valerio, Z. Xu, T. Zemen, C. F. Mecklenbräuker, M. Shemshaki, L. Ekiz, and O. Klemp, "Hybrid Communication Systems for Vehicular Communications in Intelligent Transport Systems," FTW Forschungszentrum Telekommunikation Wien GmbH, TU Vienna - Institute of Telecommunications, BMW Research and Technology, Tech. Rep., 2012.

[16] L. Ekiz, C. Arendt, O. Klemp, and C. F. Mecklenbräuker, "System Level Impact of Hybrid Radio Access for Vehicular Safety Applications," in *IEEE Transactions On Vehicular Technology*, 2014, Currently in Review.

[17] L. Ekiz, C. Lottermann, D. Öhmann, T. Tran, O. Klemp, C. Wietfeld, and C. F. Mecklenbräuker, "Potential of Cooperative Information for Vertical Handover Decision Algorithms," in *16th International IEEE Conference on Intelligent Transport Systems*, 2013.

[18] M. Kassar, B. Kervella, and G. Pujolle, "An Overview of Vertical Handover Decision Strategies in Heterogeneous Wireless Networks," *Comput. Commun.*, vol. 31, no. 10, pp. 2607–2620, Jun. 2008.

[19] ——, "An Intelligent Handover Management System for Future Generation Wireless Networks," *EURASIP Journal on Wireless Communications and Networking*, vol. 1, p. 12, 2008.

[20] E. Stevens-Navarro and V. Wong, "Comparison between Vertical Handoff Decision Algorithms for Heterogeneous Wireless Networks," in *Vehicular Technology Conference*, vol. 2. IEEE, 2006, pp. 947–951.

[21] K. Lee, J. Lee, Y. Yi, I. Rhee, and S. Chong, "Mobile Data Offloading: How Much Can WiFi Deliver," in *Proceedings of the 6th International Conference*. ACM, 2010, p. 26.

[22] S. Dimatteo, P. Hui, B. Han, and V. O. Li, "Cellular Traffic Offloading Through WiFi Networks," in *8th International Conference on Mobile Adhoc and Sensor Systems (MASS)*. IEEE, 2011, pp. 192–201.

[23] A. Aijaz, H. Aghvami, and M. Amani, "A survey on Mobile Data Offloading: Technical and Business Perspectives," *Wireless Communications*, vol. 20, no. 2, pp. 104–112, 2013.

[24] K. Dar, M. Bakhouya, J. Gaber, M. Wack, and P. Lorenz, "Wireless Communication Technologies for ITS Applications," *IEEE Communications Magazine*, vol. 48, no. 5, pp. 156–162, 2010.

[25] G. Araniti, C. Campolo, M. Condoluci, A. Iera, and A. Molinaro, "LTE for Vehicular Networking: A Survey," *IEEE Communications Magazine*, vol. 51, no. 5, p. 148157, 2013.

[26] A. Vinel, "3GPP LTE versus IEEE 802.11 p/WAVE: Which Technology is Able to Support Cooperative Vehicular Safety Applications," *IEEE Wireless Communications Letters*, vol. 1, no. 2, pp. 125–128, 2012.

[27] L. Ekiz, A. Posselt, O. Klemp, and C. F. Mecklenbräuker, "System Level Assessment of Vehicular MIMO Antennas in 4G LTE Live Networks," in *IEEE 80th Vehicular Technology Conference: VTC2014-Fall*, 2014.

[28] L. Ekiz, T. Patelczyk, O. Klemp, and C. F. Mecklenbräuker, "Compensation of Vehicle-Specific Antenna Radome Effects at 5.9 GHz," in *39th Annual Conference of the IEEE Industrial Electronics Society*, 2013.

[29] L. Ekiz, A. Posselt, O. Klemp, and C. F. Mecklenbräuker, "Assessment of Design Methodologies for Vehicular 802.11p Antenna Systems," in *3rd International Conference on Connected Vehicles & Expo*, 2014.

[30] A. Posselt, A. Friedrich, L. Ekiz, O. Klemp, and B. Geck, "System-Level Assessment of Volumetric 3D Vehicular MIMO Antenna Based on Measurement," in *3rd International Conference on Connected Vehicles & Expo*, 2014.

[31] H. Lo, C. Yip, and B. Mak, "Passenger Route Guidance System for Multi-Modal Transit Networks," *Journal of Advanced Transportation*, vol. 39, no. 3, pp. 271–288, 2005.

[32] H. Holma and A. Toskala, *LTE for UMTS: Evolution to LTE-Advanced.* Wiley, 2011.

[33] M. Alasti, B. Neekzad, J. Hui, and R. Vannithamby, "Quality of Service in WiMAX and LTE Networks," *Communications Magazine*, vol. 48, no. 5, pp. 104–111, 2010.

[34] V. Rabinovich, N. Alexandrov, and B. Alkhateeb, *Automotive Antenna Design and Applications.* Taylor & Francis, 2010.

[35] D. Bai, C. Park, J. Lee, H. Nguyen, J. Singh, A. Gupta, Z. Pi, T. Kim, C. Lim, M. Kim, and I. Kang, "LTE-Advanced Modem Design: Challenges and Perspectives," *IEEE Communications Magazine*, vol. 50, pp. 178–186, 2012.

[36] M. Matthaiou, D. I. Laurenson, and C.-X. Wang, "Reduced Complexity Detection for Ricean MIMO Channels Based on Condition Number Thresholding," in *International Wireless Communications and Mobile Computing Conference*. IEEE, 2008, pp. 988–993.

[37] J. Maurer, G. Matz, and D. Seethaler, "Low-Complexity and Full-Diversity MIMO Detection Based on Condition Number Thresholding," in *International Conference on Acoustics, Speech and Signal Processing*, vol. 3. IEEE, 2007, pp. 61–64.

[38] *TSMW Universal Radio Network Analyzer Scanner for drive tests and I/Q streaming*, 8th ed., Rohde & Schwarz, March 2013.

[39] G. J. Foschini and M. J. Gans, "On Limits Of Wireless Communications In A Fading Environment When Using Multiple Antennas," *Wireless Personal Communications*, vol. 6, pp. 311–335, 1998.

[40] A. Gerber, J. Pang, O. Spatscheck, and S. Venkataraman, "Speed Testing Without Speed Tests: Estimating Achievable Download Speed from Passive Measurements," in *Proceedings of the 10th ACM SIGCOMM Conference on Internet Measurement*. ACM, 2010, pp. 424–430.

[41] A. Molisch, F. Tufvesson, J. Karedal, and C. Mecklenbräuker, "A Survey on Vehicle-to-Vehicle Propagation Channels," *IEEE Wireless Communications*, vol. 16, no. 6, pp. 12–22, 2009.

[42] R. Hoppe, J. Ramuh, H. Buddendick, and G. Stabler, O.and Wolfle, "Comparison of MIMO Channel Characteristics Computed by 3D Ray Tracing and Statistical Models," in *2nd European Conference on Antennas and Propagation (EuCAP)*, 2007, pp. 1–5.

[43] O. Stabler, R. Hoppe, G. Wolfle, T. Hager, and T. Herrmann, "Consideration of MIMO in the Planning of LTE Networks in Urban and Indoor Scenarios," in *5th European Conference on Antennas and Propagation (EUCAP)*. IEEE, 2011, pp. 2187–2191.

[44] H. Xia, H. L. Bertoni, L. R. Maciel, A. Lindsay-Stewart, and R. Rowe, "Radio Propagation Characteristics for Line-of-Sight Microcellular and Personal Communications," *IEEE Transactions on Antennas and Propagation*, vol. 41, no. 10, pp. 1439–1447, 1993.

[45] A. Paier, "The Vehicular Radio Channel in the 5 GHz Band," Ph.D. dissertation, TU Vienna, 2010.

[46] V. Plicanic, H. Asplund, and B. K. Lau, "Performance of Handheld MIMO Terminals in Noise-and Interference-Limited Urban Macrocellular Scenarios," *IEEE Transactions on Antennas and Propagation*, vol. 60, pp. 3901–3912, 2012.

[47] *Global Positioning System Standard Positioning Service Performance Standard*, National Coordination Office for Space-Based Positioning, Navigation, and Timing Std., Rev. 4th Edition, September 2008.

[48] *ROMES4 Drive Test Software*, 5th ed., Rohde & Schwarz, November 2011.

[49] M. Geissler, C. Oikonomopoulos-Zachos, T. Ould, and M. Arnold, "MIMO Performance Optimisation of Car Antennas," in *6th European Conference on Antennas and Propagation (EUCAP)*, 2012, pp. 2750–2753.

[50] B. Hagerman, K. Werner, and J. Yang, "MIMO Performance at 700 MHz: Field Trials of LTE with Handheld UE," in *IEEE 74th Vehicular Technology Conference (VTC Fall)*, 2011, pp. 1–5.

[51] E. Ohlmer, G. Fettweis, and D. Plettemeier, *MIMO System Design and Field Tests for Terminals with Confined Space-Impact on Automotive Communication*, 2011.

[52] C. Oikonomopoulos-Zachos, T. Ould, and M. Arnold, "Outdoor Channel Characterization of MIMO-LTE Antenna Configurations Through Measurements," in *IEEE 75th Vehicular Technology Conference (VTC Spring)*, 2012, pp. 1–4.

[53] *Requirements for support of radio resource management - TS 36.133 V9.12.0*, 3GPP - Technical Specification Group Radio Access Network, June 2012.

[54] *Qualcomm eXtensible Diagnostic Monitor*, Qualcomm Incorporated, 2012. [Online]. Available: https://www.qualcomm.com/media/documents/files/qxdm-professional-qualcomm-extensible-diagnostic-monitor.pdf

[55] *QMI Network Access Service* , Qualcomm Incorporated, December 2012.

[56] M. Jensen and J. Wallace, "A Review of Antennas and Propagation for MIMO Wireless Communications," *IEEE Transactions on Antennas and Propagation*, vol. 52, no. 11, pp. 2810–2824, 2004.

[57] J. Wallace and M. Jensen, "Time-Varying MIMO Channels: Measurement, Analysis, and Modeling," *Antennas and Propagation, IEEE Transactions on*, vol. 54, no. 11, pp. 3265–3273, 2006.

[58] T. Abbas, J. Karedal, and F. Tufvesson, "Measurement-Based Analysis: The Effect of Complementary Antennas and Diversity on Vehicle-to-Vehicle Communication," *Antennas and Wireless Propagation Letters*, vol. 12, pp. 309–312, 2013.

[59] A. Thiel, O. Klemp, A. Paier, L. Bernadó, J. Karedal, and A. Kwoczek, "In-situ Vehicular Antenna Integration and Design Aspects For Vehicle-to-Vehicle Communications," in *European Conference on Antennas and Propagation*. IEEE, 2010, pp. 1–5.

[60] A. Thiel and O. Klemp, "Initial Results of Multielement Antenna Performance in 5.85 GHz Vehicle-to-Vehicle Scenarios," in *European Conference on Wireless Technology*. IEEE, 2008, pp. 322–325.

[61] J. Härri, H. Tchouankem, O. Klemp, and O. Demchenko, "Impact of Vehicular Integration Effects on the Performance of DSRC Communications," in *Wireless Communications and Networking Conference*. IEEE, 2013, pp. 1645–1650.

[62] S. Kaul, K. Ramachandran, P. Shankar, S. Oh, M. Gruteser, I. Seskar, and T. Nadeem, "Effect of Antenna Placement and Diversity on Vehicular Network Communications," in *4th Annual IEEE Communications Society Conference on Sensor, Mesh and Ad Hoc Communications and Networks*. IEEE, 2007, pp. 112–121.

[63] T. Eng, N. Kong, and L. B. Milstein, "Comparison of Diversity Combining Techniques for Rayleigh-Fading Channels," *IEEE Transactions on Communications*, vol. 44, no. 9, pp. 1117–1129, 1996.

[64] *Broadband and Omni-directional DSRC 5.9 GHz Antenna*, Mobile Mark, June 2013. [Online]. Available: http://www.mobilemark.com/images/spec%20sheets/pg%20149%20ECO-5900-spec.pdf

[65] *Cisco Aironet Omnidirectional Mast Mount Antenna (AIR-ANT2506)*, Cisco Systems, Inc., Accessed: October 13, 2014. [Online]. Available: http://www.cisco.com/en/US/docs/wireless/antenna/installation/guide/ant2506.pdf

[66] P. Noren, L. Foged, and P. Garreau, "State of the Art Spherical Near-Field Antenna Test Systems for Full Vehicle Testing," in *6th European Conference on Antennas and Propagation (EUCAP).* IEEE, 2012, pp. 2244–2248.

[67] R. Vaughan, "Switched Parasitic Elements for Antenna Diversity," *IEEE Transactions on Antennas and Propagation*, vol. 47, no. 2, pp. 399–405, 1999.

[68] *CST Microwave Studio 2013*, Accessed: October 13, 2014. [Online]. Available: https://www.cst.com/

[69] C.-X. Wang, X. Cheng, and D. Laurenson, "Vehicle-to-Vehicle Channel Modeling and Measurements Recent Advances and Future Challenges," *IEEE Communications Magazine*, vol. 47, no. 11, pp. 96–103, 2009.

[70] *FEKO 6.3 - EM Simulation Software*, Accessed: October 13, 2014. [Online]. Available: www.feko.info

[71] U. Jakobus, "Overview of Hybrid Methods in FEKO: Theory and Applications," in *International Conference on Electromagnetics in Advanced Applications (ICEAA).* IEEE, 2010, pp. 434–437.

[72] *Task Force Antenna - Status Report* -, 3rd ed., Car-2-Car Communication Consortium, November 2011.

[73] O. Brickley, C. Shen, M. Klepal, A. Tabatabaei, and D. Pesch, "A data Dissemination Strategy for Cooperative Vehicular Systems," in *IEEE Vehicular Technology Conference Spring.* IEEE, 2007, pp. 2501–2505.

[74] M. Zekri, B. Jouaber, and D. Zeghlache, "Context Aware vertical Handover Decision Making in Heterogeneous Wireless Networks," in *IEEE 35th Conference on Local Computer Networks*, October 2010, pp. 764 –768.

[75] X. Yan, A. Şekercioğlu, and S. Narayanan, "A Survey of Vertical Handover Decision Algorithms in Fourth Generation Heterogeneous Wireless Networks," *Computer Networks*, vol. 54, no. 11, pp. 1848–1863, 2010.

[76] S. Cooner, A. Cothron, and S. Ranft, "Countermeasures for Wrong-Way Movement on Freeways: Guidelines And Recommended Practices," Texas Transportation Institute, Tech. Rep., October 2003.

[77] D. Lecompte and F. Gabin, "Evolved Multimedia Broadcast/Multicast Service (eMBMS) in LTE-Advanced: Overview and Rel-11 Enhancements," *Communications Magazine*, vol. 50, no. 11, pp. 68–74, 2012.

[78] J.-H. Huang, L.-C. Wang, and C.-J. Chang, "Deployment Strategies of Access Points for Outdoor Wireless Local Area Networks," in *61st Vehicular Technology Conference*, vol. 5. IEEE, 2005, pp. 2949–2953.

[79] K. Yang, B. Qiu, and L. Dooley, "Using SINR as Vertical Handoff Criteria in Multimedia Wireless Networks," in *IEEE International Conference on Multimedia and Expo*, 2007, pp. 967–970.

[80] M. N. Halgamuge, H. L. Vu, K. Ramamohanarao, and M. Zukerman, "Signal based Evaluation of Handoff Algorithms," *IEEE Communications Letters*, vol. 9, no. 9, pp. 790–792, September 2005.

[81] T. Tran, M. Kuhnert, and C. Wietfeld, "Performance Evaluation of Feasible and Holistic CSH-MU Handoff Solution for Seamless Emergency Service Provisioning," in *17th IEEE Symposium on Computers and Communications (ISCC)*. Cappadocia, Turkey: IEEE, July 2012, pp. 317–324.

[82] P. Chan, R. Sheriff, Y. Hu, P. Conforto, and C. Tocci, "Mobility Management Incorporating Fuzzy Logic for a Heterogeneous IP Environment," in *IEEE Communications Magazine*, vol. 39, no. 12. IEEE, December 2001, pp. 42–51.

[83] J. Hou and D. C. O'Brien, "Vertical Handover-Decision-Making Algorithm Using Fuzzy Logic for the Integrated Radio-and-OW System," *Trans. Wireless. Comm.*, vol. 5, no. 1, pp. 176–185, Nov. 2006.

[84] L. Xia, L. Jiang, and C. He, "A Novel Fuzzy Logic Vertical Handoff Algorithm with Aid of Differential Prediction and Pre-Decision Method," in *IEEE International Conference on Communications (ICC)*. Glasgow: IEEE, June 2007, pp. 5665–5670.

[85] T. L. Saaty, "How to Make a Decision: The Analytic Hierarchy Process," *European Journal of Operational Research*, vol. 48, pp. 9–26, September 1990.

[86] H. Hartenstein and K. P. Laberteaux, "A Tutorial Survey on Vehicular ad-hoc Networks," *Communications Magazine*, vol. 46, no. 6, pp. 164–171, 2008.

[87] T. Mangel, T. Kosch, and H. Hartenstein, "A Comparison of UMTS and LTE for Vehicular Safety Communication at Intersections," in *IEEE Vehicular Networking Conference*, 2010.

[88] M.-A. Phan, R. Rembarz, and S. Sories, "A Capacity Analysis for the Transmission of Event and Cooperative Awareness Messages in LTE Networks," in *IEEE 18th World Congress on Intelligent Transport Systems*, 2011, pp. 1–12.

[89] C. Wewetzer, M. Caliskan, K. Meier, and A. Luebke, "Experimental Evaluation of UMTS and Wireless LAN for Inter-Vehicle Communication," in *International Conference on ITS Telecommunications*. IEEE, 2007, pp. 1–6.

[90] T. Mangel, "Inter-Vehicle Communication at Intersections: An Evaluation of Ad-Hoc and Cellular Communication," Ph.D. dissertation, Karlsruhe Institute of Technology, 2012.

[91] K. Bilstrup, E. Uhlemann, E. Ström, and U. Bilstrup, *On the Ability of the 802.11p MAC Method and STDMA to Support Real-Time Vehicle-to-Vehicle Communication*, 2009.

[92] A. A. Gómez, "Dependable Medium Access Control For Road-Traffic Safety," Ph.D. dissertation, TU Vienna, 2013.

[93] C. Lottermann, M. Botsov, P. Fertl, and R. Mullner, "Performance Evaluation of Automotive Off-Board Applications in LTE Deployments," in *IEEE Vehicular Networking Conference (VNC)*. IEEE, 2012, pp. 211–218.

[94] J. Y. Yu and P. H. J. Chong, "A Survey of Clustering Schemes for Mobile Ad-Hoc Networks," *IEEE Communications Surveys and Tutorials*, vol. 7, no. 1-4, pp. 32–48, 2005.

[95] S. Messelodi, C. Modena, M. Zanin, F. De Natale, F. Granelli, E. Betterle, and A. Guarise, "Intelligent Extended Floating Car Data Collection," *Expert Systems with Applications*, vol. 36, no. 3, pp. 4213–4227, 2009.

[96] L. A. Maglaras and D. Katsaros, "Clustering in Urban Environments: Virtual Forces Applied to Vehicles," in *International Conference on Communications (ICC) Workshops*. IEEE, 2013, pp. 484–488.

[97] A. Friedrich, B. Geck, O. Klemp, and H. Kellermann, "On the Design of a 3D LTE Antenna for Automotive Applications based on MID Technology," in *European Microwave Conference (EuMC)*. IEEE, 2013, pp. 640–643.

[98] *Frequenzplan*, Bundesnetzagentur für Elektrizität, Gas, Telekommunikation, Post und Eisenbahn, January 2014, Accessed: October 13, 2014. [Online]. Available: http://www.bundesnetzagentur.de/Frequenzplan

[99] C. A. Balanis, *Modern Antenna Handbook*. John Wiley & Sons, 2008.

[100] R. Kuonanoja, "Low Correlation Handset Antenna Configuration for LTE MIMO Applications," in *Antennas and Propagation Society International Symposium (APSURSI)*. IEEE, 2010, pp. 1–4.

[101] Y. Yao, X. Wang, and J. Yu, "Multiband Planar Monopole Antenna for LTE MIMO Systems," in *International Journal of Antennas and Propagation*. Hindawi Publishing Corporation, 2012.

[102] R. Schlueter, B. Roesener, J. Kickelhain, and G. Naundorf, *Completely Additive Laser-Based Process for the Production of 3D MIDs - The LPKF LDS Process*, 5th International Congress Molded Interconnect Devices, 2002.

[103] *Magnetic Mount Antenna - Cellular - MCA 1890 MH*, Hirschmann Car Communication GmbH, November 2012, Accessed: October 13, 2014. [Online].

Available: http://www.hirschmann-car.com/fileadmin/content/downloads/pdf/produkttabellen_3/2014-05-15_hirschmann_cc-cellular-communication.pdf

[104] J. Kurjenniemi, T. Henttonen, and J. Kaikkonen, "Suitability of RSRQ Measurement for Quality based Inter-Frequency Handover in LTE," in *IEEE International Symposium on Wireless Communication Systems*, 2008, pp. 703–707.

[105] M. Riback, S. Grant, G. Jongren, T. Tynderfeldt, D. Cairns, and T. Fulghum, "MIMO-HSPA testbed performance measurements," in *18th International Symposium on Personal, Indoor and Mobile Radio Communications*. IEEE, 2007, pp. 1–5.

[106] O. Klemp and H. Eul, "Diversity Efficiency of Multimode Antennas Impacted by Finite Pattern Correlation and Branch Power Imbalances," in *4th International Symposium on Wireless Communication Systems*. IEEE, 2007, pp. 322–326.

[107] E. Lambers, M. Klaassen, A. Koppelaar, P. Gray, and P. Alexander, *DSRC Mobile WLAN Component*, NXP Semiconductors, Cohda Wireless,, 2012.

[108] H. Holma and A. Toskala, *LTE for UMTS-OFDMA and SC-FDMA based Radio Access*. Wiley, 2009.

[109] V. Abhayawardhana, I. Wassell, D. Crosby, M. Sellars, and M. Brown, "Comparison of Empirical Propagation Path Loss Models for Fixed Wireless Access Systems," in *IEEE 61st Vehicular Technology Conference Spring*, vol. 1. IEEE, 2005, pp. 73–77.

[110] B. Sklar, "Rayleigh Fading Channels in Mobile Digital Communication Systems - I. Characterization," *Communications Magazine*, vol. 35, pp. 90–100, 1997.

[111] J. Huang, F. Qian, A. Gerber, Z. M. Mao, S. Sen, and O. Spatscheck, "A Close Examination of Performance and Power Characteristics of 4G LTE Networks," in *10th International Cconference on Mobile Systems, Applications and Services*. ACM, 2012, pp. 225–238.

[112] D. Martín-Sacristán, J. F. Monserrat, J. Cabrejas-Peñuelas, D. Calabuig, S. Garrigas, and N. Cardona, "On the Way Towards Fourth-Generation Mobile: 3GPP LTE and LTE-Advanced," *EURASIP J. Wirel. Commun. Netw.*, vol. 2009, pp. 4:1–4:10, Mar. 2009.

[113] M. Laner, P. Svoboda, P. Romirer-Maierhofer, N. Nikaein, F. Ricciato, and M. Rupp, "A Comparison Between One-way Delays in Operating HSPA and LTE Networks," in *Proceedings of the 8th International Workshop on Wireless Network Measurements WinMee'12*, 2012, pp. 286–292.

[114] P. Chatzimisios, A. C. Boucouvalas, and V. Vitsas, "IEEE 802.11 Wireless LANs: Performance Analysis and Protocol Refinement," *EURASIP J. Wirel. Commun. Netw.*, vol. 2005, no. 1, pp. 67–78, Mar. 2005.

[115] D. Krajzewicz, J. Erdmann, M. Behrisch, and L. Bieker, "Recent Development and Applications of SUMO (Simulation of Urban MObility)," *International*

Journal On Advances in Systems and Measurements, vol. 5, no. 3&4, pp. 128–138, December 2012.

[116] P. I. Bratanov, "User Mobility Modeling in Cellular Communications Networks," Ph.D. dissertation, Vienna University of Technology, Austria, 1999.

[117] S. Krauss, "Microscopic Modeling of Traffic Flow: Investigation of Collision Free Vehicle Dynamics," Ph.D. dissertation, German Aerospace Centre, 1998.

[118] Z. Nadir, N. Elfadhil, and F. Touati, "Pathloss Determination Using Okumura-Hata Model and Spline Interpolation for Missing Data for Oman," in *Proceedings of the World Congress on Engineering*, vol. 1, 2008, pp. 2–4.

[119] L. Stibor, Y. Zang, and H. Reumerman, "Evaluation of Communication Distance of Broadcast Messages in a Vehicular Ad-Hoc Network using IEEE 802.11 p," in *Wireless Communications and Networking Conference*. IEEE, 2007, pp. 254–257.

[120] *WINNER II Channel Models, Part II, Radio Channel Measurement and Analysis Results*, WINNER - Wireless World Initiative New Radio, September 2007, iST-4-027756 WINNER II, D1.1.2 V1.0.

[121] ETSI ES 202 663 v.5, *Intelligent Transport Systems*, 2010.

[122] G. Maier, "Advanced Transmission Techniques for Vehicular Communications," Ph.D. dissertation, TU Vienna, 2013.

[123] N. Sun, "Performance Study of IEEE 802.11p for Vehicle to Vehicle Communications Using OPNET," Ph.D. dissertation, Massey University, 2011.

[124] B. Pappritz, *Berechnung des Anhalteweges*, ADAC e.V., Bereich Verkehrssicherheitsprogramme, 2008.

[125] P. Papadimitratos, A. La Fortelle, K. Evenssen, R. Brignolo, and S. Cosenza, "Vehicular Communication Systems: Enabling Technologies, Applications, and Future Outlook on Intelligent Transportation," *IEEE Communications Magazine*, vol. 47, no. 11, pp. 84–95, 2009.

[126] L. Bernadó, "Non-Stationarity in Vehicular Wireless Channels," Ph.D. dissertation, TU Vienna, 2012.

[127] M. Schack, "Integrated Simulation of Communication Applications in Vehicular Environments," Ph.D. dissertation, Technical University Braunschweig, 2012.

[128] O. Renaudin, "Experimental Channel Characterization for Vehicle-to-Vehicle Communication Systems," Ph.D. dissertation, Université Catholique De Louvain, 2013.